4-14-80

Lr. 1538

ENERGY CONSERVATION

COO-2566-53-T1

FORD/D.O.E. SODIUM-SULFUR BATTERY ELECTRIC VEHICLE DEVELOPMENT AND DEMONSTRATION

Phase 1-A. Final Report

MASTER

Work Performed Under Contract No. EY-76-C-02-2566

Ford Motor Company
Dearborn, Michigan

DEPARTMENT OF ENERGY · UNITED STATES OF AMERICA

U. S. DEPARTMENT OF ENERGY

Division of Energy Storage Systems

DISCLAIMER

DISCLAIMER

Available from the National Technical Information Service, U. S. Department of Commerce, Springfield, Virginia 22161.

Price: Paper Copy $20.00
Microfiche $3.50

COO-2566-53-T1
Distribution Categories UC-94cb and UC-96

FORD/D.O.E. SODIUM-SULFUR BATTERY ELECTRIC VEHICLE DEVELOPMENT AND DEMONSTRATION

PHASE 1-A
FINAL REPORT
REPORT NO. 53

A. Topouzian
Program Manager

Research Staff
Ford Motor Company
P.O. Box 2053
Dearborn, Michigan 48121

Prepared For: The Department of Energy under Contract No. EY-76-C-02-2566, Modification A005

TABLE OF CONTENTS

FORD/D.O.E. SODIUM-SULFUR BATTERY
ELECTRIC VEHICLE DEVELOPMENT AND DEMONSTRATION

TABLE OF CONTENTS

LIST OF FIGURES

LIST OF FIGURES

LIST OF FIGURES

LIST OF TABLES

ABSTRACT

This final report presents the results of Phase I-A analyses and design studies conducted by the Ford Motor Company for the U. S. Department of Energy under modification A005 to Contract No. EY-76-C-02-2566. The objective of the Phase I-A effort was to evaluate the Sodium-Sulfur battery, in an existing conventional production automobile, as a potential power source for an electric vehicle.

The Phase I-A work was divided into five (5) major sub-tasks as follows:

1. Vehicle Specification Sub-Task
2. NaS Battery Packaging Study Sub-Task
3. Vehicle Packaging Layout Sub-Task
4. Electrical System Study Sub-Task
5. System Study Sub-Tasks covering performance & economy projections, powertrain and vehicle safety issues and thermal studies.

The major results of the Sodium-Sulfur Battery Powered Electric Vehicle Study Program are listed below:

1. The Fiesta was chosen to be the production vehicle which would be modified into a 2-passenger, electric test bed vehicle powered by a NaS battery.
2. The vehicle mission was defined to be a 2-passenger urban/suburban commuter vehicle capable of at least 100 miles range over the CVS driving cycle and a wide open throttle capability of 0-50 MPH in 14 seconds, or less.
3. Powertrain component specifications were defined.
4. Powertrain control strategy has been selected.
5. A suitable test bed vehicle package scheme has been developed.

I INTRODUCTION AND SUMMARY

This final report summarizes the results obtained from the Phase I-A analyses and design studies conducted by the Ford Motor Company for the U. S. Department of Energy under Contract No. EY-76-C-02-2566. The objective of the Phase I-A effort was "evaluate the Sodium-Sulfur battery, in an existing conventional production automobile, as a potential power source for an electric vehicle."

The Phase I Study Program Work Task was divided into five (5) major work sub-tasks as follows:

1. Vehicle Specification Sub-Task
2. NaS Battery Packaging Study Sub-Task
3. Vehicle Packaging Layout Sub-Task
4. Electrical System Study Sub-Task
5. System study Sub-Tasks covering performance and economy projections, powertrain and vehicle safety issues and thermal studies.

The program strategy developed to achieve the study objectives and milestones is defined by the following steps:

1. Develop vehicle assumptions including such items as purpose, size, weight, and performance. These assumptions will then be converted into system and sub-system functional objectives. For example, for given vehicle performance assumption, battery functional objectives of weight, power density, energy density, and volume density will be established.
2. Select a current Ford vehicle which best matches the assumptions and functional objectives.

3. Conduct analytical vehicle performance and economy (P & E) studies, including trade-off analysis, to determine the effects of various powertrain component efficiency and weight.

4. Concurrent with the analytical studies, develop vehicle package layouts to establish location, space, and weight distribution for the battery and powertrain systems.

5. Based on the above analytical and packaging studies, select the necessary powertrain and battery system components.

6. Conclude with a vehicle layout and study results in a final report to DOE.

The major results of the work are presented in each of the following sub-headings:

A. VEHICLE SPECIFICATIONS

At the outset of the study program vehicle specifications were developed for the NaS-powered electric vehicle (EV), via interchanges between Ford Research Staff and several long range planning and product planning activities within Ford. The objective was to define EV characteristics for a vehicle which could compete in a free market with an ICE-powered vehicle of similar size and function.

The ten most significant vehicle specifications developed for a NaS battery-powered EV are listed in Table I-1.

These specifications were used as program guidelines for performing battery sizing studies, vehicle packaging studies covering vehicle installations of both battery and powertrain components, as well as performance and economy studies of a selected Ford production vehicle.

B. BATTERY PACKAGING

Based upon the vehicle specifications listed in Table I-1, the computer results obtained from the Ford Research NaS cell sizing and performance

programs, and the computer results from the Company vehicle performance and economy (P & E) program, a series of battery packaging concepts were developed for vehicle application study. Early in the study program, the Fiesta was chosen as the preferred Ford production vehicle for conversion into a test bed/demonstration vehicle for evaluating the future potential of the NaS battery as a power source for electric passenger vehicles. Consequently, all battery package concepts were developed with Fiesta installation in mind.

Conceptual designs of battery packages were developed for evaluation under the following trade-off conditions:

1. Vehicle front end installation of the NaS battery package vs vehicle rear end installation.

TABLE I-1 ELECTRIC VEHICLE SPECIFICATIONS FOR PROJECTED 1985-1995 MARKET

1.	Purpose	— Shopper/commuter for multi-vehicle families
2.	Seating Capacity	— 2-passengers minimum
3.	Cargo Capacity	— Approx. 10 Ft^3 (Groceries/small packages)
4.	Size	— Approx. exterior dimisions: OAL - 125" width - 55"
5.	Range	— 100 miles over CVS cycle @ 80% battery discharge
6.	Performance	— 0-50 MPH in 14 secs.
7.	Battery Specifications	— 5 hour (max.) recharge time
8.	Vehicle Accessories	— Heater and radio mandatory
9.	Weight Penalty	— 500 lb. weight penalty over equivalent ICE powered vehicle
10.	Vehicle Safety	— Meet all FMVSS requirements for EV vehicles

2. Air cooling and/or heating of the battery package vs liquid cooling (plus resistance heating) for the purpose of maintaining temperature control of the interior of the battery package.

One of the more interesting battery package designs developed is the liquid cooled and electrical resistance heated battery package illustrated in Figure I-1. Table I-2 summarizes the key design features and dimensions of the configuration, which is shown packaged in the rear of the Fiesta, Figure IV-7, Section IV.

C. VEHICLE PACKAGING

With the vehicle specifications listed in Table I-1 as guidelines, the 1978

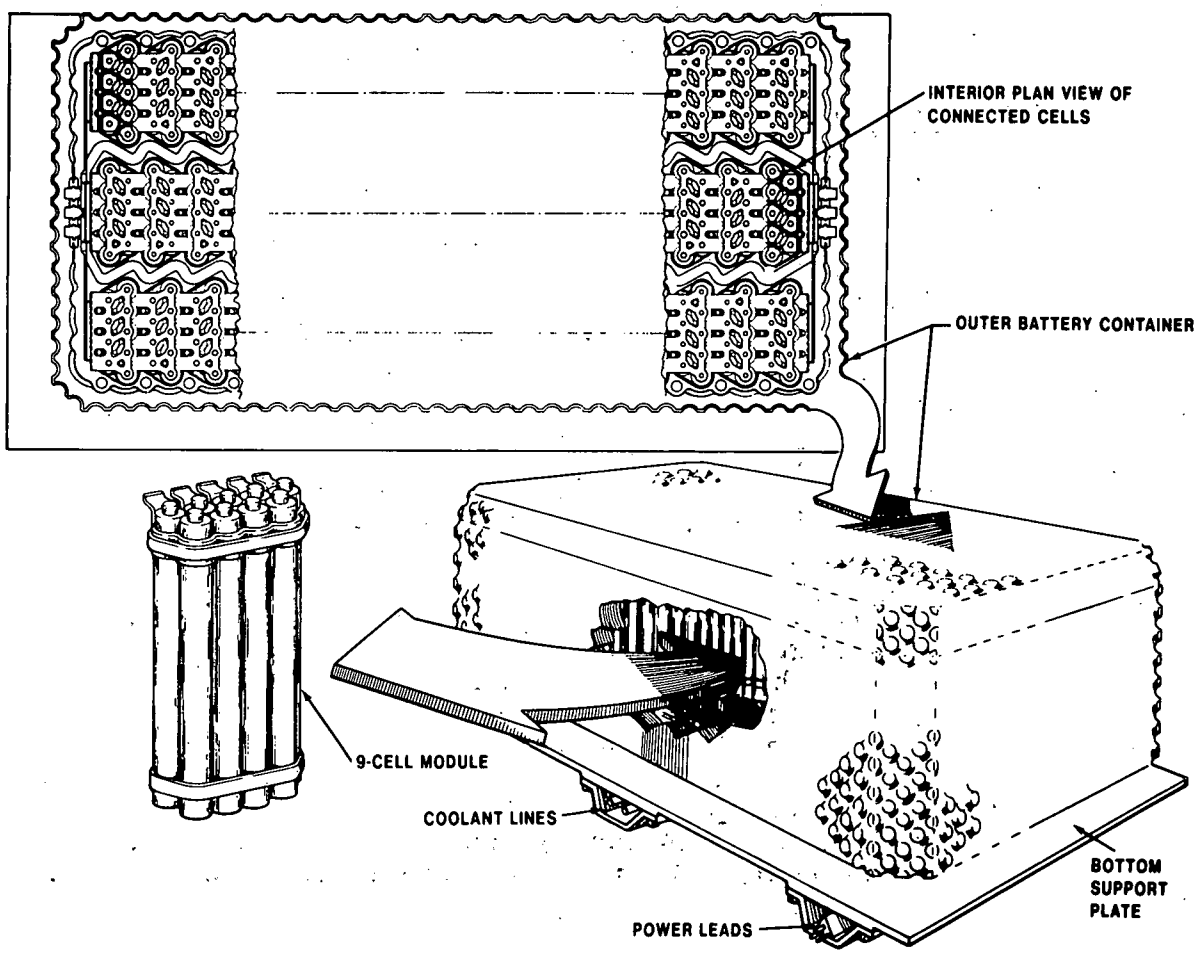

Figure I-1 Evacuated Liquid Cooled and Resistance Heated Battery Package

Ford Fiesta was chosen to be the reference vehicle for the NaS battery powered EV study program. This reference vehicle was conceptually modified to be a 2-passenger vehicle powered by a small 1.1 litre engine (a downsize from the standard I.6 L engine used in the U.S. production Fiesta), and carrying only enough fuel to achieve a CVS cycle driving range of 125 miles. The curb weight, performance, and driving cycle efficiency projected for this conceptual internal combustion powered vehicle provides the competitive criteria for the NaS-powered vehicle.

TABLE I-2 DESIGN FEATURES OF THE NaS BATTERY PACKAGE FOR THE FIESTA EV

1.	Battery Size:	Width (Inches)	39
		Length (Inches)	20
		Height (Inches)	20
2.	Battery Weight (lbs):		665
	. Clustered Cells	492.8 lbs.	
	. Electrical Connections.	19.4 lbs.	
	. Insulated Container	85.0 lbs.	
	. Tie Down Structure	50.0 lbs.	
	. Filler Material	9.0 lbs.	
	. Bus-bars/Lead Thru's	8.4 lbs.	
	Total (Est.)	665.0 lbs.	
3.	Cell & Sub-Module Details		
	. Total Number of Cells		432
	. Number of Cells Per Sub-Module		9
	. Number of Sub-Modules Per Battery Module		16
	. Number of Modules Per Battery Assembly		3
	A. Cell Data:		
	. Outer Diameter (Inches)		1.0
	. Length (Inches)		15.8
	. Weight (lbs.)		1.1
	. Power Density (Watts/lb)		82.4
	. Energy Density (Watt-Hrs./lb)		71.3
4.	Projected Performance:		
	. Power Rating -kw @ Zero depth of discharge)		40.6
	. Energy Rating — Kw-Hrs. (100% DOD in 5.72 Hrs.)		35.2

The packaging studies began with the removal of all components from the 1978 Fiesta production drawings not required for the NaS EV, for example:

- Engine, engine mounts, and cooling system;
- Fuel tank, fuel lines, and instrumentation;
- Exhaust and emission subsystems;
- Rear spare tire (by the late 1980's it is projected that "run-flat" tires will be in standard production); and
- Rear passenger seats and all rear interior trim

At the outset of the vehicle packaging program, it was believed that it would not be practical to divide the high temperature (600°-660°F) NaS battery into multiple and separate modules, each located at various points within the vehicle. The increase in thermal losses due to the large increase in exposed surface areas of multiple modules over that of a single battery package volume favored the latter approach to vehicle packaging of the NaS battery. The problem then became one of finding the largest available volume within the modified Fiesta for storage of a single battery package. Both front wheel drive with rear battery installation and rear wheel drive with front end battery installation layouts were prepared during the course of the NaS battery powered EV study. The configuration finally chosen as the preferred method of integrating the high temperature NaS battery with a 2-passenger Fiesta was the front wheel drive — rear mounted battery installation which has the NaS battery and its support structure mounted low in the vehicle just behind the front passenger seats and in front of the rear axle. Nearly all of the electrical drive and control components comprising the EV powertrain are packaged in the vehicle front end. Figure I-2 is an artist drawing illustrating the final EV configuration. Section III of the report discusses in more detail the NaS battery packaging study.

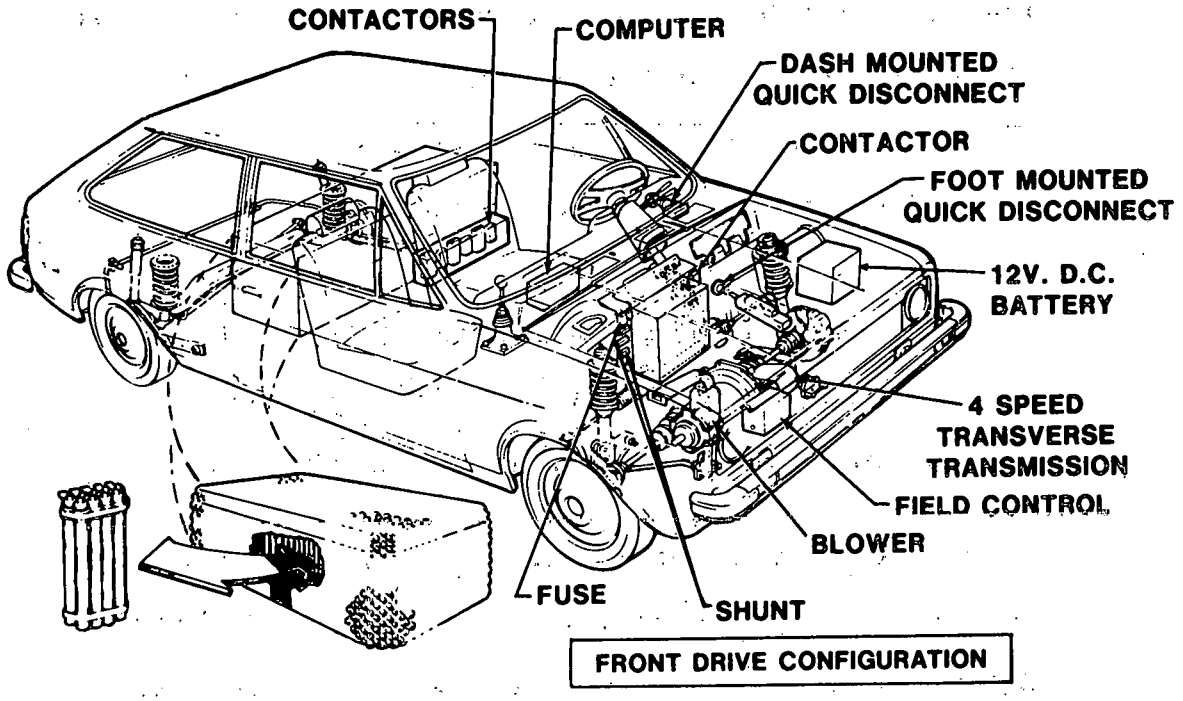

Figure I-2 Sodium Sulfur Battery Powered Fiesta Electric Vehicle

D. ELECTRICAL SYSTEMS

Based upon the contractual requirements that the Phase I Study Program focus its attention on production vehicles and non-developmental power-train components in the design study of a test bed vehicle, electrical drive motors and controllers which Ford has used in its past EV projects were evaluated. It was concluded that an earlier General Electric motor which Ford Research personnel had used in the EV conversion of a Ford Cortina four passenger vehicle several years ago, was the best choice for the NaS Fiesta EV study. It has high efficiencies over a wide speed range; furthermore, its power rating was found to be more than adequate for the wide open throttle (WOT) requirements for a Fiesta size vehicle. Its present weight of 150 lbs. could be reduced to approximately 100 lbs. with further development, thereby making this particular motor frame design suitable for use in long range EV developments.

Since the Cortina motor was extensively tested by Ford Research, along with its Ford designed controller, excellent motor input data was available

for use in the Ford developed EV performance and economy projection computer program. The test data were essential in carrying out the P & E analysis required to define the NaS battery size and performance criteria.

While the Cortina motor was examined with several controller schemes and a couple of battery voltage range splits, the final preferred motor-controller combination was chosen to be field/contactor control (parallel connection) matched to the 96/32 volt NaS battery package. Figure I-3 is a plot of regions of steady state operations for 32-v and 96-v battery terminal voltages with the motor using field/contactor control.

The Cortina motor-controller drive system was integrated with other ancillary electrical controls to form the NaS Fiesta electrical drive system shown schematically in Figure I-4. Section V of this report covers, in a more detailed discussion, the numerous electrical powertrain concepts

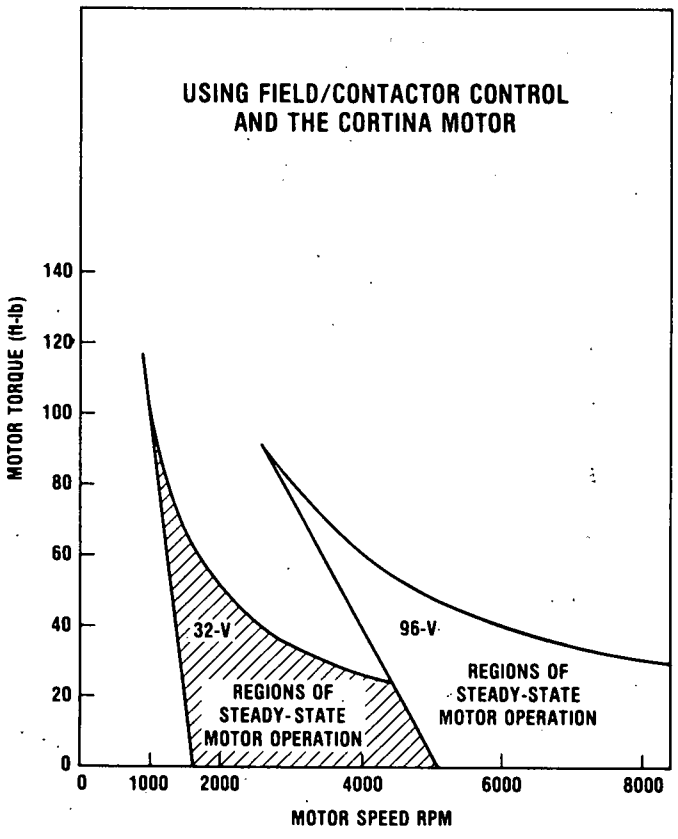

Figure I-3 Motor Torque vs. Motor Speed

evaluated and the reasoning for focusing upon the final electrical system design described above.

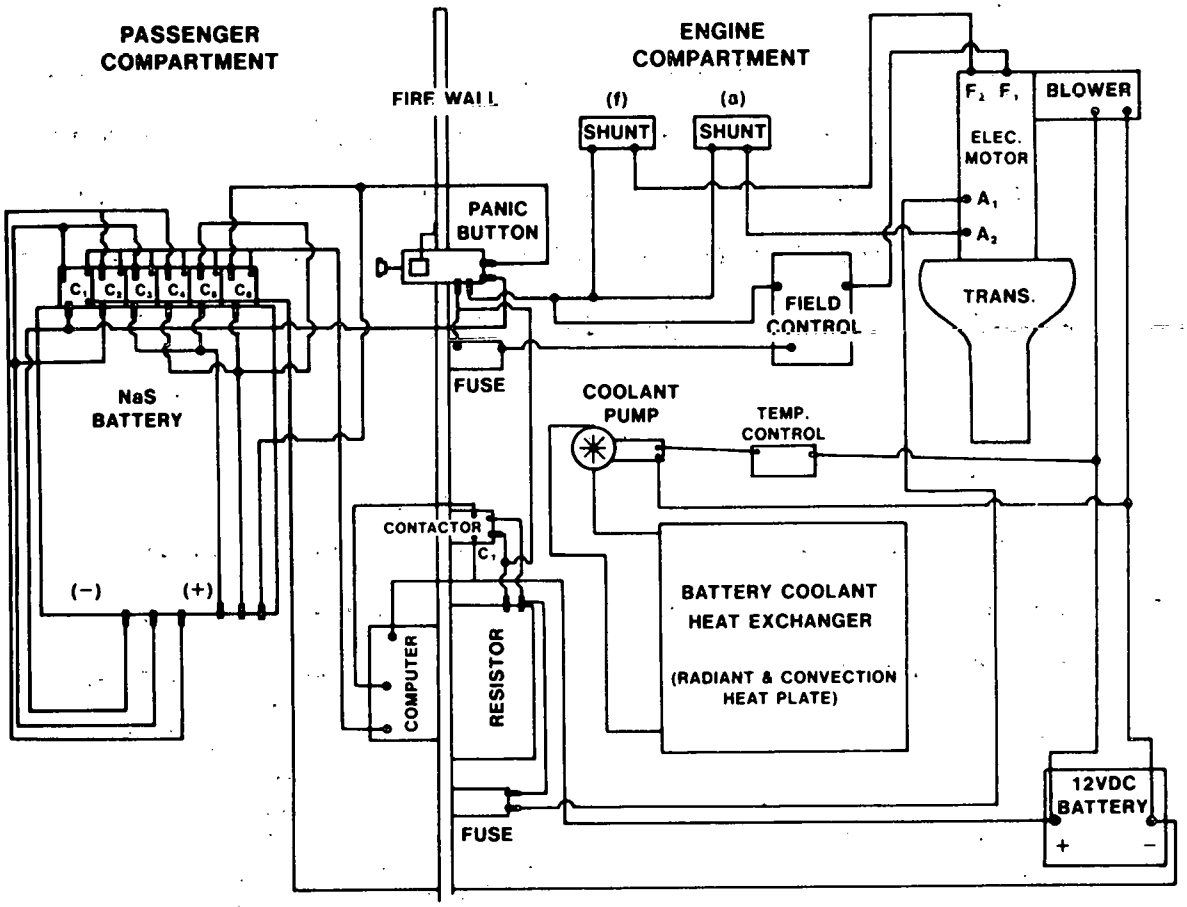

Figure I-4 Electric Vehicle Schematic

E. SYSTEM STUDIES

In support of the NaS battery work tasks, the vehicle packaging work tasks and the electrical system studies, there were additional study tasks that played key roles in guiding the overall direction of the NaS Vehicle Study Program. The major highlights of these studies are discussed below:

1. Performance and Economy Studies:

   Of the vehicle specifications listed in Table I-1, three items, numbers 5, 6 and 9, are directly related to performance and economy (P & E) goals for the NaS powered Fiesta EV. The goal of achieving 100 miles range over the CVS driving

cycle to the point of 80% battery discharge was selected to be of highest priority. Of secondary importance was the desired wide open throttle (WOT) acceleration performance of 0-50 MPH in 14 seconds (or less). The weight penalty for the NaS Fiesta EV of 500 lbs over an equivalent ICE powered vehicle was considered to be an important goal, because of its impact on vehicle ride and handling, vehicle costs, and vehicle crashworthiness. However, it was a goal which could be compromised with lesser impact upon future vehicle acceptance in the 1985-1995 markets than compromises in the range and performance goals.

The P & E analysis began with the definition of a base vehicle weight, viz., a Fiesta stripped of all ICE related components. To this base vehicle weight (1254 lbs for the Fiesta EV) was added payload weight (350 lbs), motor-controller weight (206 lbs), and variable weight allowances for the battery and its containment and support structure, to give a final vehicle test weight which is used as an input parameter in the Ford Research P & E computer program.

For each vehicle package and battery package layout developed during the NaS Fiesta EV study, P & E computer projections were calculated. For the final configurations of battery and vehicle layout, the P & E computer model description of the NaS Fiesta EV is as follows:

- Vehicle Test Weight 2470 lbs
- Vehicle Base Weight 1254 lbs
- Motor-Controller Weight 206 lbs

- Battery Weight (clustered cells and electrical leads) — 492 lbs
- Battery Support Structures and Component Weights — 168 lbs
- Vehicle Payload Weight — 350 lbs
- Vehicle Range (CVS) — 100 + miles
- Time for 0-50 MPH (WOT) — 10.5 secs
- Battery Power Rating — 34.5 kw
- Battery Energy Rating (C/20) — 29.4 kw-hr

Further detailed discussion of the P&E studies, covering various Fiesta EV and battery package configurations can be found in Section V of the report.

2. Powertrain and Vehicle Safety Studies

During the course of the NaS Fiesta EV study program, both front wheel drive vehicle packaging and rear wheel drive vehicle packaging were examined for vehicle crashworthiness and ride and handling characteristics. Since the contract terms clearly stated that the study should consider only a production vehicle and its use with minimum of modification to accept the NaS battery package, center line tunnel packaging of the NaS battery was ruled out because of extensive tear up of the vehicle (refer to Section V for further discussions of the reasons why a vehicle tunnel package is unacceptable for a NaS battery).

In discussions with Company Vehicle Safety personnel, it was concluded that a front end mounted NaS battery package offered

less safety for front end vehicle impact than a rear end battery installation inasmuch as the NaS battery package could not contribute to the vehicle front end crush. Instead, the NaS battery would have to be safeguarded by surrounding structure in order to prevent rupture of the NaS cells. When these considerations are added to the fact that there was marginally adequate storage volume under the hood and within the former engine compartment to install enough battery cells to achieve 100 miles range over the CVS cycle, the front end battery installations with rear wheel transaxle drive was dropped from consideration. Further detailed discussions of this topic are presented in Section V of this report.
from consideration. Further detailed discussions of this topic are presented in Section V of this report.

3. Thermal Studies

The thermal studies were limited in scope in the Phase I-A study due to the amount of time necessary for the development of conceptual battery designs and their subsequent trade-off studies. Once a NaS cell and battery configuration was selected, e.g. final NaS cell dimensions, number of clustered cells per module, number and spacing of modules for a given battery size, etc., the inner and outer battery containers could be designed, along with design approaches for bringing in and out the battery power leads, the coolant lines and, finally, the electrical leads for the resistance heaters and electrical instrumentation. With these critical heat leak passages defined, thermal studies could be initiated. For the battery configuration shown in Figure I-1 and discussed in construction detail in Section II, the continuous thermal loss from the battery was estimated to be approximately 150 watts which is the summation of thermal losses from the following sources:

- Thermal loss from the battery thru the container walls . . . . 63 watts
- Thermal losses thru battery support structure . . . . . 15 watts
- Thermal losses thru battery power leads (#2 wire) . . . . . 50 watts
- Coolant tubing wall conduction and instrumentation lead losses . 20 watts

For any follow-on NaS Vehicle Battery Study Program, thermal investigations covering both analysis and component mock-up for thermal experiments, should be included as an important activity.

F. CONCLUSIONS AND RECOMMENDATIONS

Phase I-A NaS battery powered electric vehicle study program produced encouraging results insofar as showing that a feasible NaS battery design can be developed for installation in an existing production vehicle, such as the Ford Fiesta. The study has shown that this NaS Battery powered Fiesta (modified to be a 2-passenger vehicle), can have adequate performance and range potential such that its use as a test bed could adequately evaluate the potential of the NaS battery as a power source for further electric vehicles.

Several other key findings and/or conclusions are listed below:

1. The battery sizing studies demonstrated that NaS tubular cells designed for load leveling are non-optimum for vehicle applications.

2. From the P&E studies, it was determined that whenever the battery was sized such that its power rating was sufficient to meet all peak power demands imposed by the CVS driving cycle, the Fiesta EV WOT acceleration goal of 0-50 MPH in 14 secs. was always met.

3. From the P&E studies, it appears that meeting the 500 lb weight penalty goal (See Table I-1 Section I) will be marginal unless one or more of the following technology advances occur:

   a. The power density of a "bare battery" viz., clustered cells without thermal protective containers, support structure, electrical connectors, etc., must be advanced to the range of 83-85 watts/lb.

   b. The motor-controller weight (206 lbs) must be reduced by 35-50 lbs.

   c. The base weight of the 2-passenger Fiesta EV must be reduced by about 50 lbs., perhaps through use of light weight materials (aluminum, plastics, composites) for hood panel, side and/or floor panels, aluminum wheels, etc.

4. Based upon the efficiency maps for the Cortina motor and its associated controller, P&E studies indicate that a manual transmission shifted at optimum speed points, e.g. 37 MPH (1st-2nd), 44 MPH (2nd-3rd), 54 MPH (3rd-4th), is more efficient than a direct motor drive system. Furthermore, increased range could be obtained by changing the production gear ratios of 3.58/2.06/1.30/1 to a higher setting of 4.50/2.50/1.75/1.00. This would require major re-work of the current pro-

duction transmission but such a change could be carried out in a future follow-on program.

5. To meet the FMVSS front and rear end barrier crash tests, the battery cells must be protected from impact ruptures to insure that the high temperature liquid reactants comprising the NaS cells do not enter the driver and passenger compartment or endanger personnel in the immediate vicinity of the crashed vehicle. This safety requirement virtually demands that (1) the battery container box structure must be capable of maintaining its structural integrity upon vehicle impact, (2) the cells should be packaged inside their storage container in such a cushioned manner that their likelihood of being impact ruptured is very small, and (3) the inner volume of the NaS cell container box should be completely evacuated or, as an alternative, evacuated and then filled with inert cover gases (such as argon, helium or dry nitrogen) in the event of cell seal failures or cell ruptures due to impact forces. By evacuating and/or use of inert gas around the NaS cells, oxidation reactions of sodium and sulfur can be avoided.

Several open issues remained at the conclusion of the Phase I-A study. These open issues could very effectively serve as the basis for follow-on work. The most critical open issues are briefly highlighted below and these areas are recommended for further contract support:

1. <u>Thermal Management Studies:</u>

   The one study area most in need of further exploration and analyses is in thermal analysis of the battery package, in-

cluding vehicle related areas such as support structures, coolant lines (or passages), power leads, etc. The very limited thermal analyses conducted to date only dealt with feasibility of various conceptual designs. There was not sufficient project time or money to conduct numerous trade-off studies regarding the heating and cooling of cell clusters, the thermal control of power lead, instrument lead and/or coolant line losses. Thermal studies of methods for rejecting the unwanted thermal energy developed by the battery, under special driving conditions, needs much more attention, since any chosen method must be capable of vehicle integration with minimum weight penalty.

Thermal growth and thermal stress studies of various sub-elements of the battery system, e.g. bottom support plates, bottom support posts for power leads, coolant inlet line support, etc., need more attention before hard-line layouts of the integrated battery-vehicle system are prepared.

2. Full Scale Engineering Mock-Up

Cylindrical NaS cells will continue to be the candidate configuration for vehicle application for the foreseeable future, and certainly up to and including the first demonstration NaS batteries for EV use. Cell dimensions developed from this early study are reasonably close to the cell dimensions obtained in a more complete optimization study for a spectrum of applications. Consequently if a full scale mock-up of the NaS battery configuration developed in this study (see Section II) were constructed from prototype materials set down by the battery design study, a "non-electrical" battery assembly could be built as an engineering "work horse" for laboratory study of the following open issues:

a. Cell modules and total battery thermal losses (covering heat leaks from the battery container, power leads, instrumentation leads, coolant lines, etc.)

b. Effect on cell and battery assembly integrity when the system is subjected to simulated road shocks, and variable frequency vehicle vibrations.

c. Assembly and disassembly techniques are open issues that can only be explored satisfactorily by using a full size model to work with. This full size model can also be used as a working design tool for testing design modifications or alternatives.

3. Battery and Vehicle Safety Issues

With an appropriately designed engineering simulation of a NaS battery especially designed as an EV battery, several fundamental safety issues related to the battery package itself, could be laboratory evaluated. For example, the problems of close temperature control of the battery via internal heating and cooling subsystems installed inside the battery container; (to insure safe operation) could be evaluated in a meaningful experimental way using an engineering simulation. Also, tests could be run wherein a certain number of cells are permitted to have seal failures of varying types and causes to determine the impact on the remainder of the battery cells and their containment structure.

An engineering simulation would be required to perform vehicle crash tests to evaluate the ability of both the vehicle structural design and the battery design to meet front and

rear impact requirements. Because of the design and assembly complexity of the battery and the large number of interfaces between the vehicle structure and the battery subsystem, math-modeling the vehicle impact tests would be impractical. Running "Cold Tests" of a simulated NaS battery would produce virtually meaningless results because the key electrochemicals in the cell solidify at low temperature and hence the response of the cells to shock and vibration would be entirely different than a "hot" battery wherein the bulk of the actual reactants, sodium and sulfur, are in a liquid state within each of their separately sealed volumes.

The above described work tasks, based on using full scale engineering simulation of a NaS battery designed for passenger vehicle application, can be performed in parallel with current NaS research and development work tasks which are primarily devoted to advancing electrochemical performance of specific cell designs, making improvements in construction materials and fabrication techniques to achieve long cell life and low cell fabrication costs, etc. Since the aforementioned engineering/vehicle application work tasks will take 2-3 years to complete, and the final tests of specially designed NaS cells for EV application will require almost the same amount of time, paralleling the two efforts would be a very cost effective plan. If the two programs are scheduled sequentially then the NaS battery program for commercial EV's will be an unnecessarily long development program.

In the Sections of the report to follow, a more detailed summary is given of the steps taken in each work task cited, the accomplishments as well as the open issues uncovered within each work task and a brief summation of the level of the state-of-the-art produced within each task area by the Ford-DOE program efforts.

II VEHICLE SPECIFICATIONS

At the outset of the Electric Vehicle Development and Demonstration Work Task effort, a tentative list of the "minimum" Electric Vehicle Market Requirements was developed. This list would serve as a guide to the final selection of clectric vehicle specifications that are, in turn, necessary design and performance guides for the follow-on vehicle development and demonstration work tasks. Mid-way in the first quarterly period a set of requirements were established, as listed below:
development and demonstration work tasks. Mid-way in the first quarterly period a set of requirements were established as listed
below:

1. Purpose — Shopper/commuter vehicle for multi-vehicle families.
2. Seating Capacity — Two passengers.
3. Cargo Capacity — Approximately 10 cubic feet (room for groceries and miscellaneous items).
4. Size — Approximate exterior dimensions, OAL: 125" — Width: 55".
5. Range — 100 Miles over Federal Test Procedure Cycle (CVS Cycle) with 20% charge remaining.
6. Performance — 0-50 MPH in 14 seconds with top speed of 65 MPH.
7. Recharge Time — Five hours maximum.
8. Battery Life — Five years/50,000 miles.
9. Safety Requirements — Meets all applicable FMVSS requirements.
10. Accessories — Heater and radio mandatory. (Note: Power steering may be required to meet Ford GPAS wherein maximum steering effort is limited to 35 lbs.)

11. Retail Price Premium — TBD but tentative goal of $800 cost penalty for EV will be used as first phase objective.

12. Cost of Ownership — TBD during follow-on Phase I-A Study Program.

13. Weight — 500 lb. weight penalty over the equivalent ICE powered vehicle.

Review of Company small car line specifications resulted in the conclusion that a Ford Fiesta size vehicle came the closest to meeting most of the above cited requirements; therefore, it was decided to use the Fiesta as the "image car" for the electric vehicle design, packaging and performance studies.

As a guide to all NaS EV study work, a tabulation of electric Fiesta vehicle assumptions was prepared. TABLE II-1 is a copy of the Vehicle Assumption List, which was reviewed monthly and updated as required. All major systems were identified by a coding system, e.g., Complete Vehicle System (0.00), Body System (1.00), Frame and Mounting (2.00), Engine/Motor (3.00), etc. The most recent results of the battery-vehicle packaging studies, NaS cell and battery trade-off studies and vehicle performance (P & E), were used to update the Vehicle Assumptions (viz. specifications) List.

TABLE II-1 ELECTRIC FIESTA VEHICLE ASSUMPTIONS

Edition No. 3 Date: December 15, 1978

System Or Subsystem Number	Primary System/Subsystem Assumptions
0.00	COMPLETE VEHICLE SYSTEM
0.10	Reference Vehicle

Fiesta 90 Inch Wheelbase

- 1.1 L OHC engine transverse mounted.
- 4-Speed manual transaxle.
- Manual rack and pinion steering.
- Curb weight 1620 lbs. (Advertised figure).
- Seating capacity — two persons.
- Fuel tank capacity for 125 mile range (CVS Cycle).

0.20 Electric Fiesta

Same as Reference Vehicle, except:

- 40 HP DC General Electric series wound motor.
- Modified 4-speed manual transaxle.
- Manual rack and pinion modified for new electric powertrain system.
- Sodium sulfur battery sufficient to yield following performance:
  - Range: 100 miles CVS at 80% depth of discharge.
  - Top Speed: 65 MPH.
  - Performance: 0-50 acceleration 14 seconds.
  - Life: 5 years and/or 50,000 miles.
  - Recharge time: 5 hours
- Two-passenger seating capacity; rear seating modified for packaging NaS battery and other powertrain components.
- Curb weight approximately 500 lbs. over Reference Vehicle.
- Safety conformance to all applicable FMVSS standards plus other unique EV safety requirements concerning battery crash worthiness and unique electric hazards.

TABLE II-1 — ELECTRIC FIESTA VEHICLE ASSUMPTIONS (Cont'd)

Edition No. 3 Date: December 15, 1978

System Or Subsystem Number	Primary System/Subsystem Assumptions
1.00	BODY SYSTEM
	Body Structure
	. Floor plan modified for sodium sulfur battery mounting and upgaged as required for additional loading.
	. New battery tray assembly with tie-down straps and crash protection structure.
	. New structure support for controller, contactors and other required electrical components.
	. Modify rear floor for removal of spare tire to maximize battery packaging volume (if required).
	. Remove radiator support and provide body structure for forced air cooling of controller, motor and contactors.
	. Modify rear structure and suspension for additional battery weight and mounting.
1.09	Rear View Mirrors
	Same as Base Vehicle
1.10	Seat, Seat Trim and Track
	Rear seat trim and track structure plus rear seat area side panel will be deleted to provide room for new battery packaging.
1.12	Instrument Panel
	Modified instrument panel for electric instrumentation such as voltmeter, battery temperature gages, battery state-of-charge unit, ammeters, etc.
2.00	FRAME AND MOUNTING
	New support mounts will be required for electric motor and modified transmission.
3.00	ENGINE (MOTOR)
	40 HP DC Series Wound G.E. Motor; (same as used in Cortina EV) — 100 volts. Control for motor is defined Section 15.00.

TABLE II-1 — ELECTRIC FIESTA VEHICLE ASSUMPTIONS (Cont'd)

Edition No. 3 Date: December 15, 1978

System Or Subsystem Number	Primary System/Subsystem Assumptions
3.02	Motor Lubrication
	TBD.
3.03	Motor Cooling
	Air Cooled — forced convection.
3.04	Battery Charging
	Off-board battery charger with 110/220-volt charging capability. Battery to sense 110/220-volt input and adjust charge rate automatically.
4.00	SUSPENSION SYSTEM
	Same as Reference Fiesta. Effect of transmission and Cortina motor on suspension to be evaluated by tests along with added front rear suspension loads due to battery and support structure weight.
5.00	DRIVELINE
5.02	Dead beam rear axle may be upgaged due to battery system weight located in rear passenger area.
6.00	BRAKES
	Same as manual Fiesta brakes except modified for regenerative braking. Power assist will be examined by drive tests to determine if required. Note: Regenerative braking will be employed down to a vehicle speed approaching 3-5 MPH at which point regeneration cut-out will occur.
7.00	TRANSMISSION
	Existing Fiesta 4-speed manual transaxle modified to have gear ratios of 3.58/2.06/1.30/1.0. An additional gear set may be installed between the electric motor and the existing Fiesta transmission if it is determined that such an addition will optimize speed range for the electric powertrain.
8.00	CLUTCH SYSTEM
	Same as Reference Fiesta unless drive tests show that a new clutch is required for driveability.

TABLE II-1 — ELECTRIC FIESTA VEHICLE ASSUMPTIONS (Cont'd)

Edition No. 3 Date: December 15, 1978

System Or Subsystem Number	Primary System/Subsystem Assumptions
9.00	EXHAUST SYSTEM
	Deleted.
10.00	FUEL SYSTEM
	Deleted.
11.00	STEERING SYSTEM
	Same as Reference Fiesta except it may be modified if drive tests show that the vehicle exceed 35 lb. GPAS steering effort, then power assist will be required.
12.00	CLIMATE CONTROL SYSTEM
	New liquid fuel space heater and fan capable of running off a 12-volt auxiliary battery under all motor modes. Forced air ventilation same as Fiesta except modified for new instrument panel, as required. Air Conditioning will not be considered.
13.00	GAGE AND WARNING DEVICE SYSTEM
	Instrument Cluster
	Same as Fiesta except with the addition of:
	. Ammeter.
	. Voltmeter.
	. State-of-charge meter.
	. Temperature gage (battery).
	. Safety meter (indicates vehicle is grounded for shock hazard).
14.00	ELECTRICAL POWER SUPPLY SYSTEM
14.01	Battery
14.02	Auxiliary Battery
	1-12 volt advanced SLI battery (NiZn if available) for lights, horn, windshield wipers, radio, emergency lights, turn signals, auxiliary lights and cooling and heating fans.

TABLE II-1 — ELECTRIC FIESTA VEHICLE ASSUMPTIONS (Cont'd)

Edition No. 3 Date: December 15, 1978

System Or Subsystem Number	Primary System/Subsystem Assumptions

14.03 Main Battery

- Type: Sodium Sulfur
- Battery Physical Characteristics (Preliminary)

Height	Width	Length	Weight
20"	20"	38.5"	865 lbs

Weight of Total/Cell	No. of Cells	No. of Modules	No. of Cells/Module
492 lbs	432	48	9

- Battery Ratings:

Power	Energy	Discharge Time
40.6 Kw	35.2 Kw-hr	5 hr (80% Utilization)

- Individual Cell Physical Dimensions:

Length	O.D.
40.2 cm (15.8 in.)	2.5 cm (1.0 in.)

- Individual Cell Ratings:

Power Density (Mass)	Energy Density (Mass)
.18 Watts/gram	.15 Watt-hrs/gram

15.00 ELECTRICAL CIRCUITRY SYSTEM

- Motor Controller (New design).
- Battery temperature sensors/controllers (New design).
- Contactors (New Design).
- Fail safe quick disconnect to off-board charger described below:

Off-board battery charger:
110/220-volt service capability. Charger automatically adjusts for variable state-of-charge of the battery and provides for vehicle safety during charging mode.

III NaS BATTERY PACKAGING

In this Section of the report, the analytical and design activities necessary to select a cylindrical cell configuration which can be used as a basis for designing a total battery package, will be discussed. Also covered in this Section, are the key battery performance, safety and vehicle integration considerations which served to guide the direction of the battery conceptual design effort.

A. NaS CELL AND BATTERY TRADE-OFF STUDIES

At the beginning of the Phase I NaS Electric Vehicle Study Program, the vast majority of NaS cell technical design and performance information available was applicable mainly to load leveling batteries. Little design data was available on NaS cell configuration optimized for EV use. Consequently, to provide a cell design data base which could provide support to the vehicle specification work task the NaS battery package design studies and the P&E computer projections, an analytical investigation of cell optimization methodologies was carried out. The objective of this early study effort was to develop parametric displays of key cell design/performance parameters which would serve as guides to selecting the cell configuration that would give either minimum battery weight, or battery volume, or both.

A previously developed computer program which was especially created for NaS cell sizing was chosen for use in conducting preliminary NaS cell parametric studies. This cell sizing computer program (Ford File Name: NaS) calculates cell size (OD, length), cell weight, cell power and energy capacity for variable inputs such as electrolyte dimensions (OD and ID), electrolyte resistance, hours to 100% discharge, and others. The primary cell characteristics investigated via parametric plots were cell electrolyte length to

diameter ratios (L/D), cell discharge times (hrs.) cell power densities (Watt/gram), cell electrolyte diameters (OD) and battery weight (kilograms) at various power levels. Figure III-2 through III-4 are Figure III-2 through III-4 are sample plots for two values of cell electrolyte length to diameter ratios, e.g., 20:1 and 14:1.

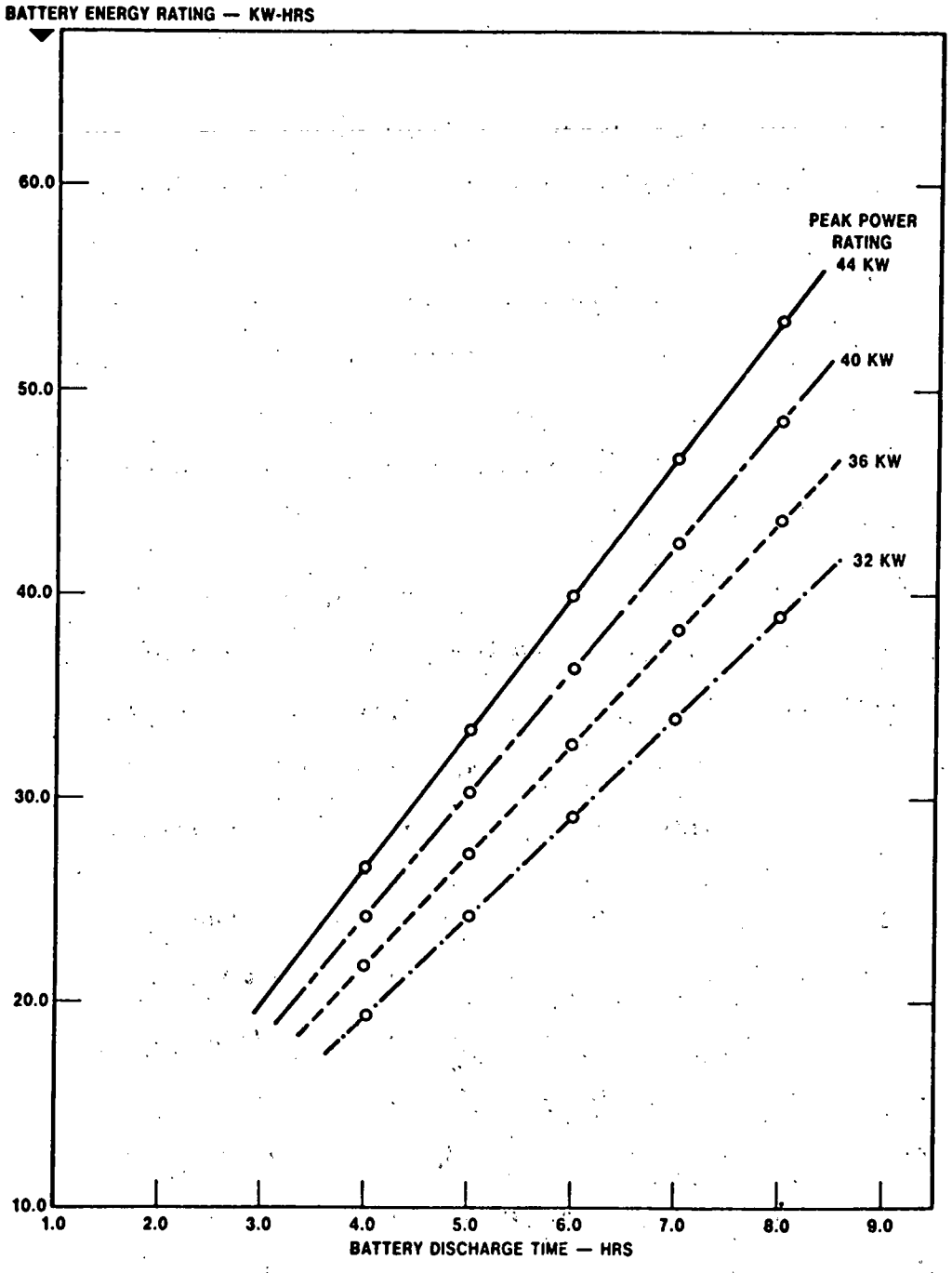

Figure III-1 Battery Rating (Kw-Hrs.) vs. Battery Discharge Time (Hrs.)

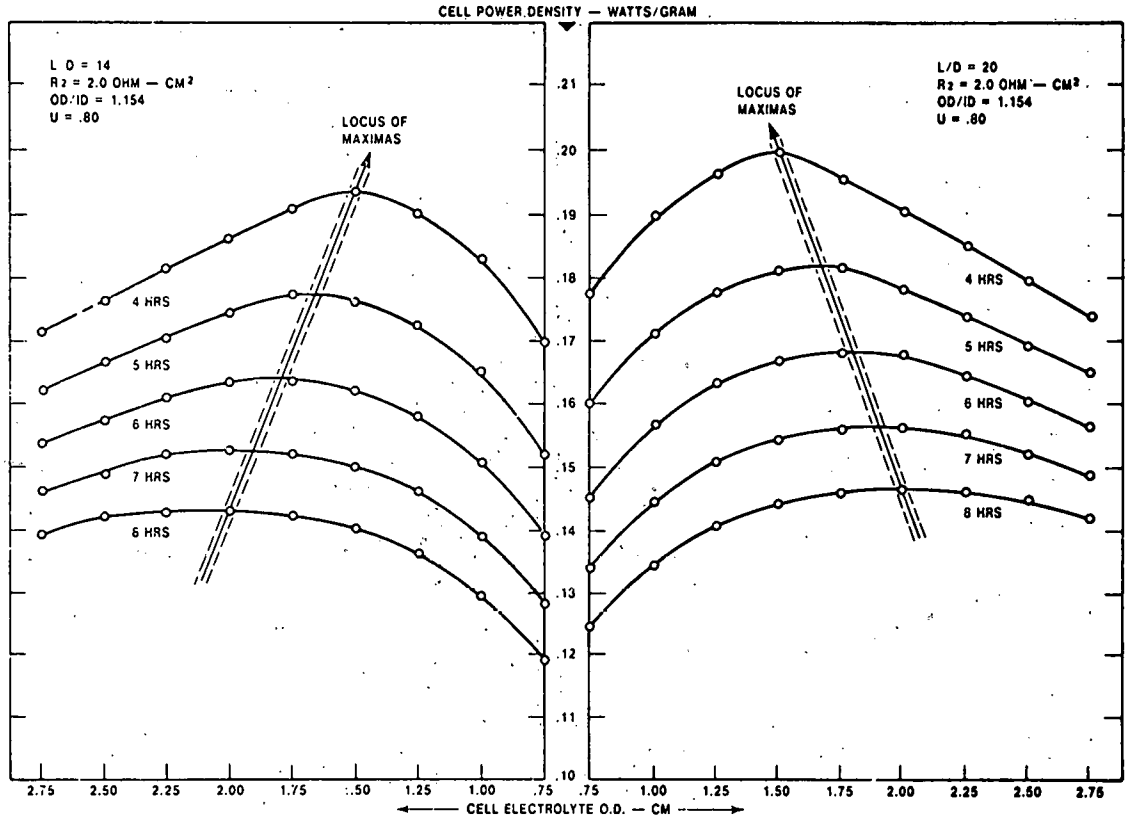

Figure III-2 Cell Power Density vs. Cell Electrolyte Outer Diameter (O.D.)

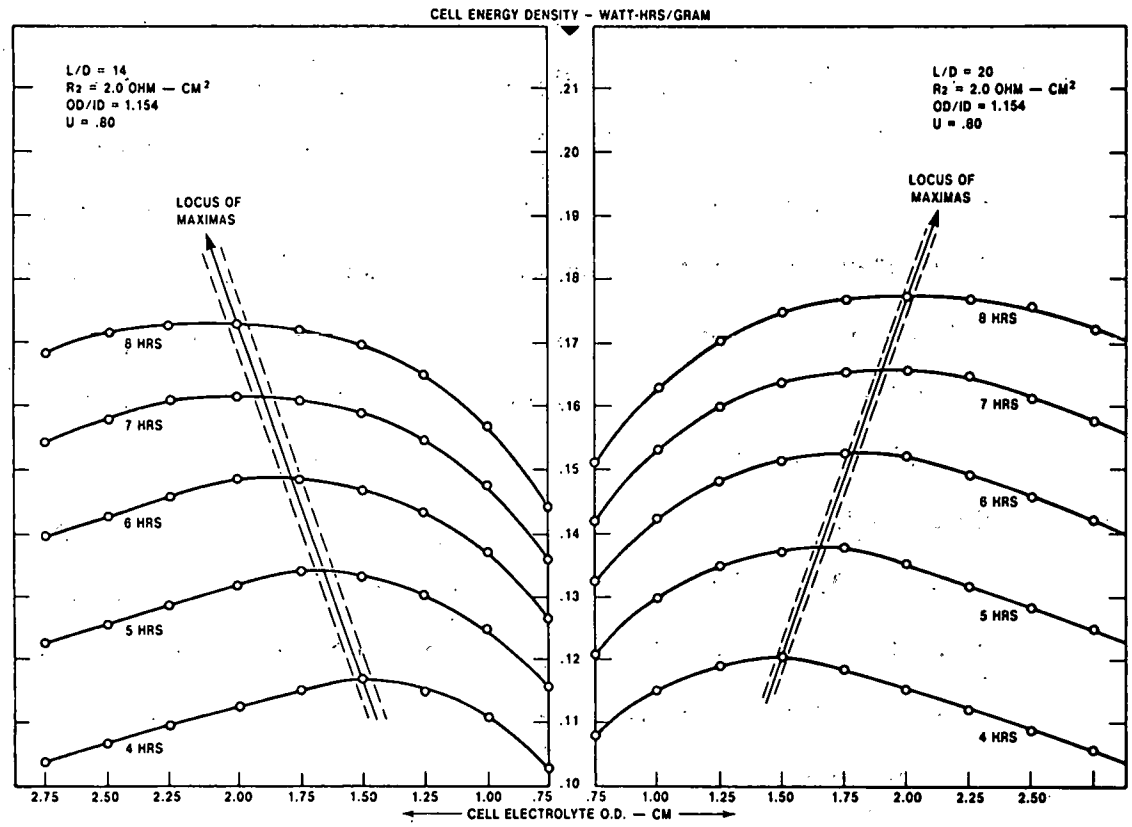

Figure III-3 Cell Energy Density vs. Cell Electrolyte Outer Diameter (O.D.)

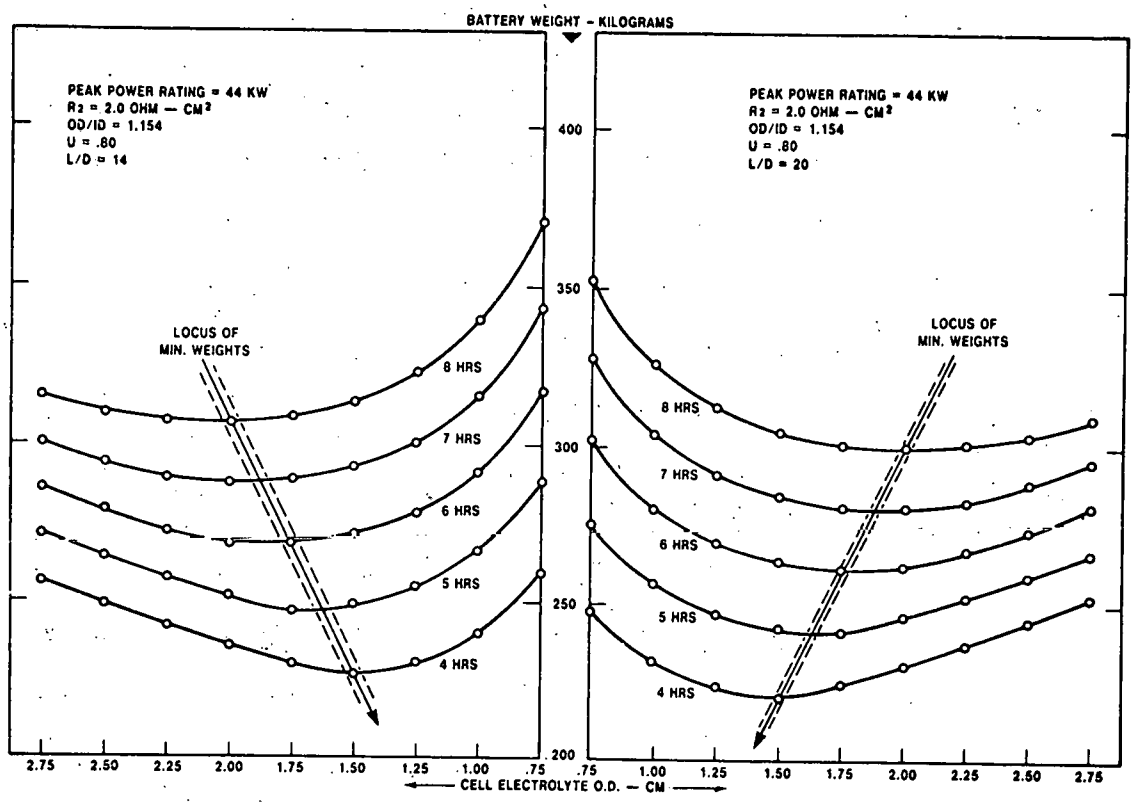

Figure III-4 Battery Weight vs. Cell Electrolyte Outer Diameter (O.D.)

Figure III-1 illustrates the variation in energy rating (Kw-hrs.) with variations in discharge time (hrs.) and peak battery power level (Kw). Figures III-2 and III-3 are graphs of NaS cell power density and energy density versus cell electrolyte OD for constant values of cell L/D. Shown in each figure is the locus of maximum values for each plot of power density and energy density as a function of constant discharge time (hrs.) versus variable cell electrolyte OD. In Figure III-2, it can be seen that the maximum power densities are achieved along the locus line when cell electrolyte OD and cell discharge times are made small. The reverse trend holds for the locus of maximum energy densities, as shown in Figure III-3. The highest value of energy density (Watt-hours/gram) occurs at the largest discharge time and for a fairly large electrolyte OD.

Figure III-4 is a parametric plot of battery weights as a function of effective discharge time for a given power rating (Kw), for two values of cell L/D. As Figures III-4 shows, the locus line of minimum battery weights for given values of battery discharge times follows the same general trend noted earlier for the plot of power density versus electrolyte OD in Figure III-2, viz., the locus of minimum battery weights moves in the direction of smaller discharge times and smaller cell electrolyte diameters. It is important to note, however, that the number of cells associated with the peak values of either power density of energy density (see Figure III-5), have a direct bearing on battery costs, and required battery storage volume. For some applications these may force a compromise in choice of cell dimensions. An example of this can be illustrated using Figures III-2 through III-5. For an arbitrary discharge time of say 6 hours, and an L/D ratio of 20/1, it can be seen from

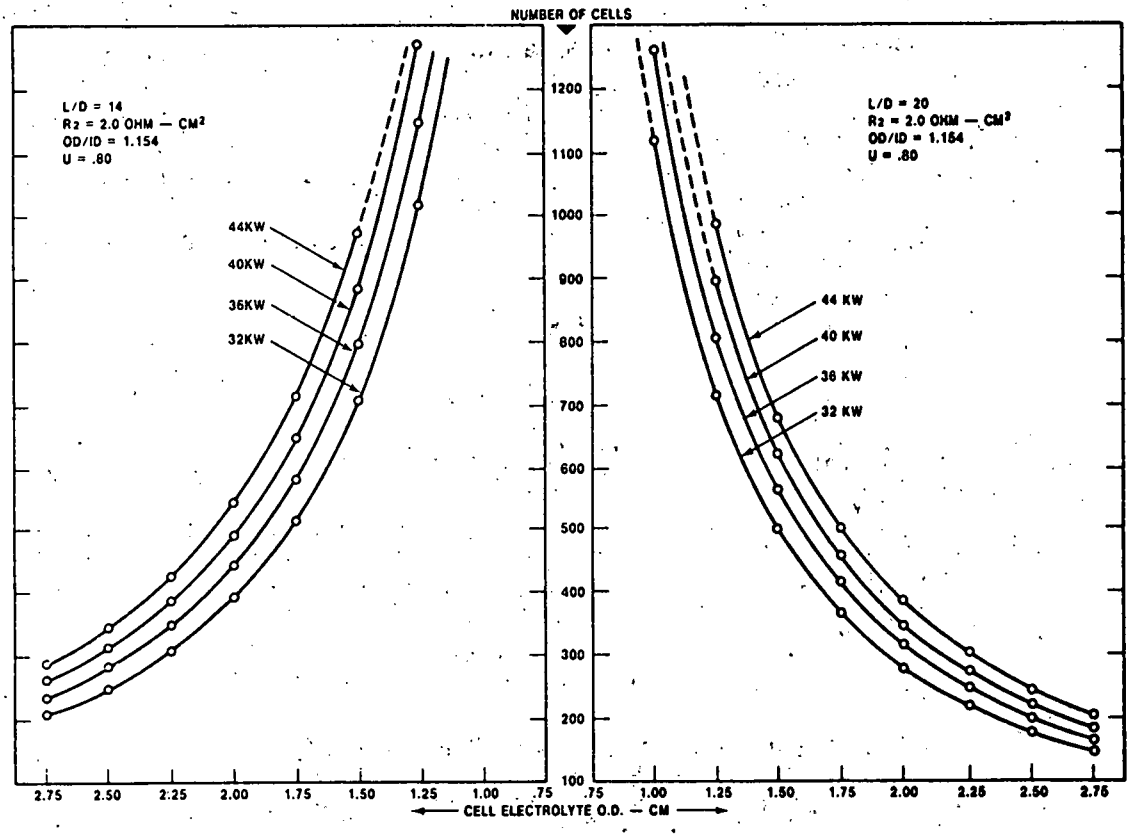

Figure III-5 Number of Cells vs. Cell Electrolyte Outer Diameter (O.D.)

Figures III-2 through III-4 that maximum power density, and minimum battery weight are achieved for a cell having an electrolyte O. D. close 1.75 cm. However, the change in these values for a cell having an electrolyte O. D. of 2.0 cm. is relatively small compared to the change in number of cells required to produce a given power level, as illustrated in Figure III-5. If, for example, a power level of 44 kw is selected, it can be seen that approximately 500 cells having an electrolyte O. D. of 1.75 cm would be required as opposed to approximately 390 cells if the electrolyte O. D. were increased to 2.0 cm. These types of parametric curves and nomographs were used to select the cell reference design which provided the basis for the battery packaging studies.

To arrive at a NaS cell reference design for EV use, P & E calculations were run for a Fiesta EV having a computed test weight of 2470 lbs. From these computer projections it was determined that, while driving the CVS cycle, the battery had to be sized such that it could deliver slightly over 32 kw of power, up to and including a state of discharge of 80%. For a range of 100 miles over the CVS cycle, the battery would have to deliver a net energy output of about 24 kw-hrs., (regeneration was accounted for in the P & E calculations) again to the same 80% state of discharge level.

It was decided that with the remaining 20% of energy available in the battery, the vehicle should be able to be driven at a constant speed of 40 MPH for a distance of 25 miles, which was assumed to be an adequate range to reach a charging station. From the P & E computer projections, this requirement would add another 5 kw-hr. energy demand on the battery, making for a total energy rating requirement of at least 29 kw-hrs.

For the P & E calculations, the battery was assumed to have cells capable of developing an open circuit voltage of 2.07 volts (at f = 0, i.e. freshly

charged condition). This voltage was assumed to be essentially constant until the state of discharge had reached almost 43%, at which point it was assumed that the battery voltage would drop linearly to a value of 1.77 volts at 100% depth of cell discharge. From these assumptions, a fresh, fully charged battery power rating of approximately 39 kw can be calculated. For the cell sizing studies, a more conservative battery rating of 40 kw was used.

Since the average driving time for 100 miles of CVS cycle driving is close to 5 hours (based on an average vehicle-speed of 19.6 MPH), and the added driving time to go 25 miles at a steady speed of 40 miles per hour computes to be 0.6 hours, a 100% discharge time of 5.7 hours was used as an estimate input to the Ford cell sizing program which assumes a constant current load.

Ford defined 20/1 to be a practical upper limit because of mechanical strength considerations for the L/D of the β " — alumina electrolyte. Figures III-2 through III-4 shown that high values of L/D give higher cell peak power and energy densities and lower over all battery weights. The following cell parameters were used to conduct parametric cell calculations to determine cell configuration for further battery conceptual design work:

Cell L/D ratio	20/1
Electrolyte OD/ID ratio	1.15
Cell resistance (R_2)	2.0 ohm-cm^2
Utilization factor (U-factor)	0.80
Hours to full discharge (H-hours)	5.7
Sulfur fill factor (Fo-dimensionless)	1.1
Sodium fill factor (F_2-dimensionless)	1.1
Power (peak-cycle)/power (max) ratio (F_1)	1.0

Power (avg)/power (peak-cycle) (P_9)	0.15
Container density (R_1-gm/cc)	7.85
Alpha-alumina thickness (L_1-cm)	1.0
Sodium container wall dimen. (X_1-cm)	0.07
Sulfur container wall dimen. (X_2-cm)	0.07
Cell open circuit voltage (@f = 0, volts)	2.07

Using the above parameter list as computer input, calculations of total cell weights for a given power level (40 kw) and various values of electrolyte O. D. were made. From a plot of battery (clustered tubular cells) weight vs cell electrolyte O. D., it was determined that minimum battery weight was achieved at an electrolyte O. D. equal to 1.75 cm. Listed below are the key dimensions and projected performance for the selected cell configuration:

Cell electrolyte outer diam. (cm)	1.75
Cell electrolyte length (cm)	35.0
Cell overall diameter (cm)	2.5
Cell overall length (cm)	40.1
Cell weight (gms)	517.7
Power density (watts/gm)	0.18
Energy density (watt-hrs/gm)	0.15

A more detailed cell design-optimization study is ongoing under the principal DOE contract. The preliminary study discussed above was performed as an expedient to allow other battery design activities proceed.

In the discussion to follow, the engineering activities related to battery conceptual design and vehicle packaging studies will be reviewed.

B. NaS BATTERY CONFIGURATION STUDIES

The initial battery conceptual design effort commenced with the clustering

of cells having an electrolyte L/D ratio in the neighborhood of 14 and a outer cell diameter approximately equal to 3.55 cm. The cells were arranged in columns with each column containing 8-cells to form a sub-module. There was a total of 48 submodules in a battery. The battery was subdivided into 4-modules, with each module containing 12 submodules (or 96 cells). All cells in a submodule were electrically parallel and all 12 submodules in a module were series connected. It was intended that, through external switching, a 48 volt rating or a 96 (nominal) volt battery rating could be achieved by proper paralleling or series connecting the battery modules.

From the basic cell arrangements just described, five conceptual battery package arrangements were generated for study. All of the arrangements had the general design features listed below:

(a) Internal heating of the modules is provided on demand (for initial battery warm-up and for constant temperature control) by electrical resistance heaters;

(b) Multi-foil super-insulation is installed between concentric battery container boxes whose internal gap volume is evacuated to minimize conduction heat loss;

(c) An outer container, filled with compounds suitable to combat Na leakages due to cell rupture, is provided. The materials could be non-iodized salt or sand; and

(d) The modules are cooled by forced air flow on a demand basis.

The battery packaging concepts differed from one another mainly in design details concerning:

(a) Method of introducing air cooling (single concentric opening for inlet and outlet air flow versus separate openings for flow control of air-in and air-out);

(b) Approach to supporting the battery container in the vehicle via side mounting rails and support brackets;

(c) Location of materials suitable for controlling sodium/sulfur leakages within the battery-insulated container; and

(d) Methods of directing cooling air around the cell clusters to achieve nearly uniform cooling within each sub-module.

Four air-cooling battery packaging schematics were developed but none were deemed fully acceptable because of resultant large sizes and weights. For example, the weight of a battery container consisting of 384 NaS tubular cells (14.6 inches long by 1.4 inches in diameter), with provision for forced convection air cooling of all cells and internal store of materials to combat NaS spills, was estimated to weigh close to 1000 lbs. Because of the large size of the flow ducts and plenums required to direct the air into the battery, around the cells and out of the battery, the package volumes were more bulky than desired. It was concluded that a considerable amount of design work would be required to reduce the size and weight of the air-cooled battery package.

Figure III-6 shows a battery design which also used the 1.4 in. dia. x 14.6 in. long NaS cells closely packaged in a double-walled container mounted low between two side frame rails that are an integral part of the body structure of the Fiesta. To achieve this compact configuration, no provision for internal cooling of the cells has been made, nor is there a provision for storage of internal materials (sand or non-iodized salt)

for suppressing fires caused by sodium and/or sulfur leakages. This configuration comes close but does not quite fit in the space available behind the front seats since the dimensions for the maximum usable volume behind the front seats are 48 inches (1) x 26 inches (w) x 24 inches (h). As can be seen in Figure III-6, which is a sketch of a NaS Battery Concept, the battery dimensions are approximately 41 inches (L) x 28 inches (w) x 21 inches (h). The width of 28 inches causes an interference with the rear axle travel. The estimated weight range of the NaS Battery package concept illustrated in Figure III-6 is 800-850 lbs., which is still heavier than the goal of 650-700 lbs. estimated for the reference NaS Fiesta EV (see Section IV for further details).

1. Conceptual Battery Cooling Designs

Of major concern was the design of an internal cooling system for the NaS battery. Figure III-7, is a sketch of four (4) possible cooling options considered for battery packages constructed from cylindrical cells. Each of the four cooling options has resistance heating elements to maintain constant temperature control and provide initial battery warm-up.

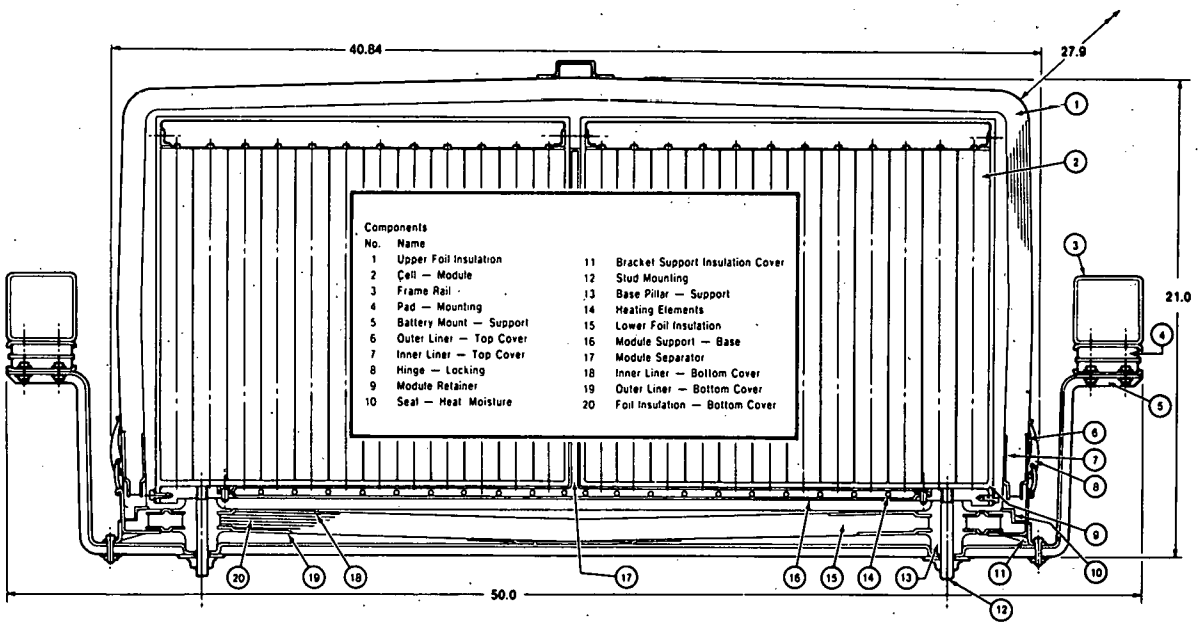

Figure III-6 NaS Battery Concept

Figure III-6 is representative of option 1. Since some form of battery cooling most likely will be required this approach is merely academic and no further interest was invested.

Option 2, either open or closed air cooling system, is the most common method used to provide a cooling mechanism for batteries. For electric vehicle application where weight, size, and exhaust temperature are key design issues, a simple air cooling concept as shown in Figure III-7 does not appear to be suitable or practical. In order to make option 2 provide the necessary cooling, rather large and bulky inlet/exit duct work, plenums, and/or high mass flow blowers would be required.

Option 3, closed liquid cooling system, offers the potential of providing an efficient battery package size, but several major problems exist. These problems are determining a suitable liquid coolant capable of func-

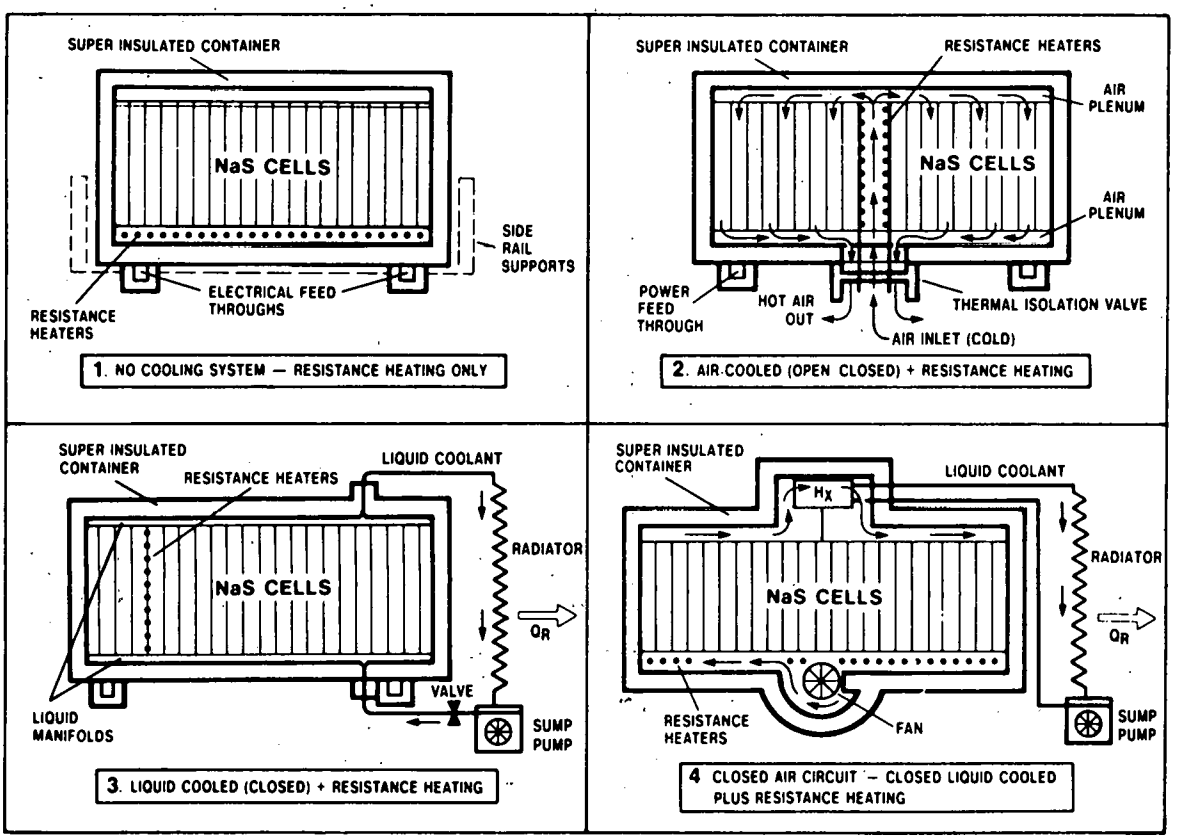

Figure III-7 NaS Battery Heating & Cooling Concepts

tioning in a NaS battery environment and determining a suitable mechanism to physically transfer the heat from the NaS cell to the liquid coolant.

Option 4, combination closed air and liquid cooling system, provides for the advantages of cooling the cells with air while eliminating the need for bulky inlet/exit plenums and ducting by relying on a secondary closed liquid system to remove the heat from the battery compartment to ambient.

Options 3 and 4 appeared to be the most feasible cooling candidates from the viewpoint of package size and weight goals. Therefore, further study was done to develop conceptual battery designs incorporating these battery cooling options.

2. Liquid Cooled Battery Design — Option 3

The closed liquid cooled battery design concept was built around the following design criteria:

(a) Reduce the NaS cell size by choosing the diameter of the β'' — alumina to be smaller than the 1.40 inches (2.56 cm) electrolyte diameter chosen for the cells used in the previously described battery package designs. Based on the cell optimization studies discussed earlier, and illustrated by Figures III-2 through III-4, an electrolyte diameter of .68 inches (1.75 cm) was chosen which resulted in a cell size of 1.01 inches (2.58 cm) in diameter and 15.8 inches (40 cm) in length;

(b) The smaller cells are clustered to form a triangular-centered array instead of the previously used column array design to achieve a slightly more compact volume for clustered cells, (see Figure III-8)

(c) Submodular cell arrangements will be formed by clustering 9 cells together and connecting them electrically in parallel, as shown in Figure III-8. These submodules will be, in turn, connected electrically in series to form three separate modules which could be connected

interchangeably to form either series and/or series-parallel arrangements to provide different battery voltage levels; and

(d) Thermal management and battery safety in case of sodium and/or sulfur leakage will be handled by either evacuation or inert gas (Helium is preferred) filling the inner battery container which contains the closely packed cell modules, the electrical resistance heaters (strip and/or rod type), the heat sink plates cooled by a high temperature heat transfer medium (Therminol-66, Dowtherm-A, Monoisopropylbiphenyl (MIPB) are candidates), and a thermal conducting filler

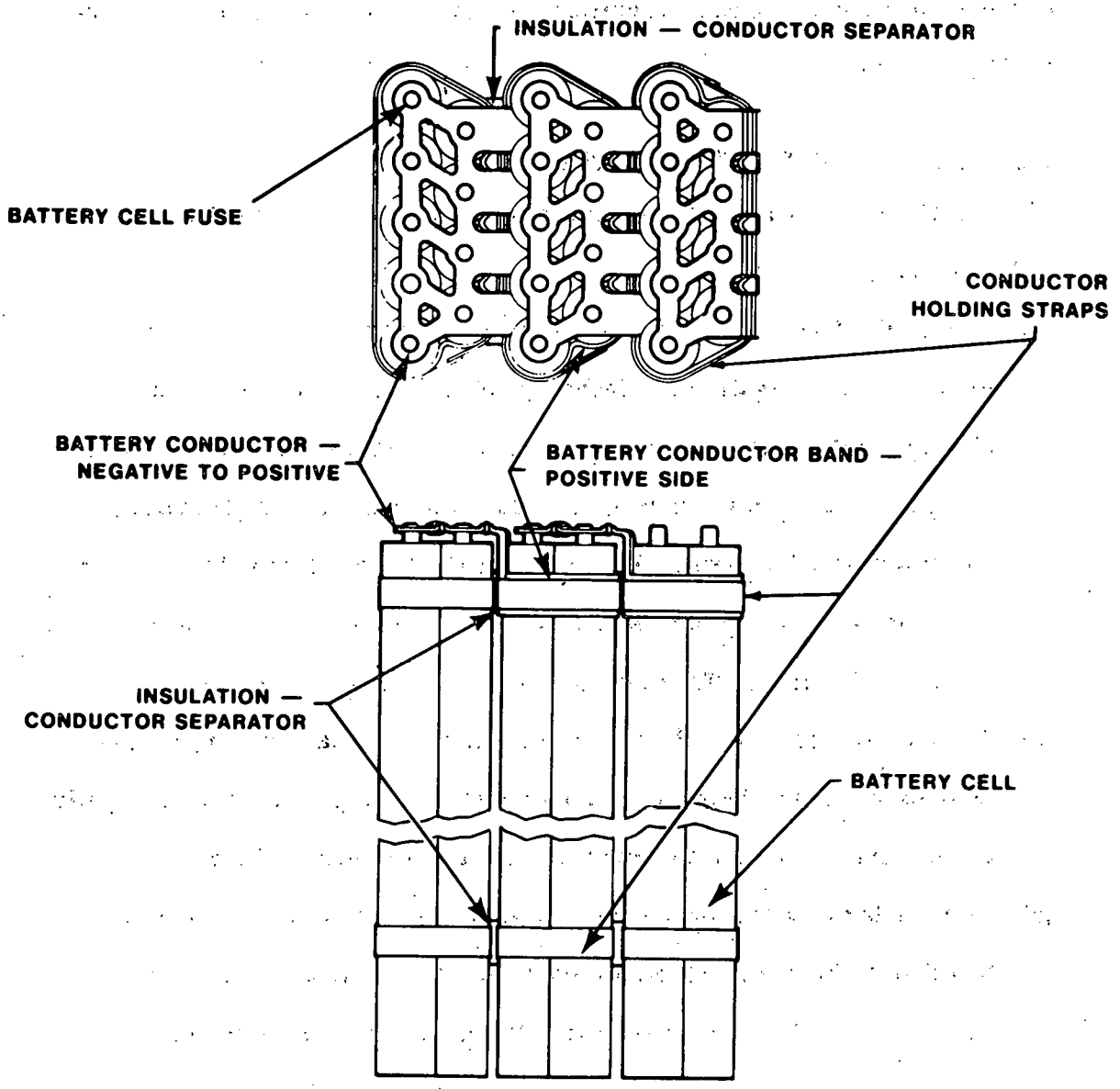

Figure III-8 Cell Module & Electrical Connection Configuration

material of low density to both support the cell modules, provide vibration damping, and aid in heat conduction from single cells and submodules, (see Figure III-9).

By the end of the third quarter, a conceptual design layout was completed. This conceptual design, shown in Figures III-10, contains the following design features:

(a) The battery is assembled as three modules, each of which is made up of sixteen submodules electrically connected in series. Each submodule contains a cluster of nine cells banded together in a triangular-centered array and electrically parallel connected. Three module design was selected rather than four for ease of packaging within the Fiesta.

(b) The battery is heated by thin-foil resistance heater sheets which are bonded to a portion of the surfaces of the heat sink plates. These commercially available heaters can be special ordered for 1000°F (536°C) service.

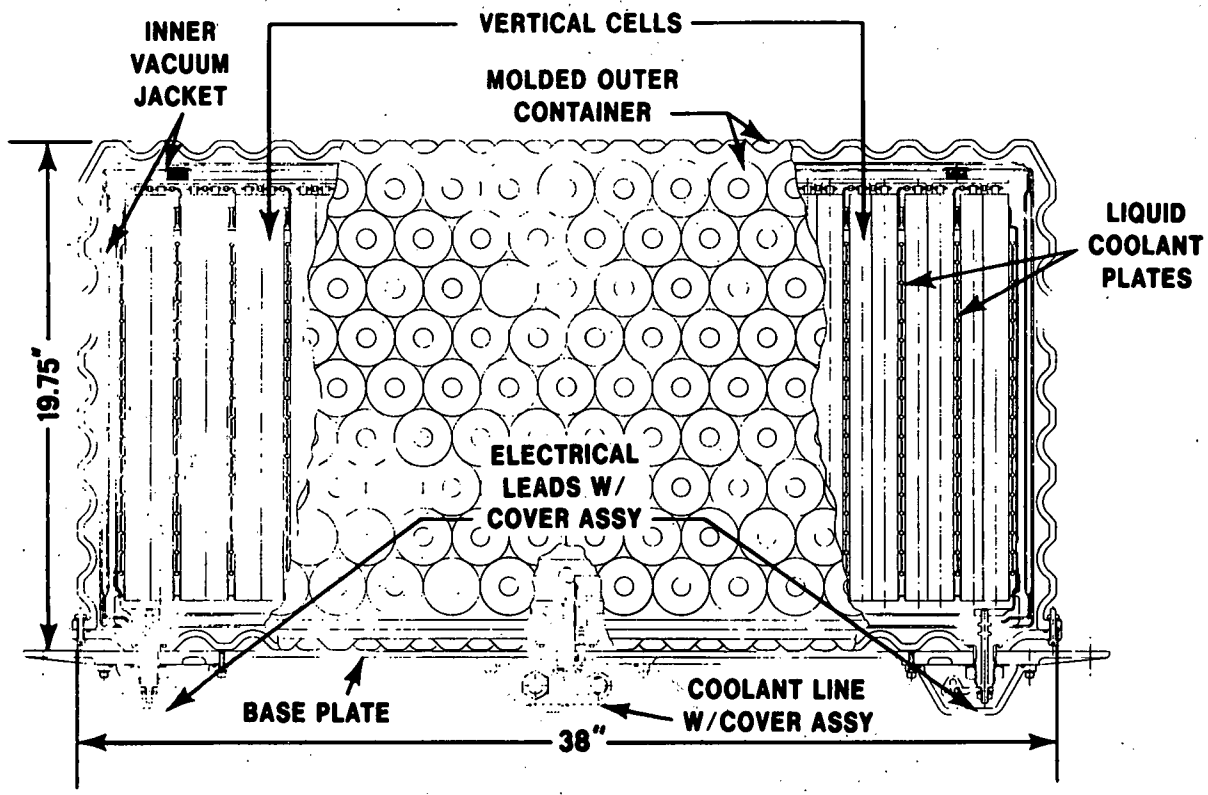

Figure III-9 Front View of Liquid Cooled Sodium Sulfur Battery

(c) Battery temperature excursions (due to high loads caused by steep grades, head winds, or extended WOT runs) are accommodated by having internal liquid cooling flow through heat sink plates which incorporate cooling flow passes created by the "Roll-Bond" (TM) fabrication technique. The pumped cooling flow is provided "on demand"

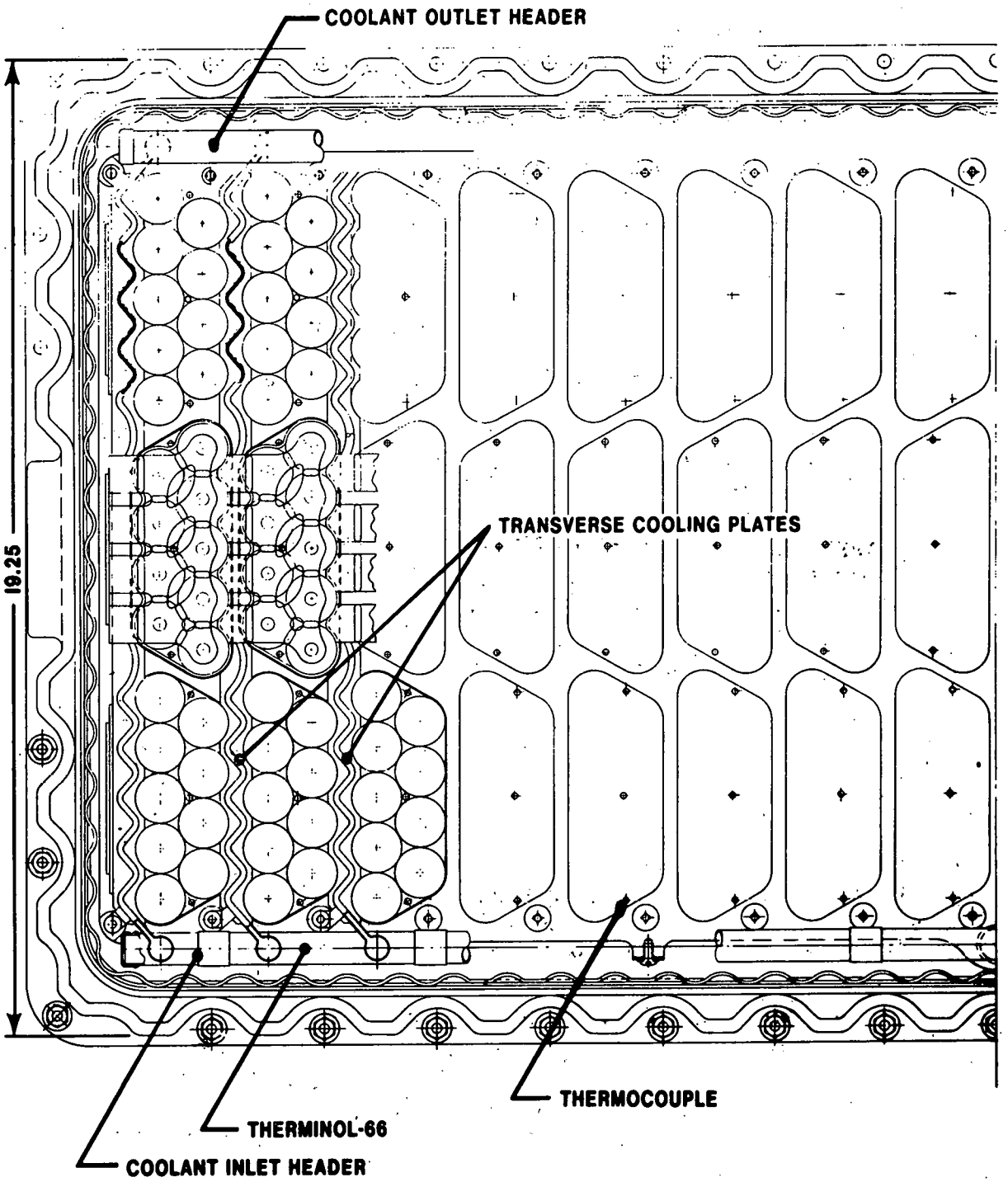

Figure III-10 Plan View of Liquid Cooled Sodium Sulfur Battery

and the heat picked up is discharged to the environment by a combination of radiation and forced convection heat transfer processes. Therminol-66, which is a high temperature heat transfer fluid (modified terphenyl) produced by Monsanto, was selected as the coolant because it can be operated at low pressures at bulk fluid temperatures of 650°F and a max. film temperature of 705°F. While Therminol-66 is not classified as a fire resistant heat transfer fluid (flash point-352°F and fire point -380°F), it can be used in the battery system at temperatures below its fire point and it is rated practically non-toxic for single doses by ingestion or dermal application.

Arrangement of the coolant flow paths is shown in Figure III-10. The coolant enters the inlet header through a line located at the bottom of the battery and at the mid-point of the battery longitudinal dimension. The coolant flows left and right in the inlet header and is drawn off through the transverse coolant plates which are installed in between the rows of cell submodules, see Figure III-10. The contoured coolant plates have parallel flow paths formed in each sheet by the "Roll-Bond" (TM) technique. The coolant is discharged from the transverse coolant plates into the outlet header which, in turn, discharges from the battery through a hermetically sealed discharge line (see Figure III-12).

(d) The inner container for the NaS cells and modules is evacuated to insure that atmospheric oxidation of leaking high temperature sodium (fire hazard) or sulfur (inhalation hazard) will not occur in the event that seal leakage occurs. To provide support to the inner container walls when the inner container is evacuated, low density material is packed in all of the void space between cells, submodules, strip heaters, heat sink plates, etc. Not only will this filler material provide support to the inner container walls but vibration damping also be provided to

the cell submodules, the heat sink plates, and electrical heaters. The filler material selected consists of hollow glass microspheres, 50-300 microns in diameter; (bulk density 9.6-12.4 lbs/cu. ft.) which can be obtained with service temperatures in the range of 482-1093°C.

(e) Internal structural support to the submodules as well as hermetically sealing the feed throughs for power, instrumentation, and coolant lines, is provided by the use of ceramoplastics. Injection moldable glass-bonded mica was chosen because it can be machined and/or metal clad, has good dimensional stability, wide operating temperature range (-273 to 1800°F) and accepts inserts well. Figures III-11 and III-12 show the uses of the molded glass-bonded mica (MYKROY, produced by the MYKROY Ceramics Corporation, has been chosen as a reference material) as a structural base plate which also provides tie down points for the battery assembly in addition to supplying hermetic feed throughs for the battery power leads, the resistance heater power leads, the instrumentation leads and the coolant lines. Also shown in the upper portion of Figure III-11, is a hold down plate made of MYKROY which is spring loaded to prevent the cell submodules from bouncing around when the vehicle is driven over rough road conditions thereby transmitting shock/vibration loads to the battery.

(f) Since the NaS cells are to be operated in the steady state temperature range of 320-350°C (600-660°F), a method must be devised to minimize the heat loss from these high temperature components to the relatively low temperature (-40° to 110°F) environment. The method chosen for the liquid cool battery package consists of using a sealed double walled container. In the space between the two container walls, multi-foil "Super Insulation" consisting of 40-60 layers of thin aluminum foil sheets (approximately .001 inches thick) each coated on both sides with zirconium-oxide chips, are installed as radiation heat transfer

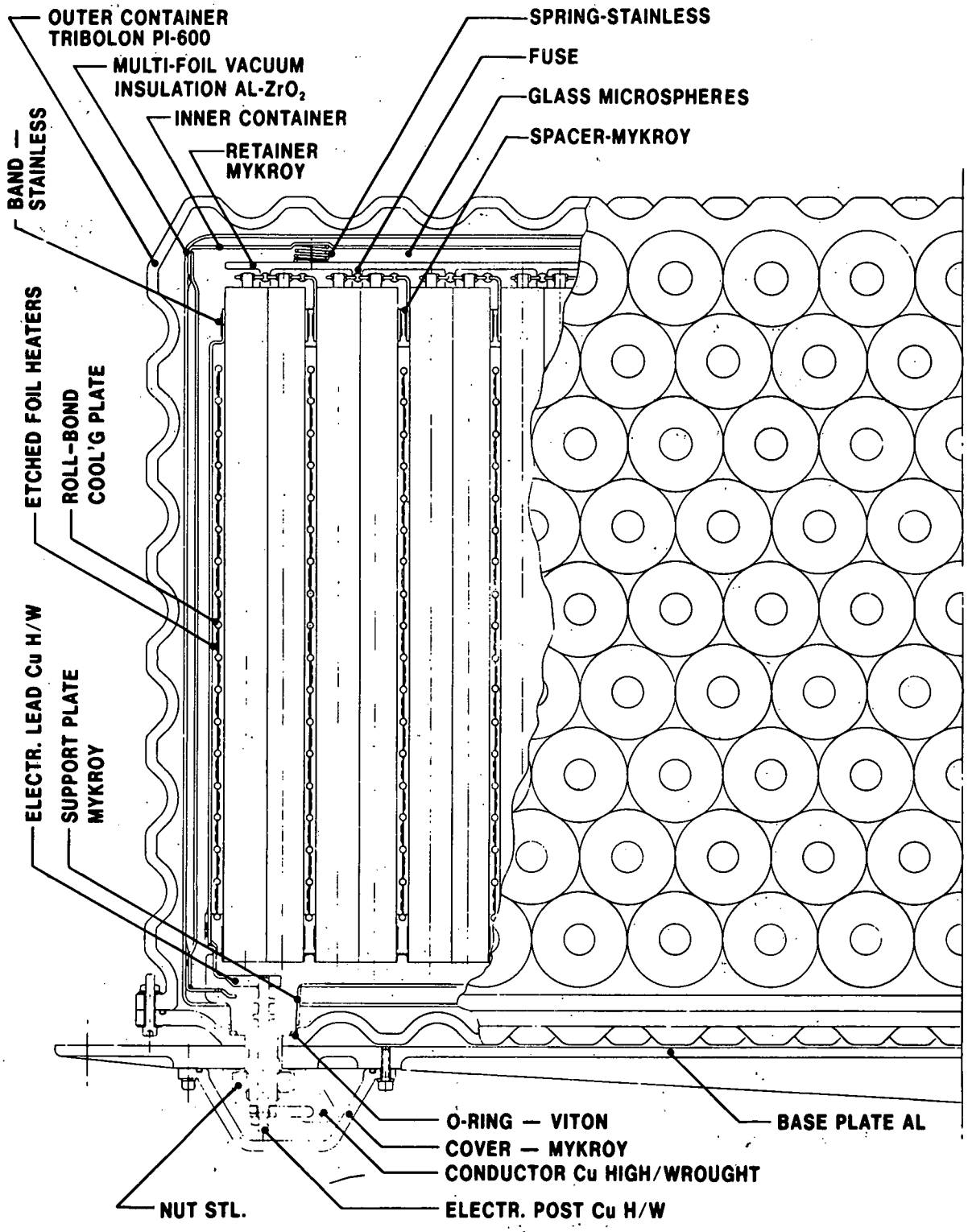

Figure III-11. Battery Side View Showing Structural Details of Final Assembly

shields. The space between the two container walls is evacuated to a vacuum level on the order of 10^{-5} torr. which, with the multi-foil radiation shields in place, should reduce the heat flux through the wall of the outer container to the order of 0.0025 watts/cm^2 (using Thermo-Electron "Multi-Foil" data as a reference).

Since the inside volume of the inner container is also evacuated to a vacuum level of 10^{-5} torr., no pressure differential exists between the inner container volume and the space between the double walls of the battery containment box. This fact permits the inner container to be made from thin walled aluminum which is surface contoured for moderate structural stiffness.

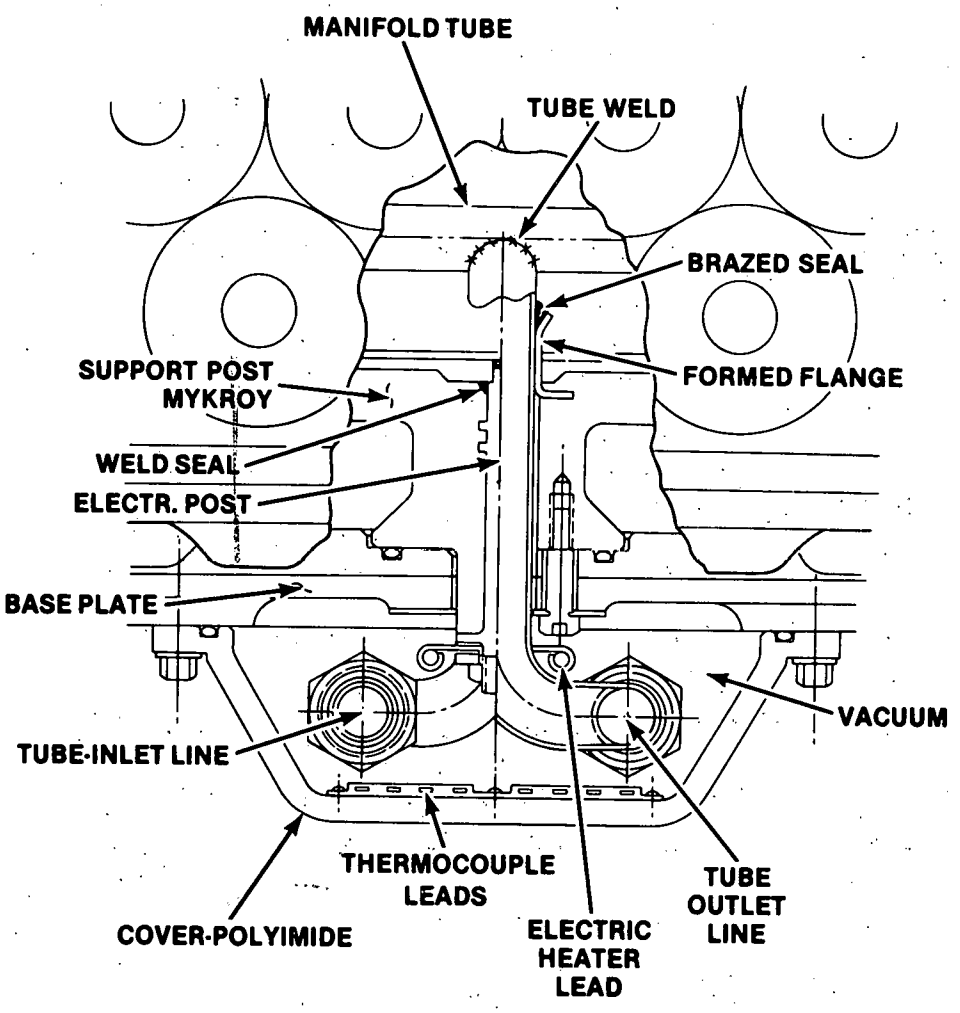

Figure III-12 Cross Section of Coolant Lines and Electrical Heater Leads for NaS Battery

The outer walls of the battery container are formed by injection molding a special formulated polyimide compound which can perform continuously at 600°F and intermittently at 800°F. As Figure III-10 show, the heavy walled polyimide outer container has its wall surfaces molded in the shape of close spaced truncated cones to provide a stiff, low-flexure, structure which should not buckle due to the pressure differential across its wall created by the vacuum inside the outer container.

(g) To minimize heat losses by conduction through the walls of the outer container box, at the points where wall penetrations by power leads, instrumentation leads, electric resistance heater leads, etc., occur, special design innovations were developed. The battery power leads are integrated into the MYKROY base plate at the points where the battery load support/tie down structure are located, see Figure III-11 for details. The leads are extended from these points for a distance of 1-1/2 — 2 feet and within an evacuated insulated jacket to insure minimum heat loss by radiation conduction and convection from the leads.

A similar approach is used for the coolant lines, the instrumentation leads, and the power leads for the electrical resistance heaters. Figure III-12 shows the assembly details whereby the coolant lines and electrical leads are brought through the bottom of the battery containment box. As can be seen in Figure III-12, MYKROY is moulded around cooling tube inserts, thermocouple inserts, and electric heater line leads to insure that a hermetic seal exists upon final evacuation of the battery inner container. To reduce conduction and convection losses to a minimum, the leads and lines are enclosed in a polyimide cover which is sealed to the bottom of the battery container and subsequently evacuated.

Following the completion of the conceptual design layouts of the liquid cooled battery package illustrated in Figures III-10-III-12, a weight estimate was prepared for a battery sized for 40 Kw. The following list covers the major battery components/subsystems:

Components	Weight — Lb. (Kg)
. Battery (Clustered Cells)	492.8 (224)
. Electrical Connections	19.4 (8.8)
. Battery Insulated Container (Double Walled/Vacuum Space)	85.0 (38.6)
. Battery Tie-down/Support Structure	50.0 (22.7)
. Filler Material (Thermal Conduction)	9.0 (4.1)
. Bus-bars and Lead Thru's	8.4 (3.8)
TOTAL ESTIMATED WEIGHT =	665.0 (302)

The battery tie-down/support structure listed above does not include vehicle structure "beef-up" required to provide adequate strengthening to the vehicle body panels made necessary by the installation of the 665 lbs. of concentrated load. Also, the 50 lbs. weight does not include structure weight that may be added to the vehicle in order to meet safety requirement. This added weight will be charged to the vehicle base weight calculations.

3. Combination Closed Air and Liquid Cooling - Option 4

The combination closed air and liquid cooled battery, option 4 has the advantage over option 2 because any sodium or sulfur leakages are contained within the hermetically sealed inner battery containment structure. The air flowing inside the inner battery container exchanges its heat gain with an air-to-liquid heat exchanger located inside of the battery container, see Figure III-7. Preliminary estimates of an air-to-air heat exchanger

to transfer the battery heat to the environment, indicated that the air ducts and plenums would be rather large and bulky and, hence, the vehicle packaging would be difficult. Consequently, an air-to-liquid heat exchanger appeared to be a better approach. Option 4 also has an advantage over Option 3 because it removes the difficult problem in finding a suitable cooling liquid and/or mechanism that would be able to provide the necessary cooling for the NaS cells. However, Option 4 will require more space than Option 3 but less than Option 2.

A combination closed air and liquid cooled battery conceptual design layout was prepared, as shown in Figure III-13. This package assembly borrowed heavily in conceptual design ideas from the work conducted

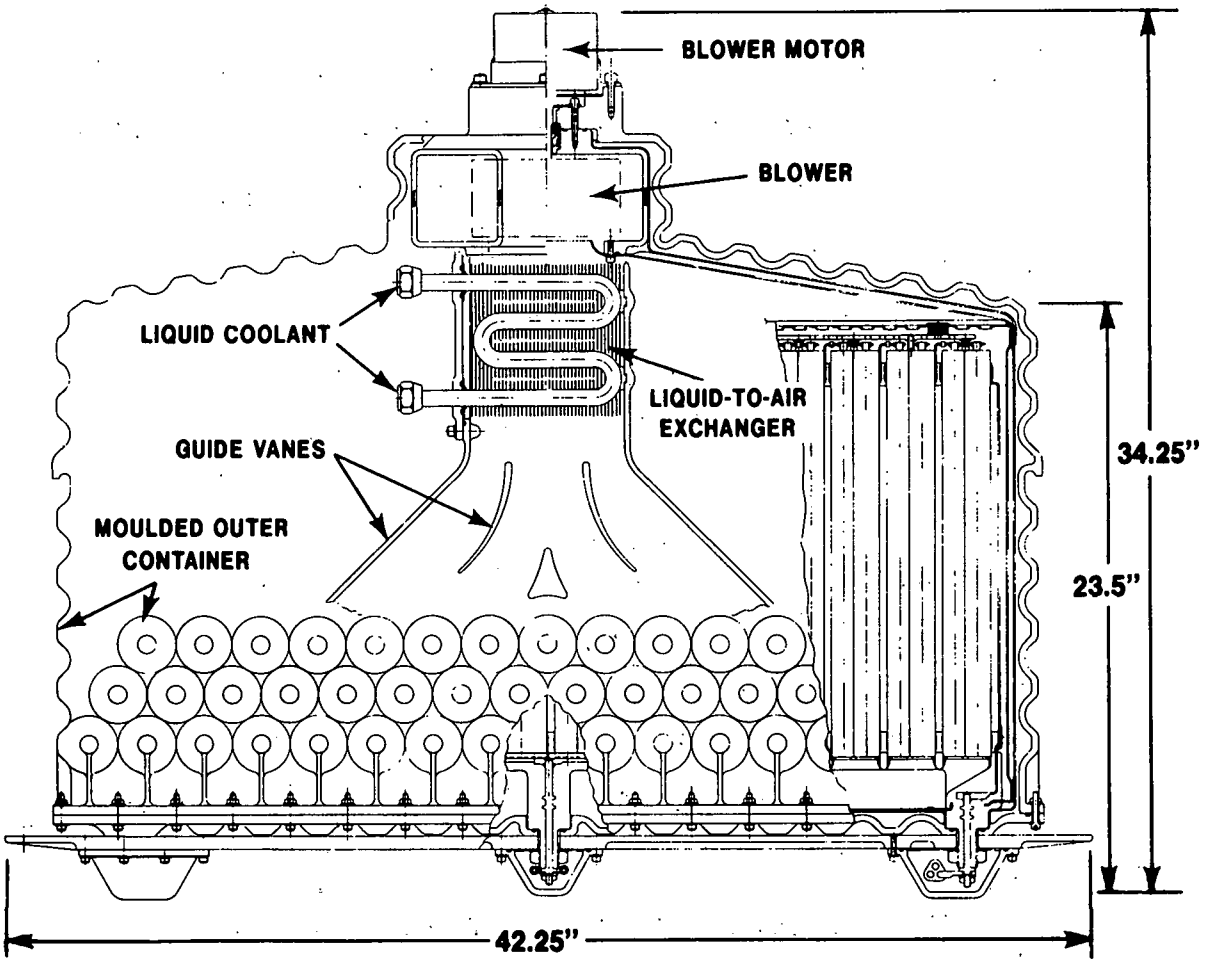

Figure III-13 Front View of Air Cooled Battery Package With Optimized Cells

on the liquid cooled battery configuration illustrated in Figure III-10. The same 9-cell module used in the liquid cooled battery package was used in the air cooled design. The cell interconnection strategy, the means for bringing the battery leads into the inner battery container were virtually identical for both.

As Figure III-7 shows, the air flow path within the inner battery container can be traced from the discharge of the internally positioned blower as follows:

a. The blower discharge air exists into a plenum formed on the back surface of the battery container structure. Within the "Chimney" portion of the plenum a heat exchanger is installed to remove the heat picked-up by the air flowing through the banks of over-heated cell submodules.

b. The cooled air existing from the back side heat exchanger is directed to a bottom plenum formed by the inner battery container and the bottom support plate formed from molded MYKROY material. The ceramoplastic base plate has molded air flow passages that line up with the vertical flow channels formed by the clustered cells forming a submodule. Spacers and baffle plates of ceramoplastic are inserted between cell submodule rows to reduce chances of air flow starvation around the outer perimeter of each cell module.

c. The air entering the contoured inlet passages in the bottom battery support plate, flows upward through the open spacing formed by clustering cylindrical cells in a triangular centered array, see Figure III-8 submodule plane view. Air also flows in channels surrounding the outer periphery of the submodules.

These flow channels are sized to insure even flow distribution around all cells and they are formed by installing ceramoplastic baffle plates especially shaped to the plan view contours of the cell submodules.

d. The heated air exiting from the top of the battery package is collected in the top plenum, shown in Figure III-13, and enters the blower which is mounted on top of the plenum. The blower is located within the double walled container and driven by an electric motor mounted on top of the battery package. The motor-blower shaft must be sealed at the point of its penetration of the double walled container and the sealed shaft assembly must be designed to reduce heat conduction through the shaft and into the motor assembly.

As Figure III-7 shows, the conceptual battery design using the Option 4 approach was larger in size than the Option 3 approach. However, the increased size may be justified as a means to overcome the problems associated with liquid cooling a NaS battery.

In Section IV to follow, the Vehicle Packaging Work Task will be discussed, commencing with the earlier battery and component installation investigations and concluding with the final vehicle packaging layout based on the battery shape, size, and weight data covered in this Section. It should be noted that the final layouts of the Fiesta EV shown in Section IV, Figures IV-7 and IV-8, contain the Option 3 conceptual battery design because it appeared to be more suitable from a packaging viewpoint. However, many issues still remain open concerning the feasibility of a liquid cooled battery. From a functional viewpoint, a more in-depth study should be under-

taken to resolve the issue of whether the NaS cells should be cooled by either air or liquid.

IV VEHICLE PACKAGING

The vehicle packaging work tasks were initiated with the final selection of the Fiesta as the "image car" for the NaS electric vehicle study program. The major sub-tasks of the vehicle packaging activity are listed below:

1. Define maximum available storage volumes for the NaS battery subsystem and the supporting EV powertrain components for
   a. Front wheel drive configuration, and
   b. Rear wheel drive configuration.

2. Investigate Vehicle Handling and Safety Issues

3. Prepare vehicle package layout.

Each of the above sub-tasks will be discussed in this Section of the report.

A. VEHICLE SYSTEMS STORAGE CAPABILITY

1. Front Wheel Drive Configuration

Beginning with the engine compartment and body layout drawings of the North American "Fiesta", preliminary layouts of available space for packaging the NaS EV components (battery, traction motor, controllers, electrical interference filters, etc.) were identified. From these studies it was determined that the volume available in the engine compartment, created by the removal of the 1.6 Litre IC engine and its radiator and support components, was adequate for the installation of the traction drive motor, controller and all other electrical/electronic support components.

Packaging studies of various high speed motor configurations revealed that even with added gear reducers and clutch assemblies for

optimum front wheel drive motor-transverse mounted transmission installations, there was ample room for these types of powertrain packages in the Fiesta front end engine compartment. The same engine compartment packaging studies also showed that, for front wheel vehicle drive, there was insufficient space to install practical volumes of NaS batteries, regardless of their individual cell configuration and, hence, the battery pack (cells, interconnections, insulation, container, tie down brackets, etc.) would have to be installed in the rear of the vehicle.

Using Fiesta production drawings, design modifications to the rear area of the vehicle were made in order to create space for use as battery storage volumes and still achieve the 10 cubic feet of cargo space specified by the Vehicle Assumptions List previously noted in Section II. Design changes to the basic Fiesta included:

1. Removal of the rear passenger seats and all floor and side wall interior trim.
2. Removal of fuel tank and tank mounts.
3. Removal of spare tire; (in the 1980-1990 time period of the spare tire is expected to be replaced by on-the-road "fail-safe" tires now under development).

These design changes to the production Fiesta resulted in development of the following volumes which could be used to store the NaS battery modules:

- Rear Passenger Compartment — 15.4 ft^3
- Fuel Tank Space — 1.3 ft^3
- Rear Passenger Seat Well — 1.8 ft^3
- Spare Tire Well — 1.9 ft^3

Total = 20.4 ft^3

Figure IV-1 is an artist sketch of the NaS battery-powered electric Fiesta following the above cited modifications to the base vehicle. In Figure IV-1 locations are shown of the key electric propulsion system components such as the traction motor, controller and controller filters, etc., along with the shape and the profile dimensions of the bulk volumes available for battery storage.

Early in the packaging study, safety considerations were given priority with the result that those volumes which offered the lowest center of gravity when occupied by insulated battery modules were preferred storage areas. As shown in Figure IV-1, Volume C provides a low profile volume having approximate floor space dimensions of 66 cm (26 inches) X 122 cm (48 inches). A single layer of cells of height equal to 30.5 cm (12 inches) would bring the battery package (cells, insulation, container, etc.) height to approximately hip level for the driver and the passenger. This was considered practical from a battery tie-down point of view in

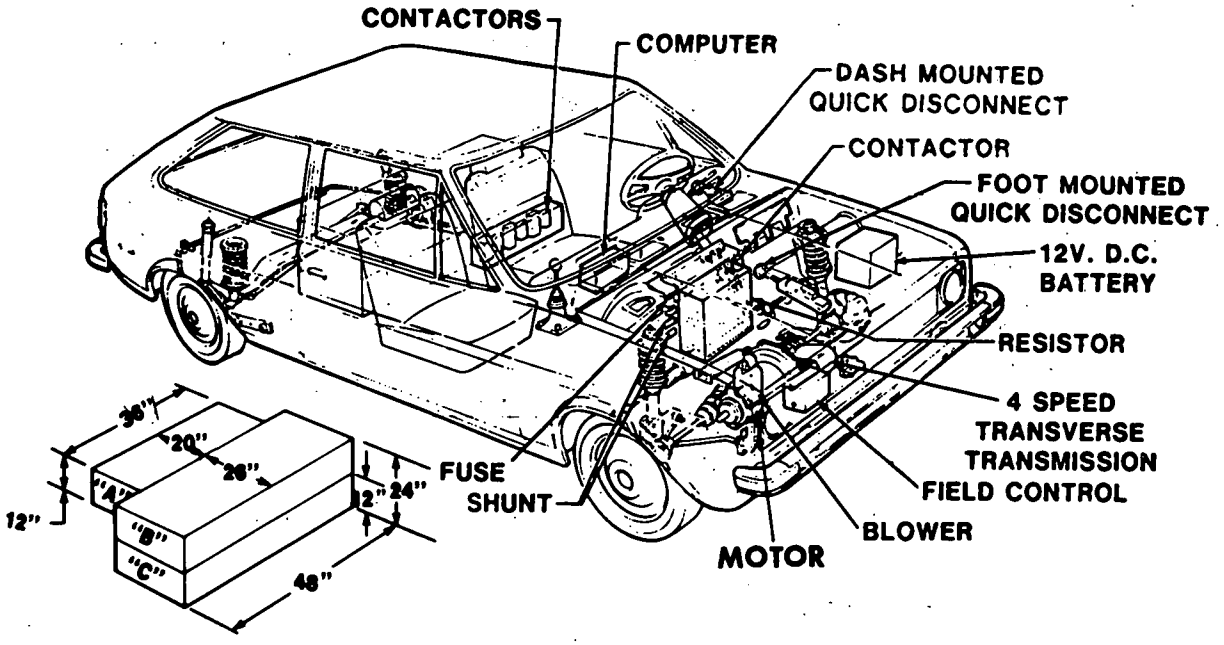

Figure IV-1 Available Battery Storage Volumes for Front Drive Configuration

the case where head-on impact protection must be accomodated in the design of an integrated battery vehicle mounting system.

A small increase in battery module height greater than the height of Volume C, e.g., battery heights of 37-40 cm (14-16 inches) can be accommodated with a corresponding intrusion of the battery pack into Volume B; (see Figure IV-1). Increasing battery heights require a corresponding increase in the weight of battery tie-down structure required to restrict battery forward travel during head-on impacts.

Volume A of Figure IV-1 is less desirable than the Volume C (or a combination of Volume C and B) from the view points of passenger safety and vehicle weight distribution; the standard Fiesta has a weight distribution of approximately 63% front loading and 37% rear loading. While it does not appear to be feasible to exactly match this standard distribution in the NaS EV, the further forward of the rear wheels the battery pack can be located, the closer will be the EV wheel loadings to the standard Fiesta loading. For this reason, Volume C would be the preferred battery pack storage volume option. Weight distribution results will be presented in discussions to follow.

As the battery packaging studies progressed it soon became obvious that Volume A, of Figure IV-1, was unacceptable, not only from vehicle load distribution considerations but from volume limitations as well. Consequently, battery and vehicle packaging studies for the Fiesta EV front wheel drive configuration, concentrated on the dimensions would not exceed the volume dimensional limits of 48 inches (l) by 26 inches (w) by 24 inches (h).

As previously discussed in Section III, the most compact battery package layout, based on non-optimized NaS cell geometries (see Figure III-6, Section III), had a package width of a least 28 inches established as a 2 inches longer than the 26 inches established as a width limit to avoid interference with the travel path of the rear axle during wheel jounce. As soon as sufficient package details were available for the liquid cooled battery package based upon the cell optimization studies discussed in Section III and illustrated in Figure I-1, preliminary vehicle packaging sketches were developed.

Figure IV-2 shows an artist's sketch of the front wheel drive Fiesta EV with the liquid cooled-resistance heated, 9-cell submodule battery package installed directly behind the front passenger seats. Also identified are the major electrical elements of the EV powertrain.

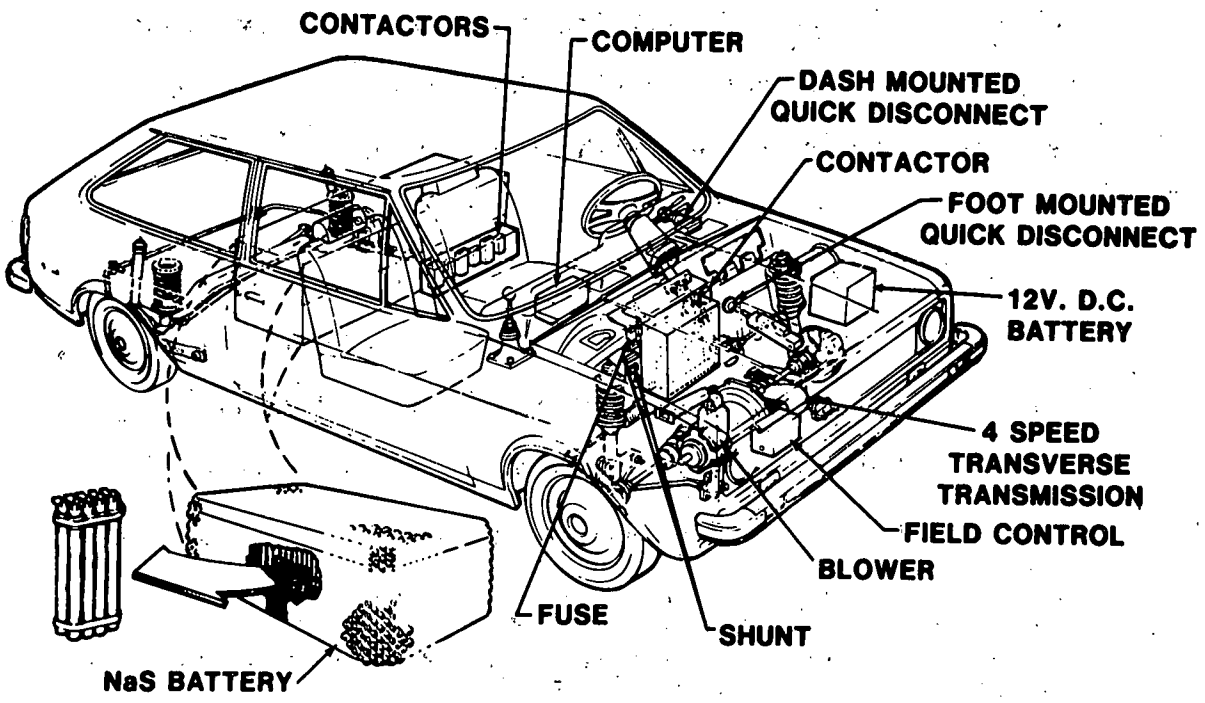

Figure IV-2 Sodium-Sulfur Battery Powered Fiesta Electric Vehicle

2. Rear Wheel Drive Configuration

Because of the significant shift in weight distribution between the front and rear wheels caused by the rear mounted battery package, in comparison to an ICE powered Fiesta package, it was decided that a front mounted battery — rear wheel drive vehicle package should be investigated. The need to use a rear drive configuration for the powertrain became clearly evident from study of the Fiesta production drawings.

The volume available for battery storage under the hood was inadequate to permit the vehicle to meets its performance and range goals if the transmission was not removed along with the ICE engine. Since major changes to the steering gear and front end suspension were neither desirable or acceptable choices, the only practical approach appear to be one of relocating the transaxle transmission to the rear and concomitantly modifying the rear axle and rear suspension systems. Figure IV-3, shows the proposed approach to redesigning the Fiesta rear end to accommodate an electric motor drive — transverse transmission assembly, along with key electrical supporting subsystems comprising the EV power train system as can be seen, this rear drive configuration represents a major re-work to the Fiesta rear end section.

With the engine compartment now free of all ICE related powertrain components, studies were made of available battery package volume and various battery package concepts that might permit the vehicle to meet the performance and range goals defined in Section II. Figure IV-4 is an artist sketch of the rear drive Fiesta EV showing the transverse motor-transmission installation previously described

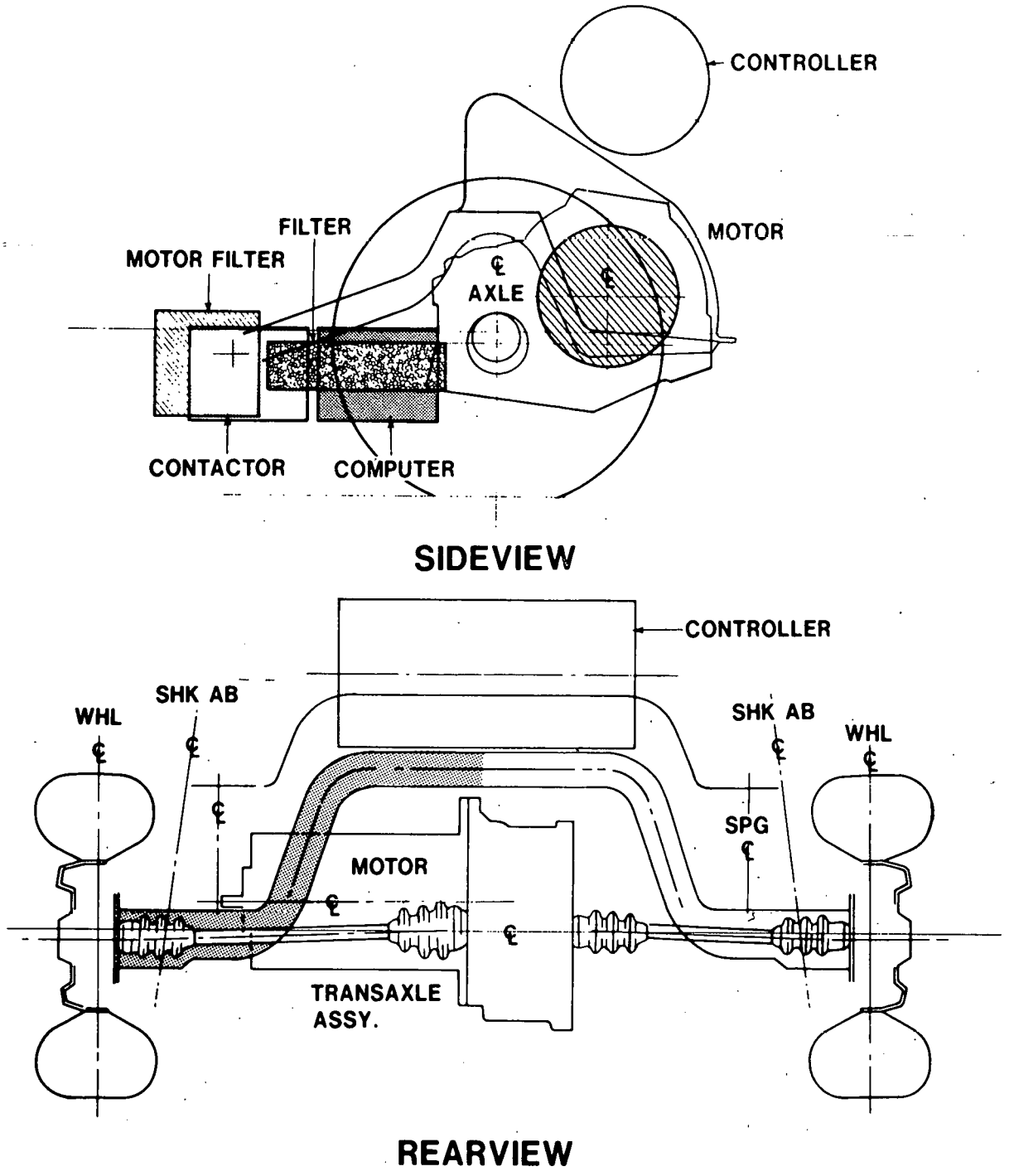

Figure IV-3 Proposed Fiesta Rear End Modification for Vehicle Rear Drive

by Figure IV-3. Also shown in Figure IV-4, is the maximum volume available for battery storage without having to make a major alteration to the hood line, an alternative considered unacceptable for the Fiesta. Within the approximately 8.0 ft.^{3} volume, various cell arrangements were tried and their performance potential was evaluated using Ford's computer program for projecting EV performance and economy. For the NaS cells defined by the Ford cell sizing program described in Section III and illustrated in Figure III-8, the range for the front battery mounted vehicle was appreciably less than 100 miles over the CVS cycle.

Figure IV-5 is a tabulation of analytical comparisons between front drive and rear drive vehicle configurations. Since this Figure showed an appreciable range difference between the front drive vehicle and the rear drive vehicle, and since discussions with Company Safety

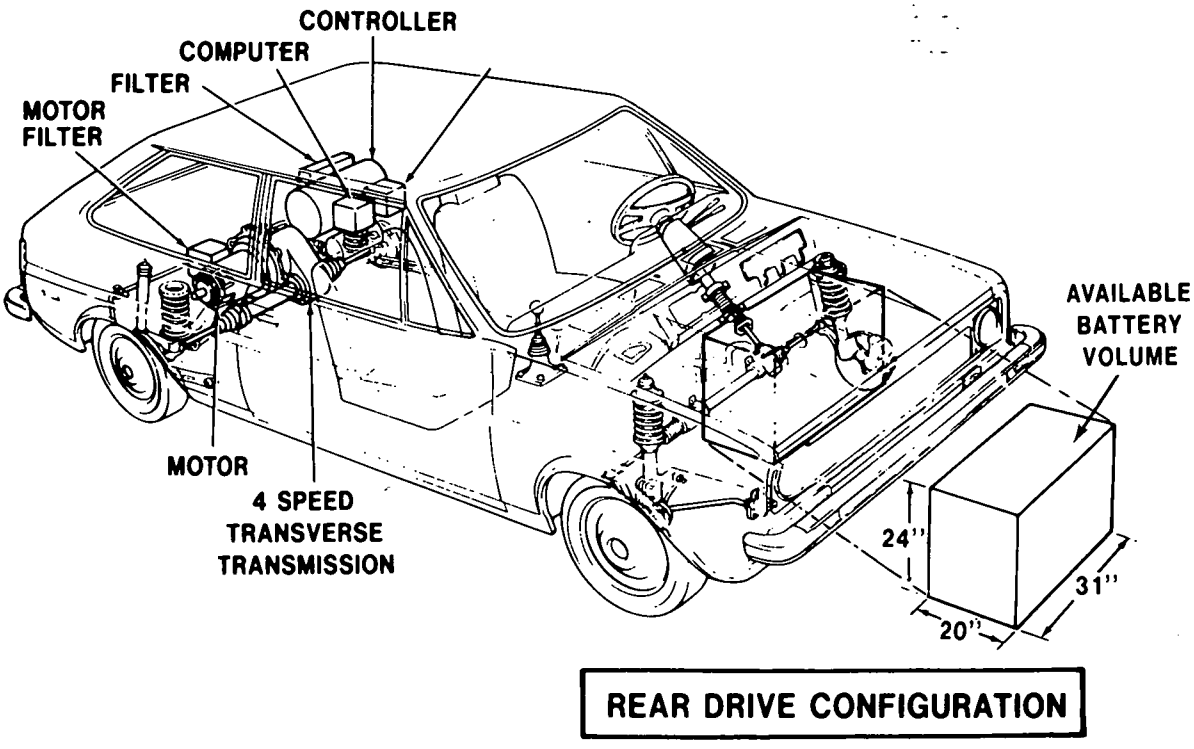

Figure IV-4 Sodium-Sulfur Battery Powered Fiesta Electric Vehicle — Rear Drive Configuration

Offices indicated that a front battery installation was considered to be less desirable from safety considerations than a rear battery installation, the front battery installation was dropped from further consideration.

KEY PARAMETERS	FRONT DRIVE — REAR BATTERY INST.	REAR DRIVE — FRONT BATTERY INST. (1)
• EV CVS RANGE	116 MILES	91 MILES
• TEST WEIGHTS	2470 LBS	2334 LBS
• BATTERY SPECS		
— CVS POWER (KW)	34.5	32.79
— CVS ENERGY (KWH)	29.4	22.68
— CELL ORIENTATION	VERTICAL	VERTICAL
— ELECTROLYTE L/D	20:1	24:1
• TIME FOR 0-50 MPH	10.46	12.22
• POWER TRAIN WEIGHT	866 LBS	740 LBS
— BATTERY (CELL + COND.)	492 LBS	398 LBS*
— MOTOR + CONT.	206 LBS	206 LBS
— STRUCTURE & COMPONENTS	168 LBS	136 LBS

(1) UNMODIFIED HOOD & BODY STRUCTURE
*BASED ON MAX. ALLOWABLE VOLUME

Figure IV-5 Comparison of P & E For Front Drive vs. Rear Drive Vehicle Installations

B. Vehicle Handling and Safety Issues

An integral part of the vehicle packaging program is vehicle weight analysis, including vehicle weight distribution. As the battery packaging program progressed to the point where battery cell weights, electrical bus bar/power lead weight, insulation and container weights and tie down structure weights could be reasonably estimated, vehicle weight distribution studies were initiated. Figure IV-6 was developed as an example of the effect of

battery weight on the percentages of distributed weight on the front and rear suspensions. This figure assumes the battery package weight of 800 lbs estimated for the battery installation illustrated in Figure III-6. The center-of-gravity of this package was calculated to be approximately nineteen (19) inches ahead of the rear axle. For these installation assumptions the EV Fiesta weight distribution percentages computes to 47% for the front wheels and 53% for the rear wheels, compared to an even 50-50 split for a four (4) passenger production Fiesta loaded with 100 lbs. of cargo.

The advantages of the battery package illustrated in Figures I-1 (Section I), III-8 and III-9 (Section III), are that its lighter weight (less than 700 lbs) and its smaller width (20 inches vs 28 inches for the Figure III-6 battery package) shift the weight distribution close to the production value of 50-50% for the front and rear wheels. This means that from a handling viewpoint, the NaS Fiesta EV (front drive configuration) with the battery configuration shown in Figure III-8 should not have driving characteristics appreciably different than that experienced by a fully loaded production ICE powered

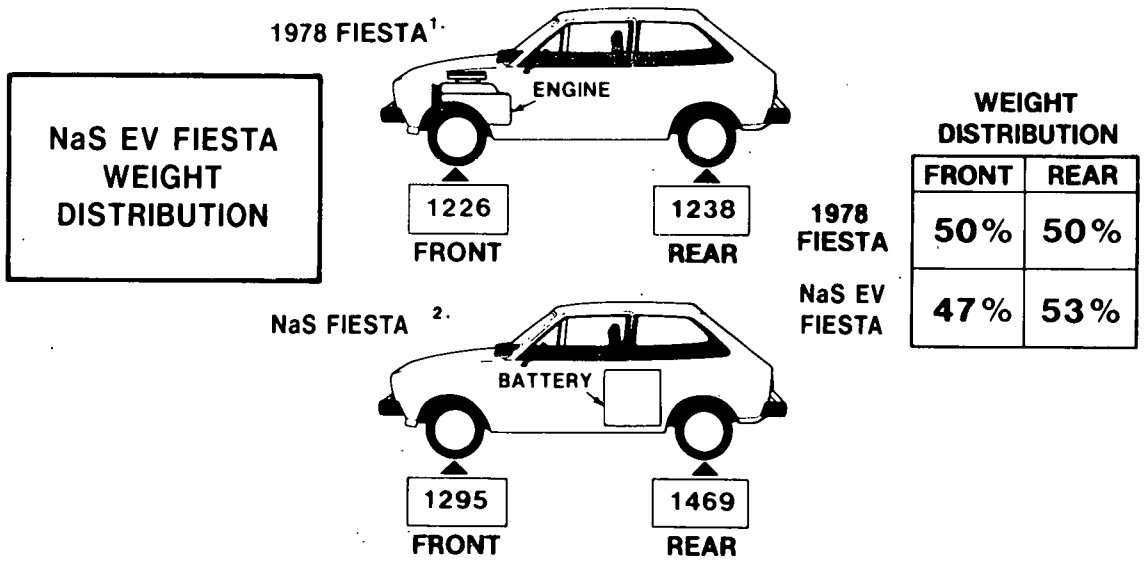

1. 1978 FIESTA WEIGHT INCLUDES 4 PASSENGERS AT 150 LBS PASSENGER, 100 LBS CARGO, AND 1764 LBS CURB WEIGHT

2. NaS EV FIESTA WEIGHT INCLUDES 2 PASSENGERS AT 175 LBS/PASSENGER, 100 LBS CARGO, AND 2314 LBS CURB WEIGHT

Figure IV-6 Fiesta Weight Distribution for 800 lb. Rear Mounted Battery Package

Fiesta. This is not to say that the front and rear suspensions and/or the wheel brakes of the Fiesta EV will not have to be modified to handle the increases in EV curb weight over the production Fiesta. These are open issues than can only be resolved in future follow-on vehicle studies and experiments.

As the battery packaging and the vehicle packaging programs progressed, numerous design review meetings were held with Ford Safety representatives (see Section VI for detailed discussion). Since it was concluded that the rear wheel drive — front mounted battery vehicle configuration was less advantages than a front wheel drive — rear mounted NaS battery, no weight summaries and weight distribution analysis were expended on the rear wheel drive Fiesta configuration illustrated in Figure IV-4.

C. Fiesta Ev Package Layout

By the end of third quarter of the NaS Fiesta EV study, the final analytical conclusion and/or system design selections were essentially established within all of the study work tasks. Consequently, a full scale layout of the Fiesta EV was started. The final master layout is presented in Figure IV-7 which shows the left profile view of the Fiesta EV, and Figure IV-8, which is a composite figure of the front end view and the rear end view of the 2-passenger Fiesta EV. For clarity, the key components and sub-systems in Figures IV-7 and IV-8 have been heavy-lined. Key design highlights and packaging assumptions are listed below:

1. The battery package and its support structure are designed to permit bottom vehicle loading of the battery. The bottom battery support is assembled to the battery and the completed sub-assembly is hoisted from underneath the vehicle into position

and secured to the body side rails that are welded into the vehicle structure as special body reinforcements.

2. The "Cortina" electric drive motor is mounted with a clutch plate adapter directly to the production Fiesta manual transmission. The EV traction motor is cooled by a separate electric motor driven blower, which only functions on demand from the traction motor temperature sensing and control circuitry.

3. All components which make up the motor controller, with the exception of six contactors mounted on the battery support structure, are located under the hood in the "engine compartment." To insure proper cooling, these components are mounted separately on either the fire wall or other vehicle body structure which serve dual functions by acting as supporting structure and heat sinks.

4. The battery support structure was constructed much like a protective cage to (a) provide a secure positioning of the battery container system during all degrees of vehicle roll, sway, pitch, jounce and rebound, and (b) tie the battery securely in position during vehicle front or rear impacts by transferring the battery inertia loads through existing and/or add-on vehicle frame members, which are integrated with the battery cage numbers. members.

5. The on-board computer which provides start-up logic, regenerative braking logic and fail-safe interlocks for normal powertrain operation as well as battery recharging and vehicle maintenance, is located in the glove compartment.

6. To provide 12 volt electrical power for all manual auxiliaries such as lights, horn, radio, instrumentation, heater blowers, etc. a Ni-Zn on board battery has been assumed and provision for its mounting has been made on the left side of the vehicle, inside the "engine" compartment and on the left hand fender apron. The maximum listed electrical load for a production Fiesta is approximately 437 watts (including a back window heater but no A/C). If it is assumed that the battery electrical support loads for contactor solenoids, a vehicle logic unit, emergency switch solenoid and instrumentation add another 168 watts, for a total of approximately 600 watts then a high performance Ni-Zn battery pack having the following approximate characteristics should be able to provide 300 watts (1560 watt-hrs.) of "keep-alive" capacity for 100 miles of CVS Cycle driving:

a. Battery Capacity vs discharge rate @ 40 amps — 230 amp-hrs

b. Battery Power density (@ 80% DOD) — 70 watts/lb

c. Battery Energy density (@ 80% DOD) — 32 watt-hr/lb

7. The floor pan behind the front seats is brought up and over the battery support structure to provide a wall seal between the passenger and the cargo compartment. The purpose of this design approach is to provide a safety shield between the front passengers and the battery system.

The vehicle package layouts illustrated in Figures IV-7 and IV-8 are soft line drawings which illustrate the general manner in which a production Fiesta could be re-worked into a 2-passenger electric vehicle using a new NaS battery package design concept and fairly conventional electrical components for the electric power system. There is much detail work yet that needs to be done before a test bed vehicle can be built for demonstration tests of the potential of the NaS battery to serve as the power source for an electric vehicle.

In Section V to follow, the electrical system study sub-tasks will be reviewed.

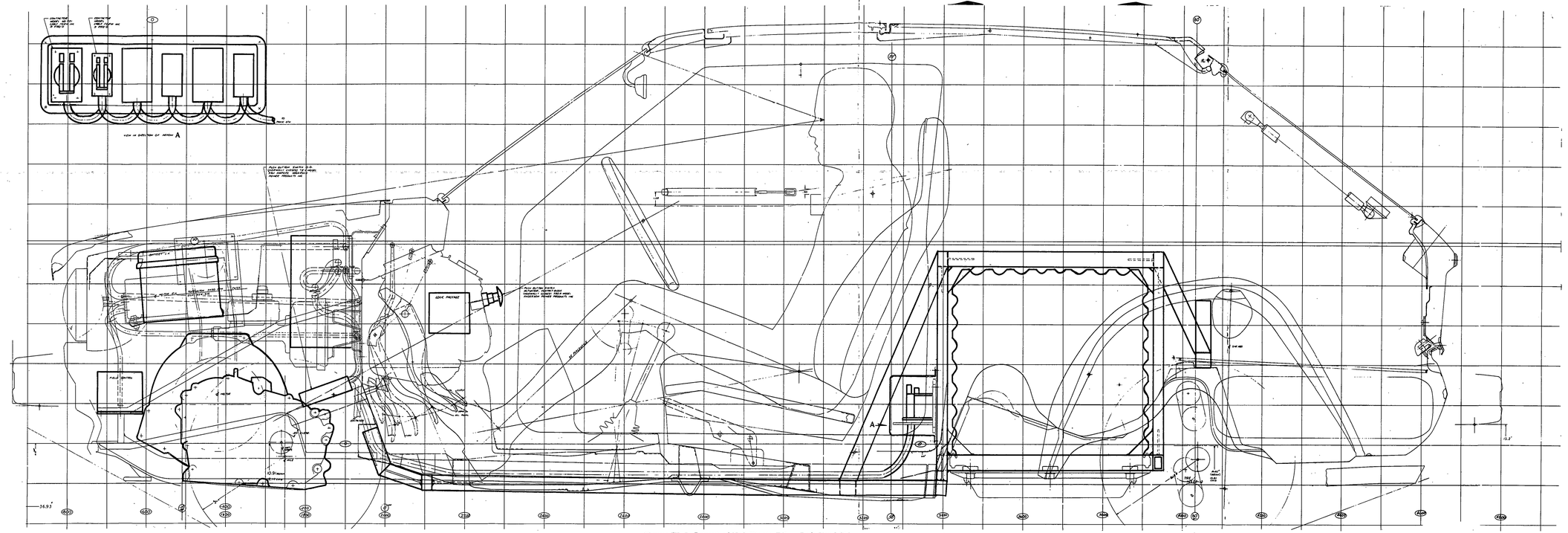

Figure IV-7 Layout of NaS Fiesta EV — Left Hand Side

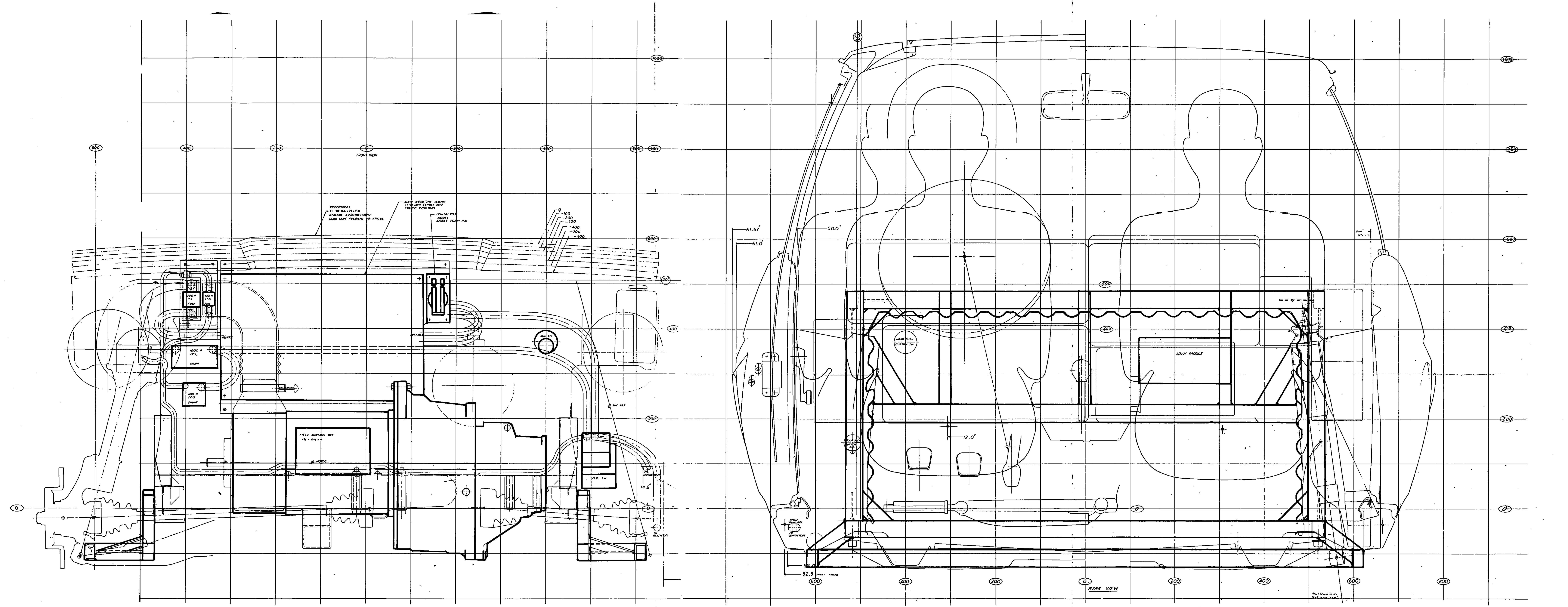

Figure IV-8 Layout of NaS Fiesta EV — Front and Rear Views

V ELECTRICAL SYSTEMS

The drivetrain of an electric vehicle (EV) consists of three major systems: an electric motor, a means of controlling the torque and/or speed of the motor (which will subsequently be referred to as the "controller" in this report), and a mechanical gearing and torque-splitting system. The latter system can generally be borrowed without significant modifications, but the motor and controller systems are unique to EV's and are by no means mature systems for this application. The purpose of the studies described in this section is to evaluate motor and controller systems suitable for use in the NaS Fiesta EV described in other sections of this report and to develop a preliminary design and packaging scheme for the electric portions of the drive train. While these studies have been aimed at a particular vehicle configuration and a particular battery system, much of the analysis is applicable to other vehicle configurations powered by other types of batteries.

Since this study has been performed by Ford Motor Company, the tenor of the study naturally reflects many of the goals and concerns of Ford. The influence of Ford on vehicle manufacture is most noticeable in three areas: economic considerations, simplicity of design, and vehicle acceleration performance. The latter consideration has already been alluded to in the discussion of battery sizing. The same considerations, of course, apply to the sizing of the motor, controller, and transmission, and the Federal Urban Drive Cycle (CVS Cycle) has been the basis for sizing the drivetrain components. The use of the CVS Cycle primarily affects the peak power rating of the drivetrain components with exception of the motor

and some of the power components in controllers. This parameter has the most influence upon component size and cost. It also brings about some modification in the way some components are specified or "rated," and the "average power rating" used almost universally for specifying electric motors is relatively insignificant for EV application. Likewise, the concept of initial component costs is a most important criterion in selecting components for use in commercial automobiles, and this criterion must also be significant in developing EV drivetrains, if it is assumed that the purpose of the development is an economically viable vehicle. The third automotive emphasis noted above, simplicity of design, is related not only to the economic need for low cost designs, but also to the need for components that are reliable and easily-maintained in the environment experienced by passenger cars and vans. This environment is one of the most demanding in which traction motors and electronic control components have ever been applied. In terms of maintenance schedules, skill and training of the vehicle operator, size and weight limitations, packaging problems and safety considerations, the private automobile environment is far difference from that of electric trains, street cars, or the English electric delivery vans, which are the only other applications in which these components have been used. The well-established technology in this field has been investigated and has been found to have little applications for EV's.

Therefore, the purpose of this study is to choose drivetrain components that have a chance for becoming economically viable in the private passenger car environment for an electric vehicle of the Ford Fiesta size with a Sodium-Sulfur battery for the energy source. More specifically, the objective of the motor/controller study are as follows:

1. Prepare a comparative evaluation of candidate motor/controller systems suitable for use with a NaS battery and constructed of

"State-of-Art" components.

2. Compare candidate systems in terms of technical performance, initial cost, system weight, energy efficiency, and relative reliability.

3. Describe technical and economic problems of candidate systems when used in a marketable vehicle.

4. Choose the optimum type of motor/controller system.

5. Prepare a detailed design for the chosen system.

6. Obtain a motor suitable for use in a NaS demonstration/test vehicle.

7. Prepare weight and volume estimates of the chosen system for use in the NaS Fiesta vehicle packaging studies.

A. VEHICLE, BATTERY, AND TRANSMISSION CONSIDERATIONS

In any type of vehicle, the vehicle weight and size and the type of drive mission have profound influence on the size, weight, cost, and technical performance requirements of the drivetrain. These vehicle related parameters which influence motor controller design are (a), the peak power rating of 45 HP (33.6 kw) for one minute; (b), 65 MPH top vehicle speed; (c) vehicle test weight limitation of approximately 2500 lbs.; (d) fuel economy based upon the Federal Urban Drive Cycle; (e) an axle ratio N/V of 56.8 RPM/MPH; and (f) the motor/controller system and all auxilliary components must be packageable under the hood of a Fiesta.

The Sodium Sulfur battery is a high temperature, liquid electrode battery quite different in almost every respect from batteries that have been used in existing EV's. However, there are relatively few restrictions imposed upon the motor/controller design due to these major differences in this

particular battery. The most significant restriction concerns the number and the size of electrical conductors required between the battery container and the motor/controller system. These conductors form a major thermal path for conducting heat out of the battery. From the standpoint of the thermal design and control of the battery, the heat transfer through this path should be minimized.

1. Regenerative Braking

A major consideration in the early design of an EV which affects the design of almost every component in the drivetrain as well as in the braking system is whether or not to use regenerative braking of the vehicle. Estimates of the relative value of regenerative braking upon increasing vehicle driving range have varied widely in the past, and disagreements among EV investigators continued during the year of this study as witnessed by several papers presented at the Fifth International EV Symposium in Philadelphia. [1], [2] In Reference 1, regeneration was estimated to increase range on the CVS cycle by about 5 — 8% based upon analytical modeling calculations. Reference 2, however, described bench tests of a lead-acid battery and conventional drivetrain in which 34% increase in battery energy capacity was measured.

The approach in this study was to follow the conclusions of previous Ford studies [3], [4] in which range improvements of from 11 — 13.5% were calculated for CVS driving using high quality drivetrain components. These studies also showed even higher range improvements resulting from regenerative braking in driving missions with more stop-start operations than the CVS driving cycle, such as driving profiles characteristics of taxis and delivery vans. The use of regenerative braking reduces battery weight somewhat when a

specific range is specified. Furthermore, the present thinking in the automotive industry is that a 5% improvement in fuel economy (which is roughly equivalent to a 5% increase in range for a given amount of energy supplied to the battery) is definitely worthwhile, unless it impairs the technical performance of the vehicle in some way or comes at a prohibitive price. The influence of regenerative braking upon vehicle driveability are relatively unknown or at least unquantified, since very few electric or hybrid vehicles have included this feature and there is almost no published data based upon test or driving experience from which potential problems due to regenerative braking might be accurately predicted. Concerning the cost penalty of regenerative braking, there is a definite cost penalty in certain types of motor/controller configurations, particularly the DC commutator motor with armature chopper control, one of the more popular types of EV drivetrains. These cost penalties are considered in the comparison of motor/controller systems described later in this section. The problems of driveability related to regenerative braking must await further driving experience with vehicles so equipped. Noting these potential problems, the use of regenerative braking was assumed in all of the analysis described in this report.

2. Mechanical Transmission

The need for a mechanical transmission has been debated among EV developers for many years. The necessity for a transmission in an internal combustion engine (ICE) vehicle — to permit engine torque at zero vehicle speed — does not exist in an EV since most electric motors have excellent starting characteristics. Therefore, following the commercialization of high power SCR's, it

was felt that infinitely-variable control of an EV should be achieved entirely through electronic means. This is a very desirable goal and has been considered one of the potential advantages of an EV over conventional ICE's. Conventional thinking tends to favor the concept of an automatic transmission and to consider manual transmissions as relatively unsaleable to the American public. The continuously-variable-transmission (CVT) under consideration for the conventional automobile has many associated technical problems, and, therefore, the smooth infintely-variable control of an SCR or power transistor controller is most attractive. The automatic transmission with hydraulic torque converter used in most conventional passenger cars today has become recognized as a relatively inefficient component, and this recognition also favored attempts to achieve even smoother drive control in an EV with highly efficient electronic control schemes.

EV with highly efficient electronic control schemes.

However, in recent years, a number of EV performance and cost tradeoff studies have produced results and conclusions favoring the use of a manual transmission where its use really isn't necessary. The only real disadvantage of the manual transmission, in fact, appears to be driver inconvenience, i.e., the nuisance of having to shift gears manually. The advantages of the use of a manual transmission in an EV include:

1. Reduced size of the required motor and controller for a given vehicle performance specification; or, stated inversely, improved vehicle performance from a motor and controller of given size. This latter improvement has been described numerically in Reference 4 and is noted quantitatively in the vehicle tests described in Reference 5.

2. A transmission permits the operation of the motor/controller system at or near optimum efficiency at most vehicle speeds. In the computer-controlled cars of future years, this feature will be essential.

3. In certain type of control schemes, a transmission permits regenerative braking over a much wider range of vehicle speeds than would be possible without a transmission.

4. Manual transmissions have a relatively high efficiency at most speed and torque conditions. Computer modeling based upon test data of manual transmission at Ford indicates an energy efficiency during CVS driving of about 94%. (3)

5. Manual transmissions are mature, reliable components with a long history of application in the conventional automobile industry. They are presently in mass production at costs far below those expected for power semiconductor controllers.

The effects of the use of a transmission on motor/controller size and cost are further illustrated by Figures V-1 and V-2 and Table V-1. These data are based upon the Fiesta vehicle and the "Cortina" motor which will be discussed in later sections of this study. The purpose here is to illustrate the effect of a multi ratio transmisson on motor size. Figure V-1 illustrates the speed-torque characteristics of this particular motor.

The peak (one-minute) torque-speed characteristics of this motor, which is typical of most EV drivetrains, is limited by different factors over the speed range, e.g. at low speeds, the current rating of the battery, control devices, and motor windings is the limiting factor; at intermediate speeds, battery power is the limiter; whereas, at very high speeds, the motor design rating itself is the limiting parameter. When this motor

torque-speed characteristic is related to the vehicle tractive effort vs. MPH characteristic, Figure V-2 results. The N/V and other drive-train parameters used to obtain Figure V-2 are show; RPBBRK is the motor speed at which the torque-speed curve changes from current limit to battery limit in Figure V-1. The manual transmission choice for this study is a four-speed with the ratios 3.58/2.06/1.29/1. The effects of using a fixed transmission ratio at any one of these values is shown in Figure V-2. For example, if the ratio were fixed at 3.58, the low-speed tractive effort would be obtainable, but the high speed tractive effort would decrease to zero at less than 50 MPH. Therefore, a much large motor/controller would be required to meed the high speed CVS requirements (shown by x's in Figure V-2) and the 65 MPH steady-state operation. Conversely, if the ratio were fixed at 1.29, the low-speed

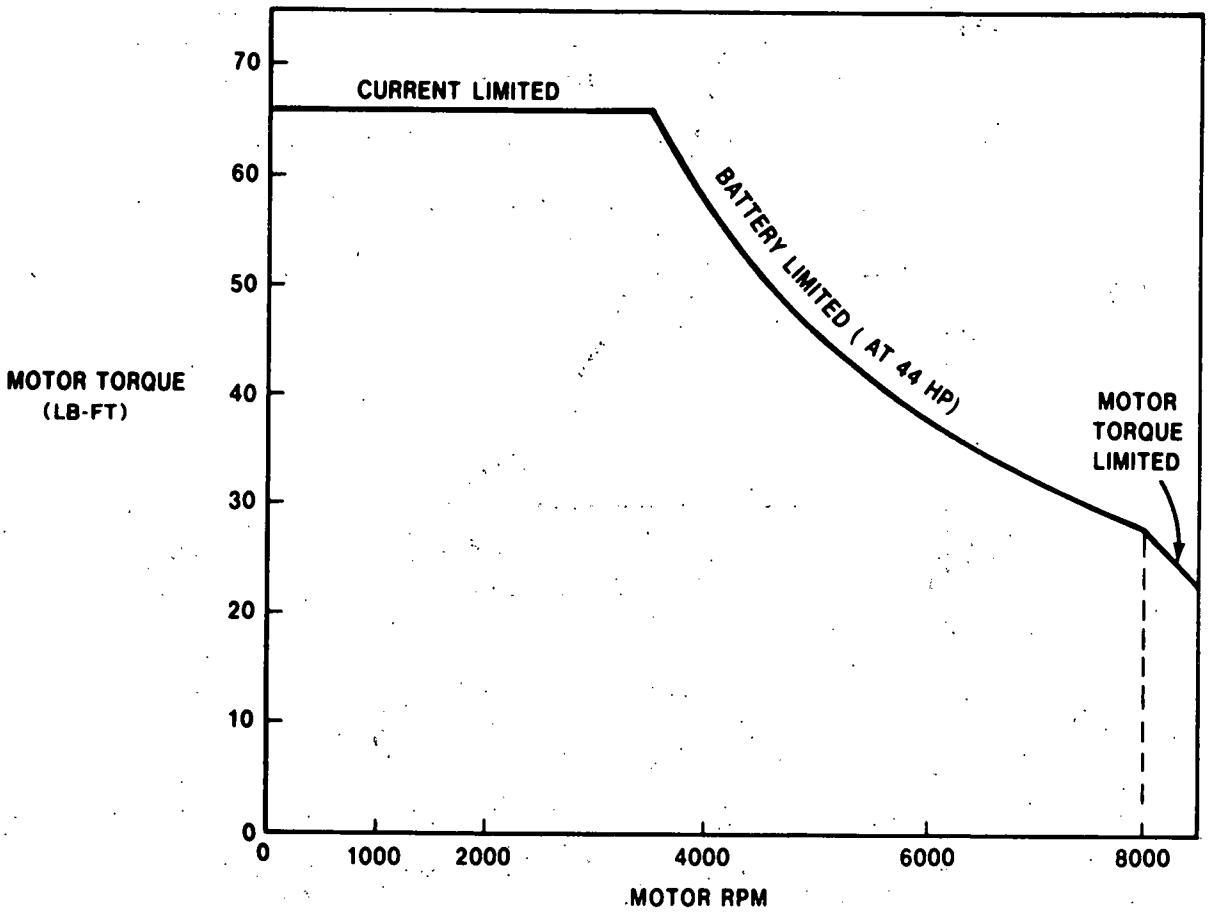

Figure V-1 Plot of Cortina Motor Torque vs. Motor Speed

capability would be drastically reduced. The effect of a fixed ratio on motor weight is shown in Table V-1. The effect upon a drivetrain cost would be much more severe due to the high current rating of the power semi-conductors in the all electronic system. Note also that the weight (and cost) penalty increases as motor speed decreases. This data will be referred to later on in the comparative analysis of motor/controller systems.

Continuously variable transmissions (CVT's) have been proposed for EV application [6], and the possibility exists that eventually CVT's could

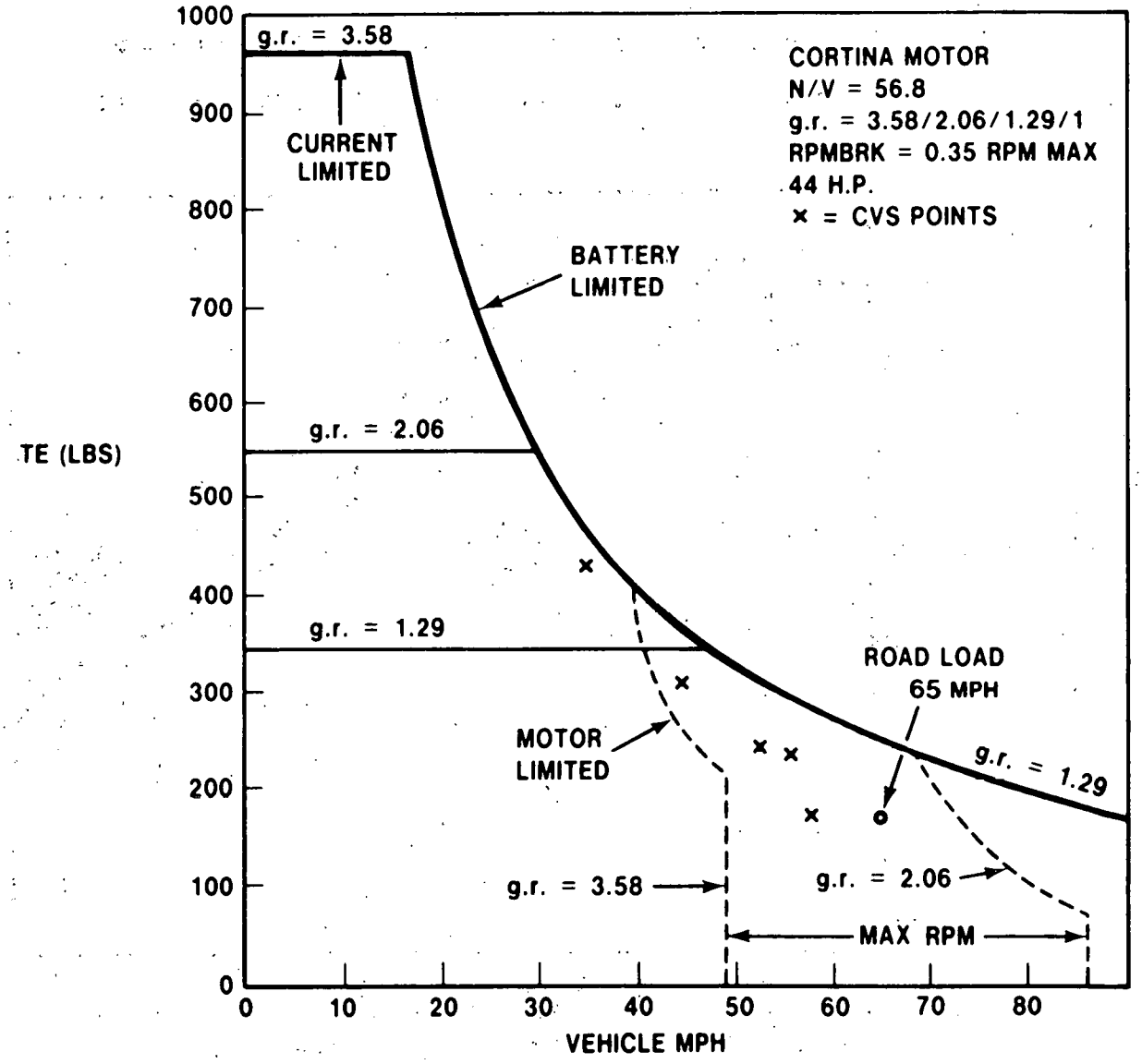

Figure V-2 Fiesta Operation with Cortina Motor

supply the infinitely smooth control in both ICE's and EV's at a lower initial cost and higher energy efficiency than possible with power semiconductor control in EV's. Ford Research has had considerable background and experience in the design and development of both traction and hydromechanical CVT's, including a DOE-funded program for a specific traction drive development. [7] There has also been close liaison with the CVT development for the University of Wisconsin's engine/flywheel hybrid work. [8]

The conclusions from the Ford Research Staff experience is that CVT's are not viable contenders for use in vehicular drivetrains in the near future — which is the time period of the present study. The efficiencies quoted in Reference 6 would augment this conclusion. Therefore, the use of CVT's in the NaS Fiesta drivetrain has not been considered.

TABLE V-1 — EFFECT OF TRANSMISSION ON TRACTION MOTOR

	CONTROL	TRANSMISSION	MAX RPM	MAX MPH	MOTOR Wt (lbs)	MOTOR TORQUE (lb - ft) MAX	MOTOR TORQUE (lb - ft) @ 65 MPH
A.	Contactor/Field/ Transmission	Man - 3.58/2.06/ 1.29/1	10000	176	100	66.1	47.5
B.	All Electronic	Fixed - 2.71	10000	65	122	87.3	23.16
C.	Contactor/Field/ Transmission	Man - 3.58/2.06/ 1.29/1	6000	106	125	66.1	62.5
D.	All Electronic	Fixed - 1.625	6000	65	174	145.6	38.5

Assumptions:

1. H. P. = 44 (max)
2. H. P. = 25 (cont.)
3. Max T. E. = 960 lbs
4. N/V = 56.8
5. Motor Wt = $K \times T^{0.7}$

B. TYPES OF EV DRIVETRAINS

In the following descriptions and comparisons of EV drivetrains, it is assumed that the reader is familiar with the fundamentals of the most common types of motors and controllers. Therefore, most of the basic principles of the different types of systems will be omitted, although references will be given to guide the reader if more detailed descriptions or theory is desired. One of the best references for detailed descriptions of motors and controllers for EV's is still considered to be Reference 9, prepared by Ford Research. Since the recent EV Act of 1976 and the subsequent DOE-funded programs, several DOE publications have summarized most of the common types of drivetrains used in EV's; References 5 and 6 are good examples of such publications.

The guidelines for evaluating drivetrains for the NaS Fiesta have been enumerated in previous paragraphs. These guidelines include the capability of meeting CVS drive cycle accelerations, the minimizing of initial drivetrain cost, the suitability for use with regenerative braking, and the use of a manual transmission, as well as the usual criteria of adequate technical performance, good energy efficiency, reasonable size and weight, packageability, and controllability for good vehicle driveability. Suitability for "near-term" (early 1980's) was also considered to be an important criterion.

Many types of motor/controller systems are suitable for EV application from purely technical considerations. Of the many systems studied with varying degrees of intensity, five systems were considered to meet the guidelines listed above and were evaluated further on the basis of initial cost. Of these five systems, two were evaluated in considerable detail and will be described below.

1. DC Commutator Motor Systems

This is by far the most common system used in all types of electric vehicular drivetrains today, from golf cars to electric trains. Most existing electric cars are powered by this class system. Four motor controller configurations have received the most attention for EV applications:

a. Separately excited motor; armature chopper; field chopper; fixed ratio transmission

b. Series motor; chopper control; fixed ratio transmission

c. Series motor; chopper control; multi-ratio transmission

d. Separately excited motor; one stage of battery switching using mechanical contactors; field chopper; multi-ratio transmission.

The second and third configurations have been the most widely used in EV's, and a considerable amount of "off-the-shelf" hardware exists from the golf cart, lift truck, and British milk truck industries that can be adapted for EV application. Configurations a and b have both been used in EV's [10], giving rise to the infinitely variable vehicle control discussed in the previous section. The fourth configuration generally cannot be applied in an EV without a multi-ratio transmission. It has been proposed for EV application relatively recently as a means of eliminating the high costs of power semiconductors required in the first two configurations.[10], [12] A qualitative comparison of the four common DC commutator motor configurations listed above is given in Table V-2.

TABLE V-2 — COMPARISON OF DC COMMUTATOR MOTOR CONFIGURATIONS

Systems a and b:	Series or separately-excited motor, power semiconductor choppers, fixed-ratio transmission
Advantages:	Infinitely smooth vehicle speed control; relatively high energy efficiency; all-electronic control; more flexibility in packaging (without transmission); requires only two battery power leads; full control over entire motor torque/speed map.
Disadvantages:	Requires motor with higher torque capability than system using multi-ratio transmissions; likewise, current rating of controller is higher; high initial cost due to cost of power semiconductors; requires large battery filter if high efficiency advantage is to be achieved; generally heavier than other systems; more susceptible to EMI; likewise, puts out more audible and electro-magnetic noise.
System c:	Series motor, power semiconductor chopper, multi-ratio transmission, contactors for field
Advantages:	Good reversal energy efficiency with a manual transmission; full control over entire motor torque/speed map; less costly than Systems a and b, lighter than Systems a and b, requires only two battery power leads; vehicle reversed

TABLE V-2 COMPARISON OF DC COMMUTATOR MOTOR CONFIGURATIONS

	by means of transmission; some commercial equipment and components available for this type of control.
Disadvantages:	Cost penalty of power semiconductors; some time delay during transistion between motoring and regenerative operation; considerable battery filtering required; susceptible to EMI; generates some audible and electro-magnetic noise; high motor speed with motor in neutral.
System d:	Separately-excited motor; two-stage battery switching to armature; chopper field control; multi-ratio transmission
Advantages:	Has potential to be lowest cost, lowest weight system in DC commutator motor class; simple electrical circuit; requires no battery filtering; least audible and electro-magnetic noise; smooth transition between motoring and regenerating.
Disadvantages:	Somewhat lower energy efficiency than other systems according to present calculations; low speed operation of the motor is not possible, and an idle or "base" speed is required; requires battery switching in most applications; battery switching increases the number of power leads out of the battery; vehicle durability may be more of a problem than in other systems.

A more quantitative comparison of three of these DC commutator motor configurations (Systems a, c, and d) is given in Table V-3. Two types of brushless machines are also shown in this comparison. This comparison has been calculated for a Fiesta vehicle (2650 lb. weight) with a 100 mile range on the CVS Cycle. Other assumptions used in preparing Table V-3 are listed.

TABLE V-3 – COMPARISON OF DC COMMUTATOR AND BRUSHLESS MACHINES

	CONTROLLER		MOTOR			TRANSMISSION			DRIVETRAIN SYSTEM		
MOTOR	Type	Wt (lbs)	RPM	H.P. (Cont.)	Wt (lbs)	Type	Ratio	Wt (lbs)	Wt (lbs)	Cost ($)	Eff.
DC - Shunt	Contactor/ Field	40	10000	25	100	Man	3.58/2.06 1.29/1.0	60	200	520	.66
DC - Shunt	Contactor/ Field	40	6000	25	125	Man	3.58/2.06	60	225	570	.66
DC - Shunt	Armature/ Chopper	70	10000	25	122	Fixed	2.71	37	240	1078	.72
DC - Shunt	Armature/ Chopper	70	6000	25	174	Fixed	1.625	37	290	1209	.72
DC - Series	Chopper	50	10000	25	100	Man	3.58/2.06 1.29/1.0	60	220	604	.68
PM	Inverter	80	24000	25	25	Man	3.58/2.06	60	115	905	.72
Disc	Chopper	60	6000	25	60	Man	3.58/2.06 1.20/1.0	60	190	582	.70

Assumptions

1. Fiesta Car; 65 MPH top speed for 10 minutes
2. Max. power required = 44 HP for 1 minute
3. RPM BRK = 0.35 RPM Max
4. TEMAX = 960 lbs
5. DC motor wt = K x $T^{O.T.}$ (T in ft - lbs)
6. Regeneration
7. Controller costs based on 100,000 controllers/y
8. DC motor cost = $3.30/lb x 1.1 if high speed
9. Other costs & wts based on "EV Systems Study" (Ref. #9)
10. N/V = 56.8
11. Efficiency is the product of motor, controller, and transmission energy efficiencies during CVS driving.
12. Battery waveform - smoothing filter weight included in Systems 3-7.

The technology for all four of the above DC commutator motor configurations, as well for many variations of these configurations, is well developed. All four systems have been used in electric passenger cars or vans. A great many chopper circuits using power SCR'S have been developed and these offer a wide variety of characteristics for both armature and field control. These are well discussed in the literature and except for the series motor/controller,

will not be further discussed in this report. References 5, 6, 9 — 12, give descriptions of several other types of chopper circuits. Power transistors and Gate Turn-off SCR's are suitable for the lower-current field chopper service today. In recent years, several very high current power transistors have been developed. It has been proposed that these devices may offer a considerable cost reduction in the initial cost of armature choppers or series motor choppers due to the elimination of the commutation circuitry required in SCR choppers.

The characteristics of three high power transistors are given in Table V-4

TABLE V-4 — HIGH POWER TRANSISTOR CHARACTERISTICS

	Toshiba	RPM	GE
Max. Voltage (V_{ceo})	300	120	400
Max. DC Current ($I_{c\text{-}ave}$)	400	200	350
Current Gain (h_{FE})	100 (I_c = 400)	1000 (I_c = 200)	5000
Power (P_T)	2500	500	Unk.
Pulse Frequency	0.3 MHz	Unk.	1 MHz

The RPM device has been used in armature choppers for lift-truck applications, but it is understood that manufacture of this unit has been discontinued. The GE device has been developed under a DOE contract and is not commercially available at the present time. High power transistors in armature chopper applications offer some simplification in circuitry, weight reduction, and high chopping frequencies as compared to SCR choppers. However, conversations with GE engineers and marketing people indicate that the total cost of a transistor armature chopper will probably be little different than the total cost of an SCR armature chopper for

many years ahead. Therefore, the cost penalty of the systems requiring high-power semiconductors noted above will probably remain for some time.

A final word concerning this class of systems concerns the brush/commutator system of the motors, the principal identifying feature of this class of machines. The brush/commutator system is often the design feature that limits motor torque and/or speed, and has long been considered the principal disadvantage of these machines. This has fostered continued development of the "brushless" class of DC machines (which are really synchronous machines with electronic commutation). Some of the brushless DC machines are received in this report. However, for many years, most traction motors in all applications have been of the commutator type. Therefor, the brush/commutator system cannot be considered too much of a limitation. Even more surprising is the fact that although the "brushless" motors themselves are usually lighter (lower specific weight) and less costly than DC commutator motors, the cost — and sometimes even the weight — of the electronic control required for brushless systems usually far exceeds that of the DC commutator motors. This is observable in the comparisons shown in Table V-3. However, in recent years, the brush/commutator system has not received enough research and development aimed specifically at traction motor applications. This class of motor could probably be improved considerably, in terms of its lifetime, reliability, and efficiency (i.e, reduced losses). The General Electric "Cortina" motor, which will be described in this report, and recently developed motors of the Garrett Corp. are examples of good brush/commutator system design. Further studies of improved brush/commutator designs might give a considerable improvement in DC commutator

performance at a very low cost.

2. DC Homopolar Motors

The homopolar machine is based upon the principles of the Faraday Disc and has long been proposed for EV use. Commercial homopolar generators are known as Acyclic generators and are used as sources for very high DC currents in such applications as aluminum refining. The homopolar machine consists of a rotating solid magnetic cylinder excited by a very simple winding solenoidal in shape. Therefore, it has potential as a low cost machine. It also has low specific weight and operates at high efficiency. The principal limitation in the development of this machine for traction applications has been the high-current, high-speed liquid metal slip rings required for current collection in the rotating cylinder or armature of the machine. The best embodiment of these slip rings has used liquid metal systems. However, the technical problems associated with high-speed liquid metal slip rings have not been fully solved and this approach has placed a cost penalty on the machine.

The homopolar motor is the only true DC machine, that is, armature and field currents are steady and unidirectional and no commutator or electronic switching devices are required. It is also inherently a low-voltage, high current machine and is therefore well matched to battery energy sources. With all of these favorable attributes, it is surprising that it has not found more of a place as a potential candidate for EV drives. As part of an extensive study in the 1960's, (13, 14) the Ford Research Lab designed, built, and tested several homopolar configurations for traction applications. The principal effort of this study was directed towards an "electric transmission" to replace conventional transmissions. However, much of the work

is applicable to EV drives. For the transmission applications, a homopolar motor was built and tested with a specific weight of approximately 0.7 pounds per horsepower (peak); for reference, the specific weight of the DC commutator Cortina motor is about 1.5 pounds per horesepower (peak). Most DC commutator motors have specific weights of from 2-4 pounds/peak horsepower. Efficiencies of 80% - 90% were achieved at these power levels. The controlled speed range was 4:1. A recent Ford patent [15] describes another homopolar motor configuration in which the motor assembly is integrated into the sodium-sulfur battery assembly, with the potential for considerable weight savings, reduced power loss in connecting electrical conductors, and improved thermal management for a vehicle with a high temperature battery source.

The homopolar motor cannot be considered for near term EV application and therefore was not seriously evaluated for this study. However, it shows much promise for long range electric and hybrid vehicle applications and should receive more study and developmental effort.

3. Brushless Synchronous Motors (Permanent Magnet Motor)

Another important class of motors for potential EV application is the brushless synchronous class, i.e., synchronous machines operated from a DC source by means of electronic control. These systems are discussed in some detail in Reference 9. There is one type of these motors that is in limited production for variable speed applications. Reluctance synchronous motors are used in many applications in the textile industry and are generally lighter weight, more efficient, and have improved speed control characteristics compared to the induction motor drives they are gradually supplanting. However, existing machines are industrial designs and generally not suitable

for traction applications. Another motor type, the homopolar inductor motor, has been used successfully in several electrical vehicle drives for the US Army.[16]

At the present time, the most promising motor type in this class appears to be a permanent magnet machine. Several configurations are under investigation and in various stages of development, including the Turner Claw Motor,[17] and configurations at the General Electric Research Center and at the Garrett Corp. The Turner motor has been investigated as a possible candidate for the NaS Fiesta. However, it is considered to have several deficiencies in its magnetic circuit design that will result in high leakage (resulting in high input currents and poor equivalent power factor) and high eddy current losses. Although it has been used in an electric bicycle, there are still some basic design problems to be solved before it can be considered as a viable EV motor.

The Permanent Magnet motor does have the potential, though, for very low specific weight and probably the highest average energy efficiency of any class of machines. At the present though, the use of high energy-product magnets, such as platinum-cobalt or the Rare-Earth-Cobalt magnets,[18] are required to achieve these excellent operating characteristics. At the present time, motors using such magnets are quite costly. The data prepared for Table V-3 in which the permanent magnet system is compared with other traction drives, was based upon these costs and upon performance characteristics presently available in various aerospace PM machines. Obviously, this class of motor deserves a lot more development, and has potential for EV use.

The other cost limitation on systems using any of the brushless synchronous machines is the cost of power semiconductors. With few exceptions, a full two or three phase inverter is required for control of this class of machines from a battery energy source, and, in general, a minimum of six high-power semiconductors is required for such systems. Therefore, the controller costs (and operating complexity) is always higher than for the DC commutators motors, DC homopolar motors, and the Ford Disc Motor. Therefore, the applicability of brushless synchronous machine for EV applications is almost exclusively a function of power semiconductors costs.

4. Permanent Magnet Commutators Motors

This class of motor is often called the "printed circuit motor," and is a disc-shaped device widely used in control and low power (under 5 HP) applications. In the larger sizes, the conductors are "stamped" rather than "printed." The commutation process takes place on the conductors themselves, eliminating the separate commutator/brush assembly of the conventional commutator motor with obvious savings in size and weight. A beefed up version of this configuration has recently been developed by Campbell [19] and is proposed for EV applications. Generically, this is identical to the DC commutator motors discussed under paragraph B.1 in this section, with the wound field replaced by a permanent magnet field. Therefore, the use of "field control" in any form is not possible and speed and torque control must be through armature current control. Control-wise, the Campbell motor is analogous to System 1 with a fixed, separately excited field. The Campbell motor uses a separate commutator/brush assembly rather than the simpler technique applied in printed circuit machines. There

are certain advantages to the disc-shaped construction: lower windage losses, generally low rotating inertia, high speed operation (since there are no conductors on the rotating element), and the possibility of integration into a vehicle wheel assembly. The Campbell motor is a viable candidate for future EV applications.

5. Ford Disc Motor

This is a disc-shaped reluctance motor operated from a DC source by means of high-current pulses. Along with the homopolar DC motor, it is among the simplest and lowest cost motor configurations conceivable and does not require any brushes or slip rings. Prototypes have been developed and tested at the Ford Research Lab and are described in References 9 and 20. The principal merits of the Disc Motor are:

a. Simplest and least costly motor structure

b. Low-cost electronic control, almost idential to that required in armature control of a DC commutator motor

c. Can regenerate using the same electronic controller as required for motor operation; this requires fewer power semiconductors than a DC commutator motor with armature control when regeneration is required

d. Low windage loss

e. High average energy efficiency

f. Low rotating inertia

The principal problems of this configuration are:

a. It is still in the developmental stage; requires housing development for practical application

b. Audible noise problems

c. Lower low-speed torque than DC commutator motors

Of the truly brushless configurations, the Disc Motor and the synchronous permanent magnet motor care considered to have the greatest potential for long-range EV applications.

6. Cage Induction Motors

A number of EV drivetrains have been built using a high-quality polyphase squirrel-cage induction motor controlled by a full-wave polyphase electronic inverter from a battery source.[21, 22] A decade or so ago, this type of electric drive-train was considered to be the eventual replacement for DC commutator motor drives. However, experience from the drive-trains that were built and subsequent analysis has shown that the cage induction motor is not well suited for this application, even though it is basically a low-cost motor and probably in more wide-spread use in industrial and residential applications than any other type of motor. In general, its efficiency is below that of several types of synchronous machines due to high rotor losses. Further-more, it is more difficult to control from a solid-state inverter, plus the fact that SCR inverters driving induction machines require more commutation circuitry than with synchronous machines, and induction motor construction costs are higher than those of reluctance, inductor and permanent magnet (using conventional magnets) synchronous machines. Reference 9 gives a thorough comparison between induction motor traction drives and those using DC commutator machines, Ford Disc Motor machines, and inductor synchronous machines. Therefore, induction motor drives have not been seriously evaluated for this study.

C. ELECTROMECHANICAL DRIVES

There is a host of drive schemes proposed for EV application that attempt to minimize the amount of electronic control required in hopes of minimizing system cost. Some of these schemes go back to the early days of electric train and streetcar control and are well tried as far as any technical problems are concerned:

1. Battery Switching

This is one of the oldest control methods used in electric drive-trains and has many merits. It consists of an array of contactors that reconnect a number of batteries, usually in a minimum of four series/parallel combinations, to the armature of a separately-excited or series DC commutator motor. With a separately-excited motor, some amount of field control is often used, and the field/contactor scheme described as System d in Table V-2 is a modified battery switching scheme with only two stages of battery switching and full field control. The disadvantages of straight battery switching for EV control are the jerkiness in vehicle driving that results, possible time delays in contactor switching that might further impair vehicle driveability, and, especially where high temperature batteries are used, the large number of power conductors into the battery which results in an excessive heat transfer from the battery. However, at the same time, it is probably the simplest, lowest-cost, and most efficient means of motor control when ambient-temperature batteries are used.

2. Countertran

This is a DC commutator rotating machine with two sets of counter-rotating brushes in addition to the conventional set of

brushes. [23] In this configuration, often called a DC rotating transformer, the conventional brushes are connected to the source battery and the two sets of counter-rotating brushes provide a variable voltage supply for armature control of a DC commutator drive motor. The Countertran has full four-quadrant control (positive and negative motoring and generating control) with no added circuitry. Control is infinitely variable, including the transition between motoring and regenerative braking. The cost, weight, and efficiency of a Countertran unit are roughly comparable to the motor it is controlling; hence, such a controller would be heavier and less efficient but less costly than an equivalent electronic controller. Generally, the Countertran falls into a class of rotating machines known as Metadynes, the best known example of which is the Amplidyne. Metadynes have long been proposed for traction drive control and have been applied in some European railroad applications. Besides a small weight and efficiency penalty when compared to electronic control, this class of controllers also has exaggerated brush/commutator problems that often result in high maintenance costs. Also, the speed of response of the control is longer than electronic control systems. Until there is some definitive practical operating experience in an EV with this type of control, a good comparison with most of the other types of control described above is not very realistic.

3. MTI Motor-Transmission System

This is a combined electromechanical motor/controller unit that offers infinitely-variable control over four-quadrants with only low-power field control required electronically. Although a great number of mechanical configurations are possible, that

shown in Figure V-3 seems to be the preferred configuration by the developers.[24] In Figure V-3, units 1 and 2 are in the same outer housing. Unit 1 is operated much like a conventional DC commutator machine, with a rotating machine armature and commutator and a fixed field and brush structure. The field of Unit 2 is mounted on bearings and is driven by the armature of unit 1; the armature and commutator of Unit 2 are also mounted on separate bearings and can rotate at an independent speed. The electrical connection to the armature is through bushes mounted on and rotating with the field. Slip rings are required to connect both the field and the armature brushes with the stationary outside world. A small prototype unit has been built and successfully operated by the developer, Mechanical Technology, Inc.

The electrical connections are as shown in Figure V-4, with both armatures connected directly across the battery source. The

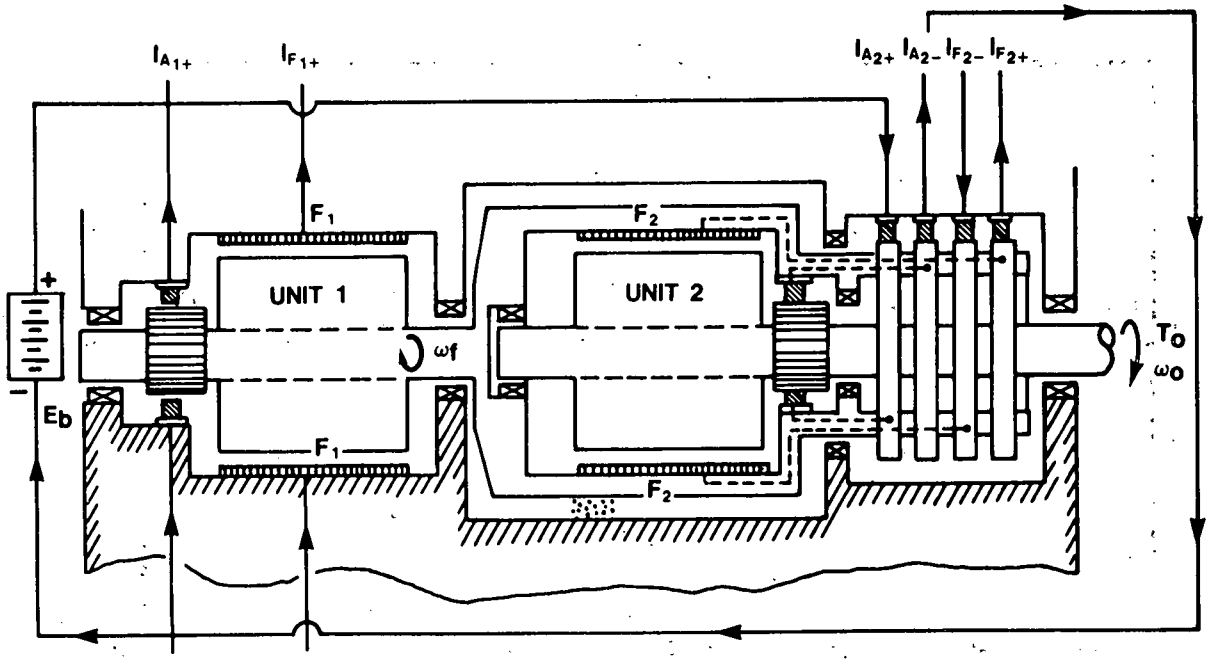

Figure V-3 Current Flow in Mechanical Technology, Inc., (MTI) Transmission

principal merit of this scheme is that the low-speed, high torque (or starting) motor operation can be achieved at high efficiency and without the excessively high currents resulting from field/contactor control and without the use of high-power semiconductors.

Since the power flow among the many members of the motor-transmission is rather complex during this mode of operation, it will be explained with the aid of the schematic power flow diagram shown in Figure V-4: Assume that the output shaft is driving the vehicle differential at a very low speed, ω_o, during startup and supplying torque, T_o. The field structure, F_2, will be rotating in the same direction at a much higher speed, ω_f, and driving the directly-connected armature, A_1, while field, F_1, is stationary. With both field currents, I_{f1} and I_{f2}, at their proper values, power is supplied to the system through armature current, I_{a2}, and input power is equal to approximately $E_b I_{a2}$. Part of this power ends up as the output

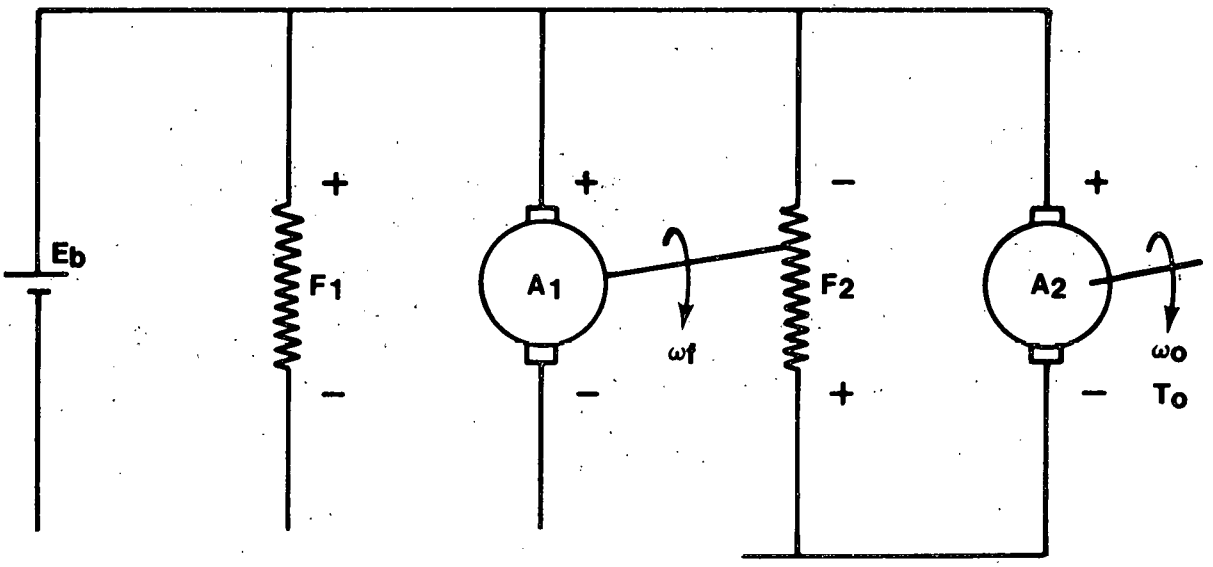

Figure V-4 Electrical (Connections) in MTI Motor-Transmission System (Ref. Fig V-4)

power, $T_o \omega_o$. The remainder is used to drive the field structure, F_2, which in turn drives the other armature and Unit 1 acts like a generator returning power into the battery. Neglecting losses, the output power is the difference between $E_b I_{a2}$ and $E_b I_{a1}$. A calculation on a unit sized to drive the NaS Fiesta showed that under the low speed condition of ω_o = 50 rad/s (477 RPM) and T_o = 80 n-m (59 ft.-lb.), I_{a2} = 118 Amps. when F_2 was rotating at 249 rad/s (2380 RPM) and 5000 watts were being returned through I_{a1}. If an armature chopper control scheme were used with the identical motor, the required armature current would be over 200 Amps. In a contactor/field control scheme, a higher current would exist.

There are many other operating modes possible with this motor-transmission system, and at a higher speed, lower torque conditions, the output is supplied only with the use of Unit 2 with its field structure locked stationary by means of a clutch.

The goal of this development has been to eliminate the need for either armature chopper control or a mechanical transmission and still achieve infinitely-variable speed control. However, preliminary calculations show that, in order to achieve full speed control over the entire speed range of the NaS Fiesta as presently specified, the total weight of the required motor-transmission system would be in excess of any of the DC commutator motor systems described in Table V-2. And there are other advantages of this system:

a. The efficiency increase at the low-speed, high-torque condition is not as great as might be expected due to the losses associated with the power circulation through Unit 1.

b. Excessive windage losses associated with the rotating field structure.

c. Many problems associated with rotating the high-inertia field system.

d. Many problems with the large number of brush/commutator and slip ring systems.

e. An unknown assembly cost.

D. DRIVE SYSTEM FOR THE NaS FIESTA ELECTRIC CAR

From the analysis of various types of EV drivetrains, some of which has been summarized in Table V-3 it was concluded that the field/contactor system, discussed in Table V-2, shows the most overall potential for near term electric vehicles. The principal advantages of this system are its low cost and its capability in the regenerative braking mode. At the same time, it was recognized that there are several technical problems associated with this control scheme and that there has been relatively little practical experience in EV's with this type of control. Therefore, an alternate control scheme, the tried and true series motor system, has been studied throughout this program and compared with the field/contactor system in more detail. Since a commercial controller for the series motor system is available with a rating suitable for the chosen Fiesta drive motor, this control system might have an additional advantage for near term prototype construction.

E. PRELIMINARY DESIGN AND ANALYSIS OF THE FIELD/CONTACTOR SYSTEM

The term, "field/contactor', has been coined to describe the two major elements used in this control scheme: (1) controls of the machine's field current, and (2) contactors to reconnect the bat-

teries to give different output voltages. The third distinguishing feature of this type of control is the manner in which the field windings are connected with respect to the armature windings of the DC commutator machine. In field/contactor control, the field is said to be separately excited, that is, the field is excited or energized from a separate power supply than that supplying the armature. In modern field/contactor systems, the field power supply is an electronic system called a DC chopper, and is a low-power version of the armature choppers used for armature control. Historically, in this type of control, the field circuit was connected in series with a variable resistance and this combination was connected electrically in parallel or "in shunt" with the armature circuit, and the system was called a shunt machine. Contactors are electrical switches or contacts controlled by solenoids from a separate control source. Contactors are an established product used in the related golf cart, lift truck, and electric milk truck applications. They are light weight, rugged, very efficient, and relatively low-cost components. The field chopper can likewise be a relatively light weight, low cost item. The power requirements of the field circuit in a typical separately excited machine are from 1 - 3 KW. Hence, the current rating of the power semiconductor required for a chopper operating off a 100-volt source is approximately 10 - 30 A. This permits the use of low-cost, mass-produced transistors, SCR's, or GTO's. The power circuit for the proposed NaS Fiesta drivetrain is shown in Figure V-5. The contactors used to change the battery connections from series to parallel are shown on the left side of Figure V-5. The choice of the three-sectioned battery shown, giving the two possible voltages of 32 and 96, was dictated by considerations of the battery housing and thermal management and is discussed

elsewhere in this report. From purely drivetrain considerations, there are both merits and problems associated with this choice as compared to the use of a two-sectioned battery giving 48 v and 96 v. The principal disadvantage is the need for six rather than four power cables between the battery housing and the contactors, which increases thermal management problems of the battery. The effect of this battery connection on the motor performance is discussed below. In Figure V-5, R_1 is an external armature resistance used to reduce surges in armature current during contactor switching; during all other operating conditions, R_1 is shorted by contactor, C_7. M_1 and M_2 are manually operated switches to insure personnel safety while the drivetrain is being maintained or to provide a manual disconnect in case the automatic protective features built into the electronics fail to operate properly. Fuses are also provided for overcurrent protection. The diode, D_1, often called a "free-

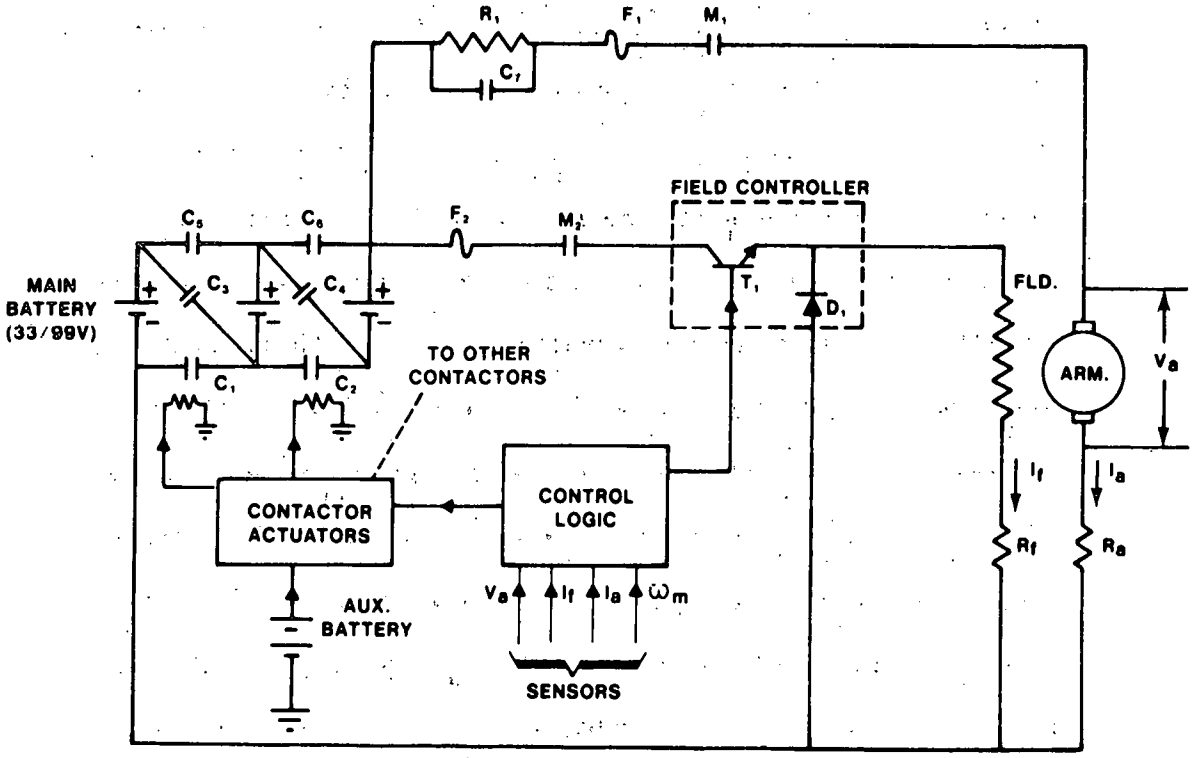

Figure V-5 Schematic of Contactor — Field Motor Control

wheeling" diode, is used to improve the wave form of the highly inductive field circuit and to reduce voltage pulses on the power semiconductor, T_1. It is assumed that reversal of the vehicle will be accomplished by means of the mechanical transmission as in a conventional vehicle, although this could easily be accomplished by reversing either the machine field or armature windings. There are no changes in the circuitry shown in Figure V-5 for either motor or generator operation of the DC commutator machine. Changing from motoring to regenerative braking or vice versa in a vehicle with field/contactor control is a smooth transition and is accomplished by varying the magnitude of the field current, I_f.

It is theoretically possible that the vehicle and the motor could be started from standstill simultaneously, at least with the use of the armature resistance, R_a. This method of startup is possible with armature chopper control and is one of the advantages of this type of control, as has been discussed in Section III-A. However, with field/contactor control, there is very little control available at low motor operating speeds, other than the armature resistance, R_1. Therefore, the vehicle is started with the transmission in neutral and the motor is brought up to a no-load or "idle" speed before the transmission is shifted into a drive gear. This process takes less than a second, as will be shown by dynamic studies described below, so it involves a negligible time delay in startup as compared to vehicle equipped with armature chopper controlled motors. The complete "drive scenario" of an EV equipped with field/contactor control is shown in Table V-5.

TABLE V-5 — VEHICLE OPERATION WITH FIELD/CONTACTOR CONTROL

(Reference Figure V-5)

A. DRIVING

1. Transmission in neutral
2. Turn on ignition switch; manual contacts, M_1 & M_2 closed.
3. Press on accelerator pedal
   a. Field transistor actuated to maximum I_f.
   b. 32V contactors close; I_a builds up — motor speeds up to base speed (less than 1 sec.).
   c. Motor is at "no-load" condition — minimum arm. current; maximum I_f.
   d. Blowers, if required, will be initiated.
4. Shift into 1st gear
   a. Let out clutch slowly and increase accelerator pedal depression.
      . Field weakening — field current is reduced
      . Vehicle accelerates due to motor torque
      . Armature current increases
   b. Clutch slipping until "X" MPH ("X" depends on motor characteristic)
      . Electric motor will have slowed somewhat.
5. Drive as normal car shifting when desireable
   a. Above "Y" MPH or above a certain acceleration setting, batteries will switch to series (96V); control system will re-adjust field current to give identical torque, minimizing jerkiness.

b. If torque demand is reduced, batteries will eventually flip back to parallel — there will be considerable hysteresis in switching of batteries.

c. Note: Vehicle or motor cannot be caused to overspeed under normal conditions since as speed increases (due to decreasing I_f), torque capability decreases.

B. COASTING

1. When there is no accelerator pedal depression, control system will adjust field current so that armature current is zero — hence, no motor torque.
2. Below certain speed, coasting will be impossible. If the batteries are in series, they will be switched to parallel.
3. Note that during coasting
   a. There is very low power dissipation in the drivetrain and this is due to motor field excitation and motor windage and friction loss — this is a motor no-load condition.
   b. There is no regeneration.
   c. There is less drivetrain drag than in an ICE vehicle.

C. BRAKING

1. Step on brake pedal; accelerator pedal has zero depression.
2. Field current increases immediately to produce negative armature current.
3. If brake pedal is further depressed, batteries will be switched to parallel (if not already so).
4. Further depression of brake pedal initiates mechanical braking.

5. If battery should become fully charged, the first section of the control coming out of the brake pedal potentiometer will be eliminated and mechanical braking will start immediately.

6. Below a certain motor speed, regenerative braking will totally disappear. The vehicle speed at which this occurs can be extended by downshifting; the speed for downshifting will be indicated by a signal light.

D. GOING DOWNHILL

1. Motor overspeed protection:

   . If motor exceeds a certain speed, field current is automatically set at max., which will introduce maximum braking.

2. If this doesn't reduce speed sufficiently, mechanical brakes will be called for by overspeed signal.

E. STOPPING

1. When mechanical brakes are called for:

   a. If motor speed is above the minimum speed where regenerative braking is still possible, regeneration will be used as described above.

   b. If motor speed goes below the minimum regen speed in any gear, armature contactors will be opened (or else motoring would commence). The contactor opening will be preceeded by the warning signal described in C-6 above.

   c. Field control will reduce I_f to zero after armature contactors open.

2. Automatic downshifting would be highly desirable during braking.
3. When zero speed is reached, blowers will be shut off when component temperatures fall below prescribed values.
4. There is now zero power dissipation (except for auxiliaries).

Components have been selected for the proposed field/contactor control system. These have been selected for a near-term prototype vehicle rather than for an eventual mass-produced vehicle and therefore the ultimate cost objectives have not been achieved. A specification for a motor suitable for the long-range production objectives is given later in this report. The weight and cost objectives of such a motor are reflected in the comparisons previously given in Table V-3.

1. Motor

Table V-6 summarizes the characteristics of some of the motors that have been evaluated for potential application in the prototype vehicle. All motors listed are existing machines with known characteristics. The first motor was developed by General Electric specifically for EV applications and was used in the late 1960's. Since two of these machines are available, it was chosen for the NaS Fiesta prototype and most of the remaining motor and drivetrain characteristics presented in this report are based upon this machine. Another factor entering into this choice was that a considerable amount of test data was already available from earlier Ford EV development work. The conclusion from this study and many other searches for EV motors is that there is no motor more suitable for EV applica-

TABLE V-6 — DC COMMUTATOR MOTORS FOR POTENTIAL EV APPLICATION

Designation	Wt. (lbs.)	T_{max} (ft. lb.) (one minute)	Break * Speed (RPM)	Max Speed (RPM)	H. P. @ Brk. RPM (one minute)	Volts
GE - Cortina	150	106	6000	10000	121.0	106
GE - Erie	140	52	1800	6000	17.8	48
GE - Fort Wayne	75	42	2200	7500	17.6	24/48
Jack & Heintz	65	48	1800	7000	19.8	48
Garrett/Airesearch	105	44	3200	10000	26.8	106
Siemens 16V1161-Z	198	118	2250	6700	51.0	144
Gould EM1213932	255	80	(series)	4800	-	48
Gould - Post Office	220	75	(compound)		-	72

* Break Speed = maximum speed at which T_{max} can be developed.

tion than this "Cortina" motor. The Cortina motor has a name-plate rating as follows: 40 HP, 96 v, 356, A, 8000 RPM. This is the continuous rating. Much more important for EV operations are the short time (usually one-minute) ratings. Figure V-6 illustrates the full torque vs. speed capability of this motor, assuming no limitations due to the controller or battery. It is seen that the peak one-minute horsepower capability (found by multiplying the torque and speed at the "break point" speed, 6100 RPM) is approximately 125 HP. The characteristic of the Cortina motor with a 44 HP limit imposed by the battery and controller has been shown previously as Figures V-1 and V-2.

With the field/contactor method of control, the torque capability is limited at some speeds below the torques shown in Figures V-1 and V-6. This can best be described with the aid of some analytical expressions relating torque, speed, motor currents, and battery voltage:

The torque developed in a DC machine can be expressed as:

$$T = k I_f I_a \qquad \text{n-m} \tag{1}$$

The induced voltage (or "back emf") in a DC machine is:

$$E = k I_f \omega_m \qquad \text{volts} \tag{2}$$

The battery voltage/motor back emf are related by:

$$V_b = E \pm I_a R_{eq} \tag{3}$$

where the + sign goes with motor operation and the minus sign with generator operation. In the above equations, k is a constant depending upon the internal construction of the specific machine. I_f is the field current, and I_a is the armature current. ω_m is the mechanical speed of the motor shaft in radians/sec., whereas R_{eq} is the resistance in ohms between the battery terminals and the

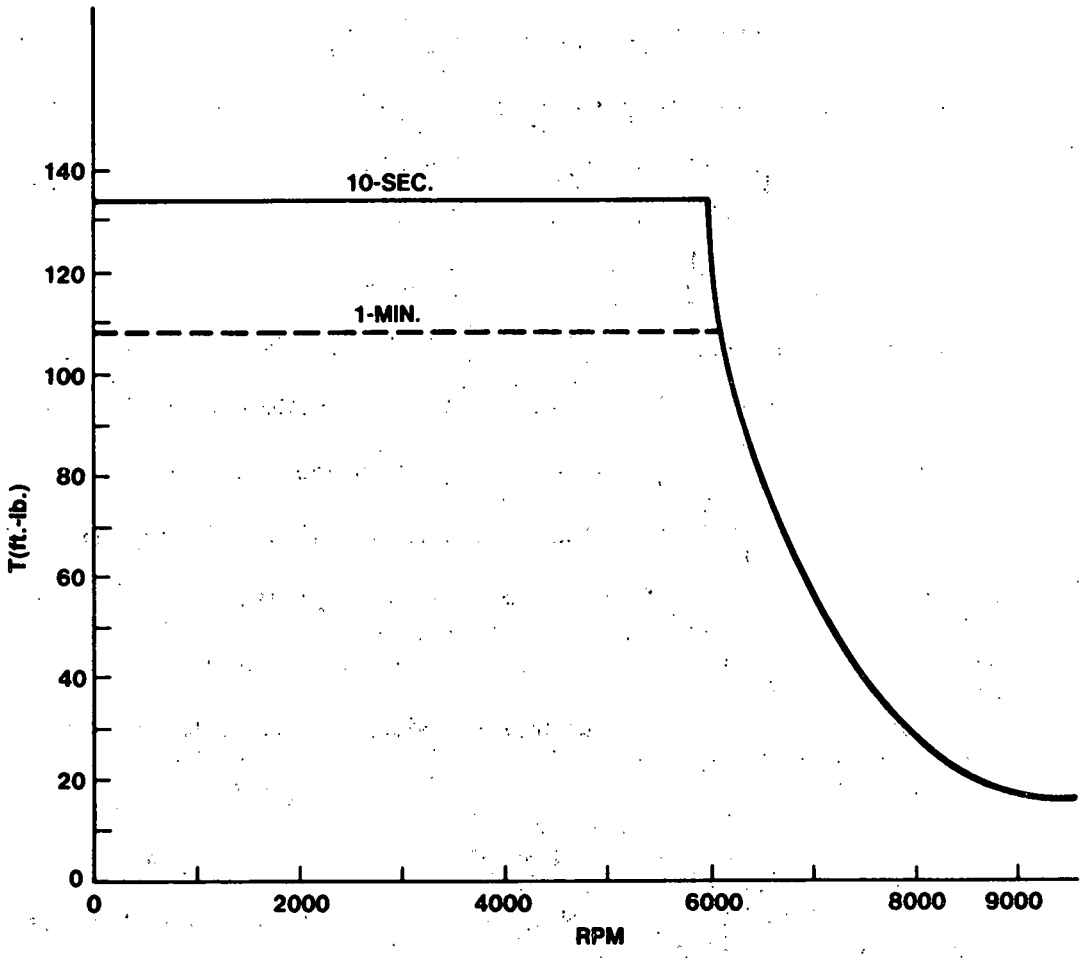

Figure V-6 Cortina Motor Torque vs. Speed Showing 10 Sec. Torque Limit

back emf (mainly armature resistance); and V_b is the battery voltage. Eliminating armature current in these equations gives

$$T = (V_b\ I_f - k\ I_f^2\ \omega_m)\ (k/R_{eq}) \qquad \text{n-m} \qquad (4)$$

Equation (4) shows that the torque produced in a field/contactor-controlled machine is dual-valued, i.e., the same torque can result from two different values of field current. It will be seen that only one of these field currents gives a stable operating condition of the motor. It is also seen from Equation (4) that there is a value of field current for which the torque is maximum. This can be derived by taking the derivative of Equation (4) and setting it equal to zero. The results are:

$$T_{max} = V_b^2/(4\ \omega_m\ R_{eq}) \qquad \text{n-m} \qquad (5)$$

$$\text{Field current at } T_{max} = k\ I_f = V_b/2\ \omega_m) \qquad (6)$$

$$\text{Arm. current at } T_{max} = V_b/(2\ R_{eq}) \qquad (7)$$

$$\text{Back emf at } T_{max} = V_b/2 \qquad (8)$$

$$\text{Efficiency of motor at } T_{max} = 50\% \qquad (9)$$

Equation (4) also illustrates that the torque will become negative under certain conditions. This indicates generator action and the transition between positive and negative torque and vice versa is a smoothly varying function of field current or speed as indicated by Equation (4). The maximum torque condition described by Equations (5) - (9) is the normal operating limit of the motor, beyond which steady-state operation is not possible, although transient operation in this condition is possible and sometimes required. Maximum torque at a given condition of speed is approached by decreasing the field current, which is the main control parameter. The control characteristic is, therefore, increasing torque with decreasing field current, as described in the drive secenario of Table V-5. If maximum torque

is exceeded, this characteristic is altered and becomes decreasing torque with increasing field current, an unstable control characteristic. Therefore, the logic control system must prevent this condition from occuring.

The Cortina motor control characteristics with field/contactor control have been calculated on the vasis of equations (1) through (9) and are displayed graphically in Figures V-7 through V-15. These characteristics have been calculated by means of several BASIC computer routines. The piecewise linear approximation used to describe the motor magnetic circuit relations is given in Figure V-7. The basic torque vs. field

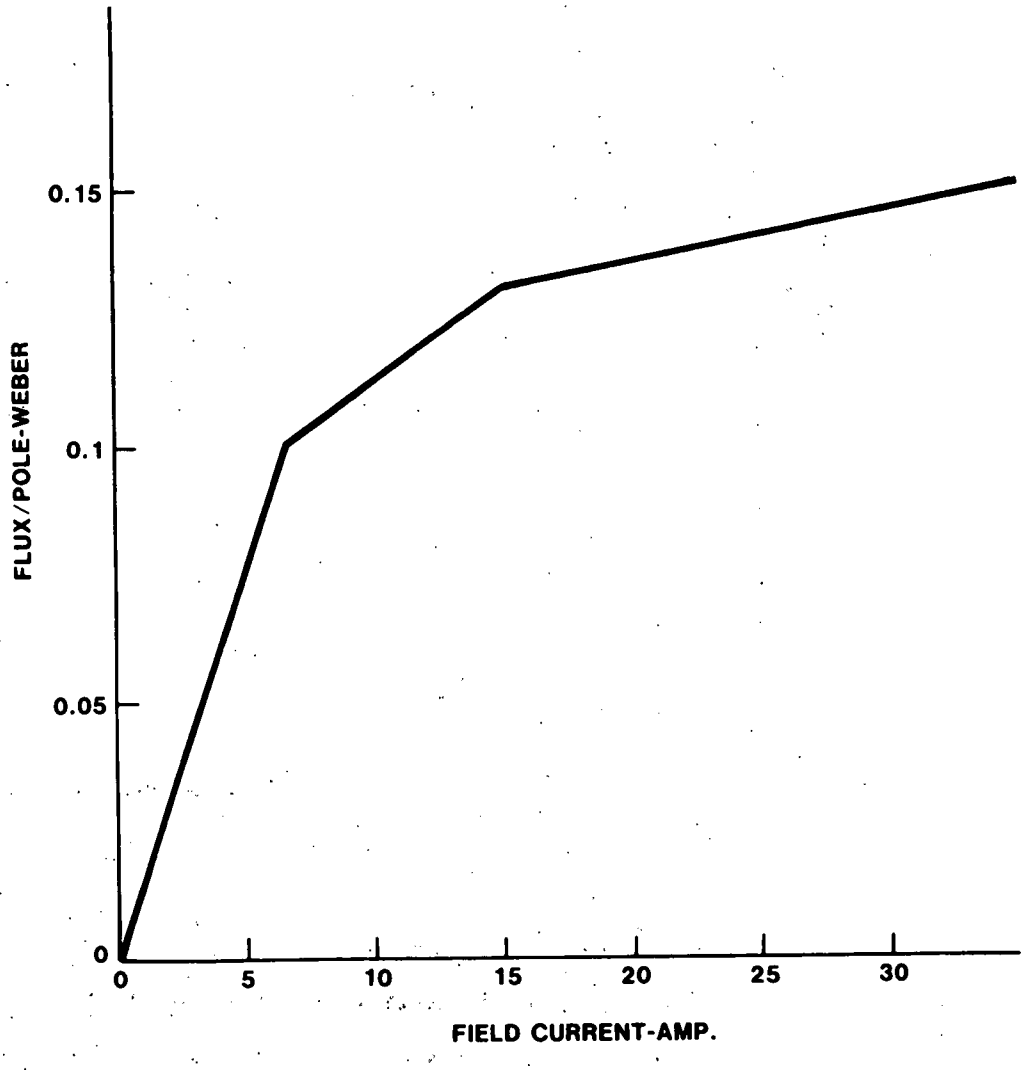

Figure V-7 Motor Magnetic Characteristics

current, or control functions are shown in Figures V-8 through V-10 for battery voltages across the armature of 32, 48, and 96 v, respectively. Figure V-11 illustrates armature current variations with field current at 48 v. Figure V-12 is an effeciency matrix as a function of motor speed and torque. Figure V-13 illustrates the steady-state torque

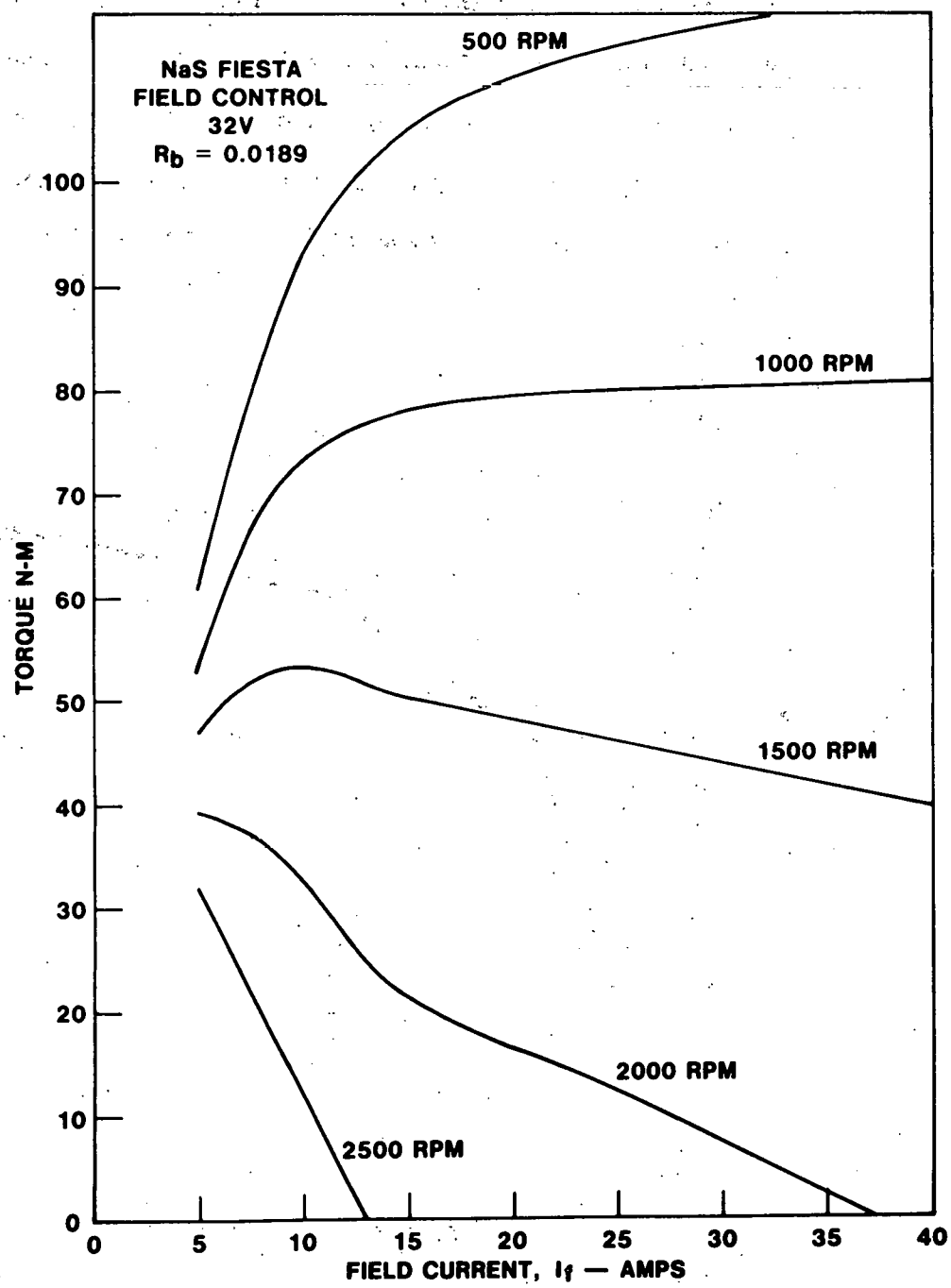

Figure V-8 Field Control (Parallel Connections)

vs. speed regions with field/contactor control. Figures V-14 and V-15 relate this torque/speed characteristic through the transmission and show the actual permissible operating regions of the motor and its controller as a function of vehicle tractive effort and speed, for two different values of N/V (the ratio of transmission output speed in RPM to vehicle speed in MPH). Also shown on Figures V-14 and V-15 are the peak tractive efforts and speeds required for the NaS Fiesta while driving the Federal Urban (CVS) Drive Cycle.

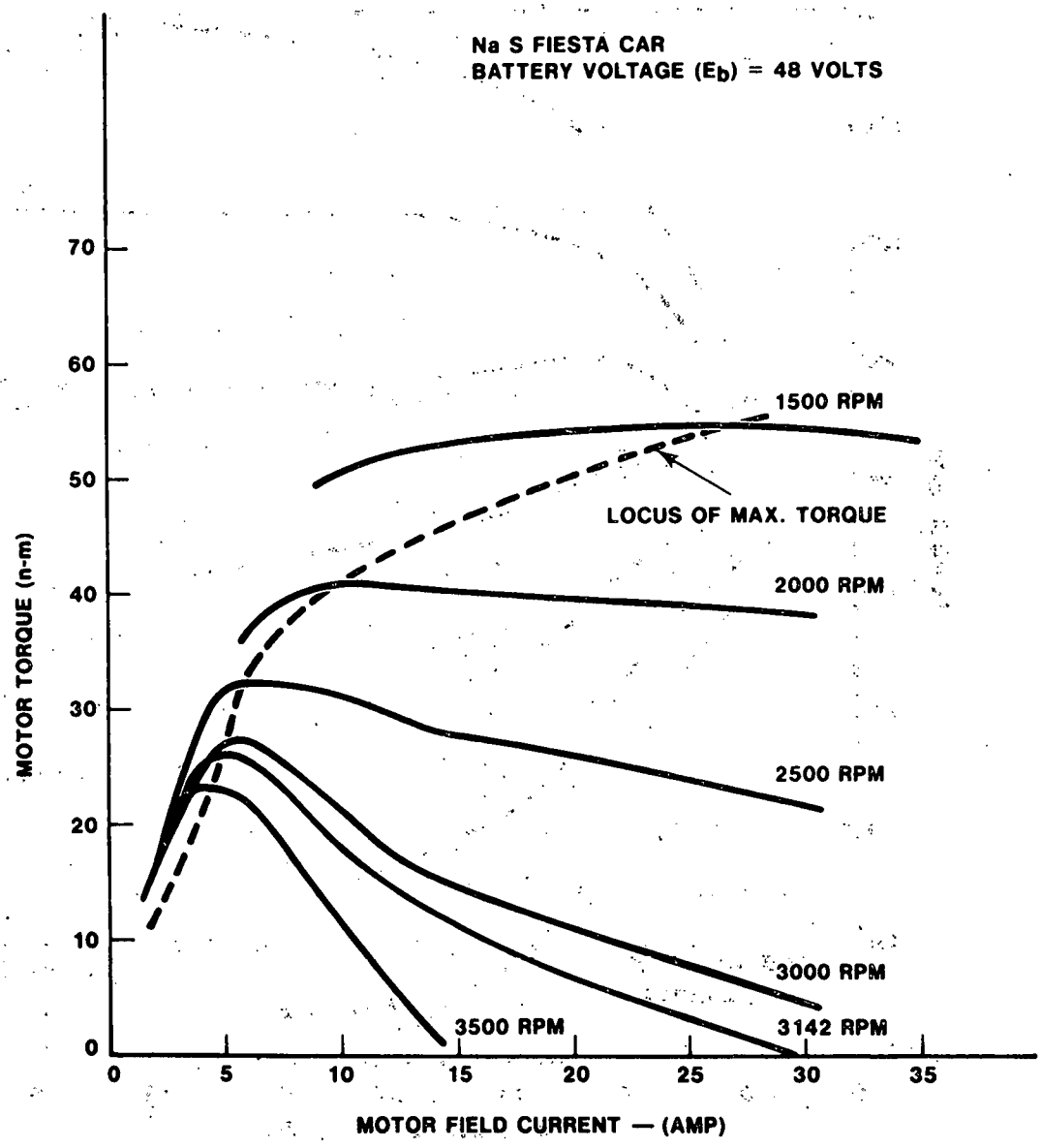

Figure V-9 Motor Control Characteristics

It is seen that the use of field/contactor control reduces the capability of the motor. This reduction is somewhat greater than if series motor control had been used, as will be illustrated below. However, with the use of the proper transmission ratios, good control at all required operating conditions is possible. One of the few EV's using this type of control is the recently developed VW Electric Rabbit, [25] and driving experience with this car indicates that good driveability and rapid response can be realized with this quite simple control scheme.

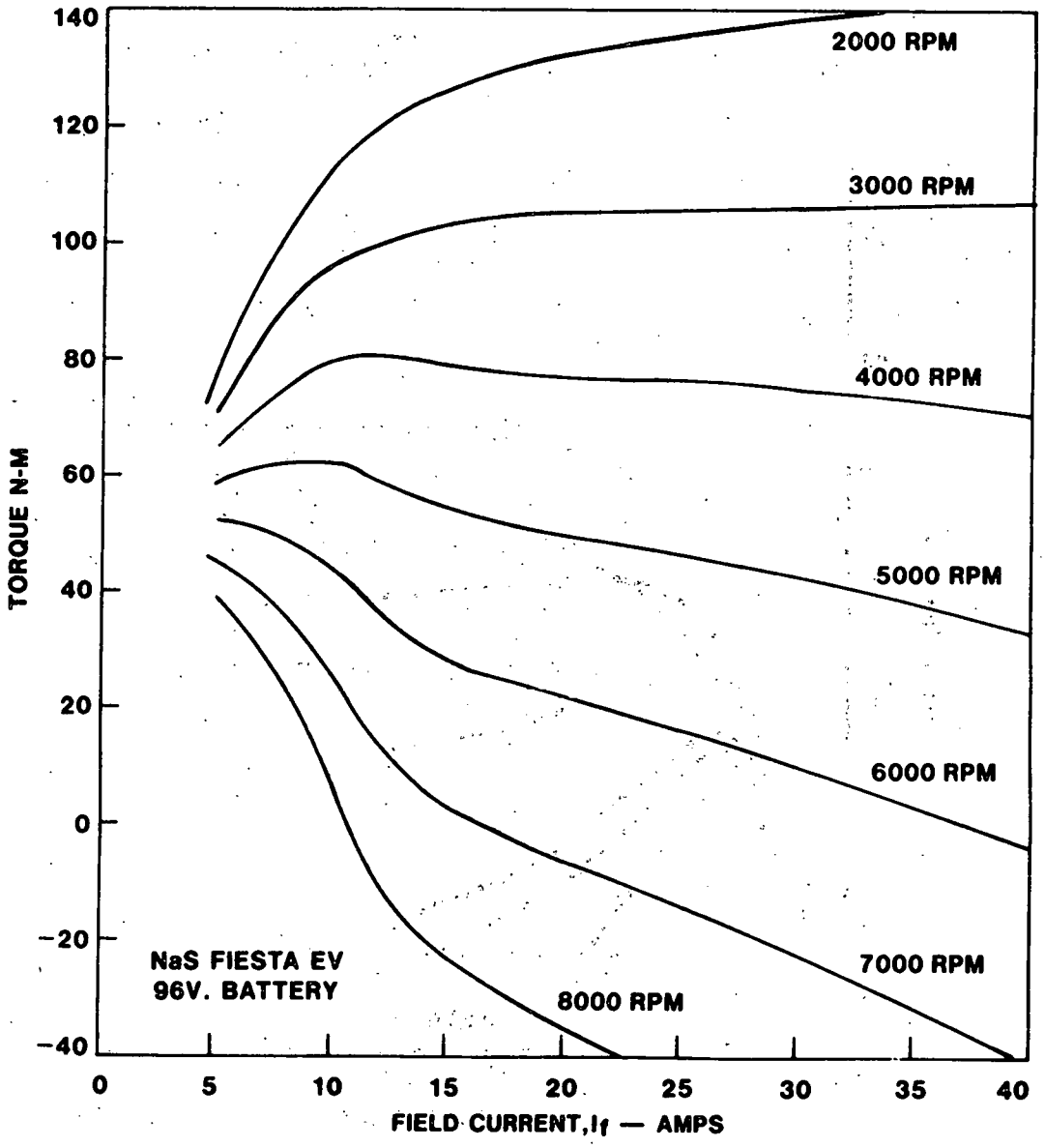

Figure V-10 Field Control (Series Connection)

2. Contactors And Battery Switching Investigation

Several commercial types of contactors are available. Principal suppliers are the General Electric Corp. and Cableform Ltd. of England. Double throw and double pole units are available. Single-pole, single-throw units have been assumed in Figure V-5. The use of the 32/96 volt battery configuration requires more contactors than the 48/96 volt configuration. Other disadvantages of the 32/96

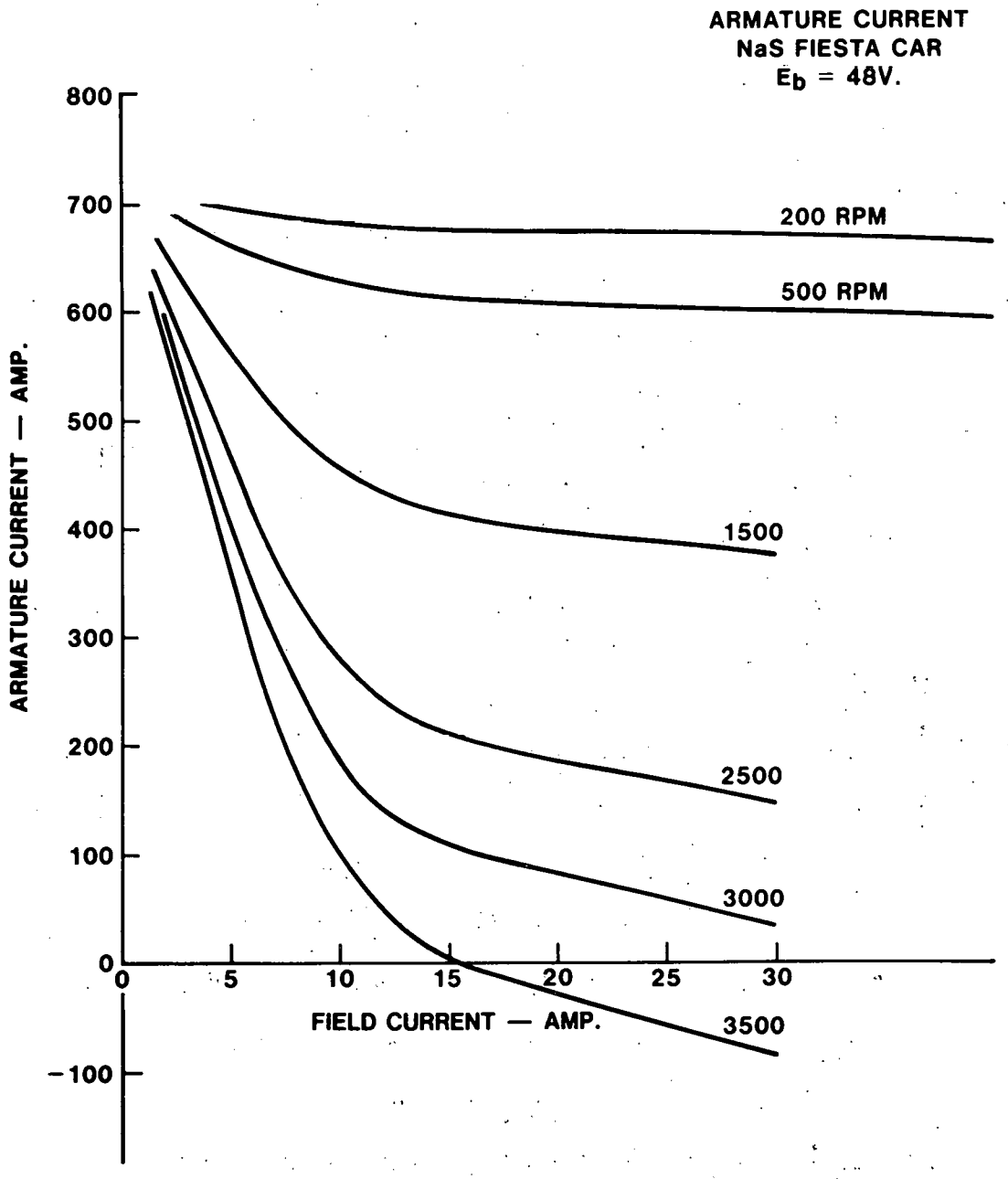

Figure V-11 Field Control (Parallel Connection)

↓T / → RPM	500	1000	1500	2000	3000	4000	5000	6000	7000	8000
10				.50	.60	.80	.48	.82	.83	.8
20				.77	.70	.88	.68	.91	.93	.87
30			.51	.83	.77		.87	.92	.87	.89
40			.63	.80		.83	.89	.84		
50			.70	.61		.86				
60			.74							
70			.68		.76					
80										
90										
100		.55								
110										

TORQUE (FT-LBS)

RPM

Figure V-12 Field/Contactor Motor Efficiency (Motor Only)

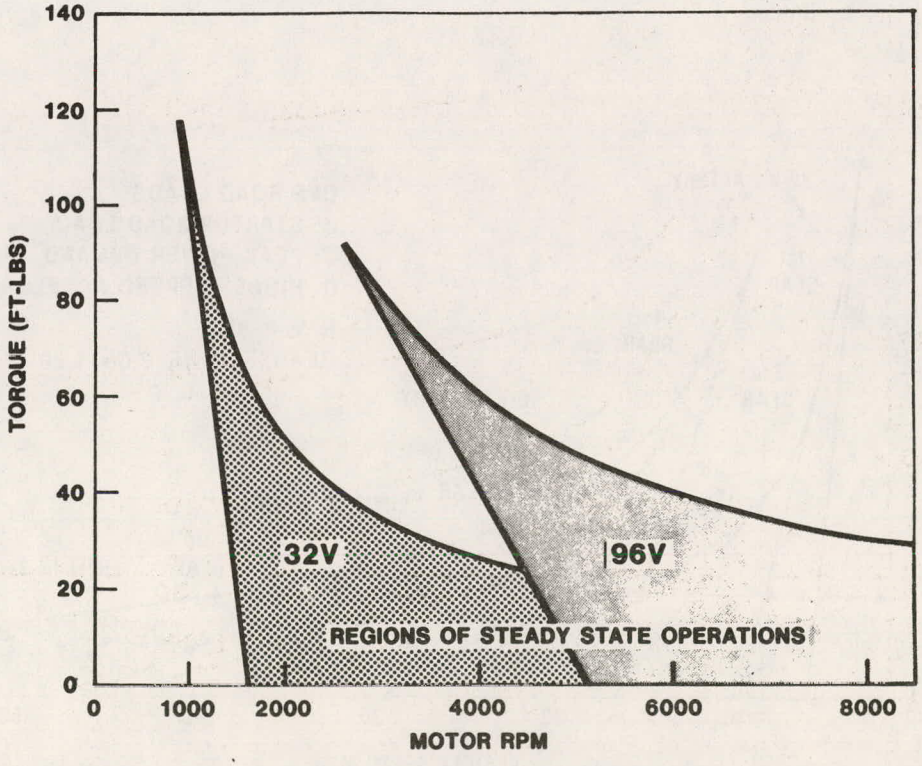

Figure V-13 Field/Contactor Control Cortina Motor Torque vs. Speed

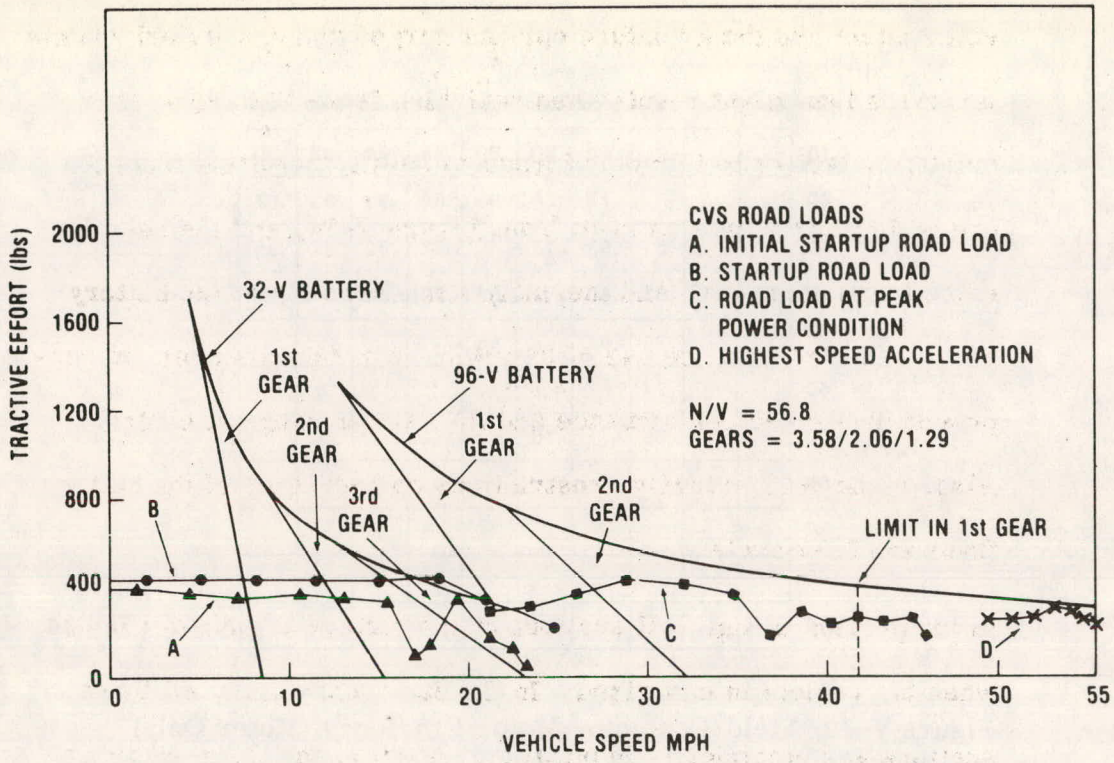

Figure V-14 NaS Fiesta Tractive Effort vs. Vehicle Speed Using Contactor/Field Control & the Cortina Motor

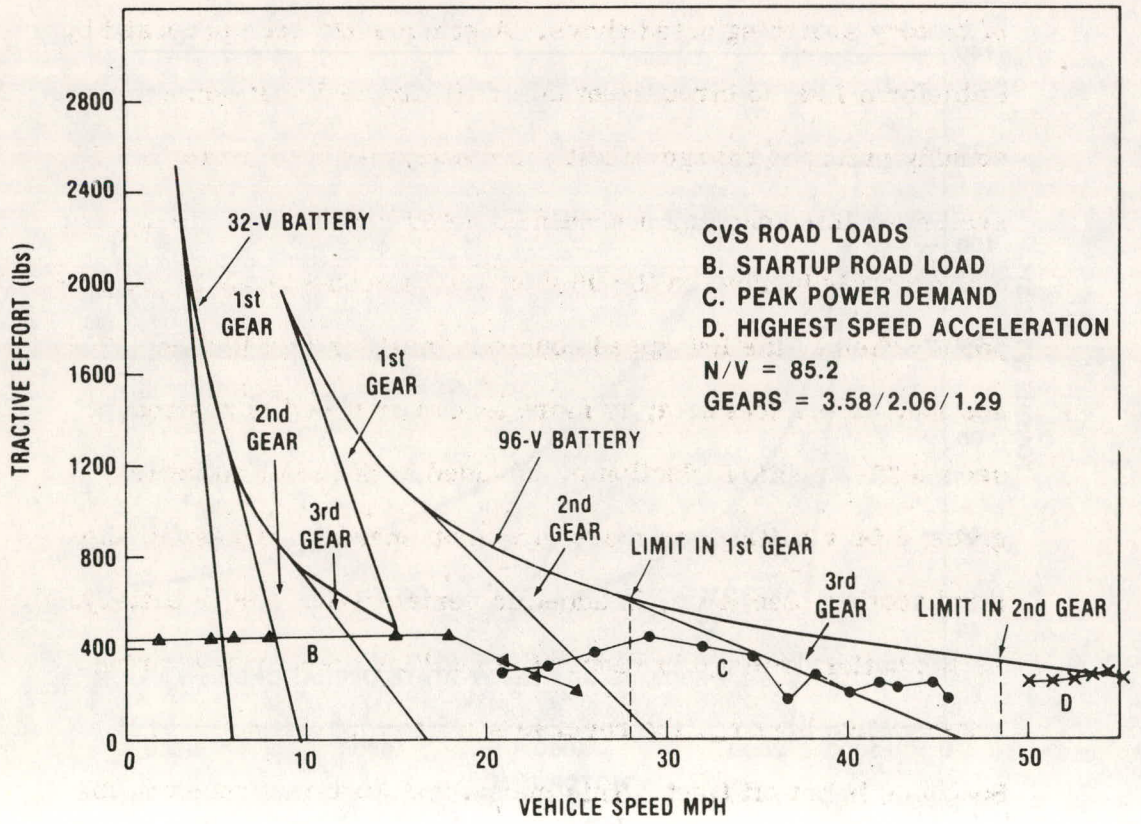

Figure V-15 NaS Fiesta Tractive Effort vs. Vehciel Speed Using Contactor/Field Control, Cortina Motor, and 1.5:1 Motor Gear Ratio

volt system are the armature current surges and associated vehicle jerkiness that might result when switching from 32 to 96 v, the relatively large gap in motor torque capability resulting from the use of 32 and 96 volts as seen from Figure V-14, and the need for more large electrical (and thermal) conductors out of the battery box. The merits of the use of 32 rather than 48 volts are: (a) improved low-speed performance and (b) a wider range of control. Also, as noted previously, restrictions on packaging of the battery favor the 32-v system.

In the present design, all sections of the battery are always in use when the vehicle is energized. In the 32-v connection, all three sections are electrically in parallel. At 96 v, the three sections are in series. This insures equal charge levels of the three battery section. However, it also is responsible for most of the problems of battery switching noted above. A scheme has been proposed by Cableform Ltd. to circumvent this difficulty and still achieve reasonably balanced charge conditions among the three sections. In evaluating this scheme, it should be noted that most of the driving will probably be done in the 96 v or series connection. In the proposed scheme, the low speed condition starts out on just one 32-v section, called Section a; as more torque or speed is desired, a second 32-v section, Section b, is added to Section a in series, giving a 64-v battery; as more torque or speed is requested, the third section, Section c, is added in series giving a 96-v battery. As the battery voltage is reduced to facilitate recharging during regenerative braking, the reverse sequence is applied, i.e., Section c is cut off first. This means that Section a receives the most recharge energy, which is proper. During the next vehicle acceleration when increasing battery voltage is required, the above

sequence is repeated but beginning with Section b and going through the section sequence, b-c-a. For the following acceleration operation, sequence c-a-b is used, and so on. Hopefully, as the battery is discharged to its final depth of discharge, each section will have received approximately equal usage. Besides simplifying the contactor circuitry somewhat (as compared with that of Figure V-5), this approach also adds the 64-v battery connection which will fill in the "torque gap" between the 32-v and the 96-v regions of Figures V-14 and V-15. If hardware for this approach is available, it is suggested for use in the prototype NaS Fiesta.

3. Field Current Chopper Considerations

As noted previously, this component can be constructed using an SCR, power transistor, or GTO as the power chopping device. A power diode is also required. The rating for the chopper semiconductor and the diode should be approximately 30 A. Power semiconductors with 20 A ratings are presently available in plastic packages at large quantity costs of less than $1; therefore, the total large quantity cost of the proposed field chopper packages could be less than $5 at 1978 prices. There are a great many potential suppliers of the field chopper, both prototype models and in production.

4. Electrical Cables Selection

The wiring diagram for the prototype Fiesta EV is shown in the Packaging Section of this report. The choice of power cables between the battery external terminals and the motor and the contactor location are based primarily upon the power limitation of the battery. The power capability of both types of control systems is very sensitive to the resistance between battery terminals and

motor armature. From maintenance and safety considerations, it would be desireable to have the contactors mounted under the vehicle hood and on the motor side of the "panic switch". For the 32/96 volt field/contactor system, this would require six power cables from the back to the front of the car. While the weight and copper loss of such cabeling is not excessive, the resistance of the cables in the 96-volt (series) connection significantly reduces the power that can be supplied to the motor. A comparison for various wire sizes is shown in Table V-7 below:

TABLE V-7

COMPARISON OF WIRE SIZES

Wire Size (AWG)	OHM/1000-ft.	Pounds/ 1000-ft.	Resistance (ohms)	Weight (lbs.)	Copper Loss (watts)
#4	0.2534	128.9	0.0215	11.0	660
#2	0.1594	204.9	0.0135	17.4	414
#1	0.1264	258.4	0.0107	22.0	328
1/10	0.1002	325.8	0.0085	28.0	260

Both the weights and copper losses of most of these cable sizes are probably tolerable. However, the resistance of each choice is relatively large compared to the 96-volt battery resistance of 0.0567 and armature resistance of 0.0056. As a result, it was concluded that the contactors must be located adjacent to the battery in the rear of the vehicle, with only two power cables between battery and motor. Accepting this conclusion, #2 wire was considered acceptable for the 32-volt field/contactor system and for the series motor system.

5. Power Resistor and Motor Dynamic Studies

During the starting of DC commutator motors, an external resistance is often added in series with the armature to limit the magni-

tude of the armature current. Since the motor in the proposed field/contactor drivetrain is started under a no-load condition (refer to Table V-2), the motor achieves its no-load speed in a very short time period. The peak instantaneous armature current that could occur during startup, neglecting the effects of armature inductance, is 1800 A at 32 v and 1875 A at 48 v. These high current values result primarily from the unusually low resistance of the armature circuit in the Cortina motor. The possibility of these high currents during motor starting indicated a need for added armature circuit resistance. To further evaluate motor dynamics with field/contactor control, a dynamic model of the motor and control circuitry was developed using the IBM software program, CSMP. This is a program that allows analog programming (using numerical integration methods) on a digital computer and is a powerful tool for evaluating dynamic time response or transient analysis of electromechanical systems.

The CSMP program used to evaluate the proposed Cortina motor and field/contactor control system is shown as Table V-8. Some of the interesting features of this model are:

a. The use of a nonlinear motor magnetization curve (Figure V-8).

b. The use of the nonlinear road load coefficients of the Fiesta vehicle.

c. The use of a linear clutch model with a variable engagement time.

d. Variable contactor switching times.

A number of transient studies were performed to evaluate dynamic response. Among the conclusions of these studies were, first of

TABLE V-8 CONTINUOUS SYSTEM MODELING PROGRAM

```
                    *** VERSION 1.3 ***
/       DIMENSION GEAR(5)
/       GEAR(1)=3.58
/       GEAR(2)=2.06
/       GEAR(3)=1.29
/       GEAR(4)=1.
/       GEAR(5)=1.
METHOD  RKSFX
FIXED   I,JFLG
INCON   REQ=.062, LEQ=3.0E-5
INCON   RF=2.9
INCON   NOV=56.8, WT=2466.
INCON   JM=.0057, D=.0037
INCON   CO=.01286, C1=.04555, C2=.02294
INCON   WTHRS=1.0, JFLG=0
INCON   S1=50., S2=50., S3=55., S4=65.
INCON   AML=0
INCON   CTIME=1.
INCON   DLL=.30
INCON   TSW=1.5
INCON   TR=.25
INITIAL
        KTT=14./(.7376*NOV)
        RR=60./6.2832
        IAO=0.
        WMO=0.
        IFOO=0.
        MPHO=0.
DYNAMIC
NOSORT
        IF(MPH.LE.S1) I=1
        IF(S1.LT.MPH.AND.MPH.LE.S2) I=2
        IF(S2.LT.MPH.AND.MPH.LE.S3) I=3
        IF(S3.LT.MPH.AND.MPH.LE.S4) I=4
        IF(S4.LT.MPH) I=5
        AM=GEAR(I)
        IF(AM.EQ.AML) GOTO 200
        AML=AM
        DEL=TIME
        IF(I.EQ.1) DEL=DLL
200     CONTINUE
        F=0
        IF(TIME.LE.DEL) GOTO 1
        F=(TIME-DEL)/CTIME
        IF(F.GT.1.) F=1.
1       CONTINUE
        VF=90.
        IF( F.GT.0.) VF=45.
        EB=48.
        IF(TIME.GT.10.) EB=90.
        LF=.054
        KPHI=.0156*IF
        IF(IF.LT.6.5) GOTO 4
        IF(IF.GT.15.) GOTO 5
        LF=.039
        KPHI=.077+.003754*IF
        GOTO 4
5       LF=.02
        KPHI=.11786+.00103*IF
4       CONTINUE
        CA=0.
        IF(TIME.GT.DLL/2.) CA=1.
        IAD=0.
        IF(CA.LE.0.)GOTO 6
        IAD=(EB-E-REQ*IA)/LEQ
        IA=INTGRL(IAO,IAD)
6       CONTINUE
        IFOD=(VF-RF*IFO)/LF
        IFO=INTGRL(IFOO,IFOD)
        IF=IFO-.263*IA/130.
        E=KPHI*WM
        TD=KPHI*IA
        FP=0.
        IF(0.0.LT.F.AND.F.LT.1.0) FP=1./CTIME
        H=RR/(NOV*AM)
        G=KTT/AM
        A1=1.05*C1*WT*H*G
        WMD=(TD-(D+A1*F*FP)*WM-F*G*(CO*WT+C2*MPH*MPH))/(JM+A1*F*F)
        WM=INTGRL(WMO,WMD)
        MPHD=H*(F*WMD+WM*FP)
        MPH=INTGRL(MPHO,MPHD)
        TL=KTT/AM*(CO*WT+C2*MPH**2+1.05*C1*MPHD*WT)
        IF(F.EQ.0.) TL=0.
TIMER FINTIM=20., DELT=.00005, OUTDEL=.1
PRTPLT WM(WMD,IFO,E)
PRTPLT MPH(MPHD,IA,VF)
PRTPLT IA(IF,WM,MPH)
PRTPLT TD(TL,IA,IF)
END
STOP
```

all, that an armature resistance was not required to limit armature current at the instant of motor startup, since inductive effects resulted in a current peak of only about 650 A at 48 v, which is tolerable. However, during battery switching, the added armature resistance did appear to be required in order to prevent vehicle jerkiness during this operation. Traces of some vehicle and motor parameters during startup on a 48/96 v battery sustem are shown as Figure V-16. The control operations during startup are shown at the top of Figure V-16. The big current surge during battery switching from 48 to 96 and the associated step change in motor torque is considered to be not acceptable from the standpoint of vehicle driveability. Therefore, the use of an external armature resistance during battery switching was added to the proposed control system and is shown in Figure V-5.

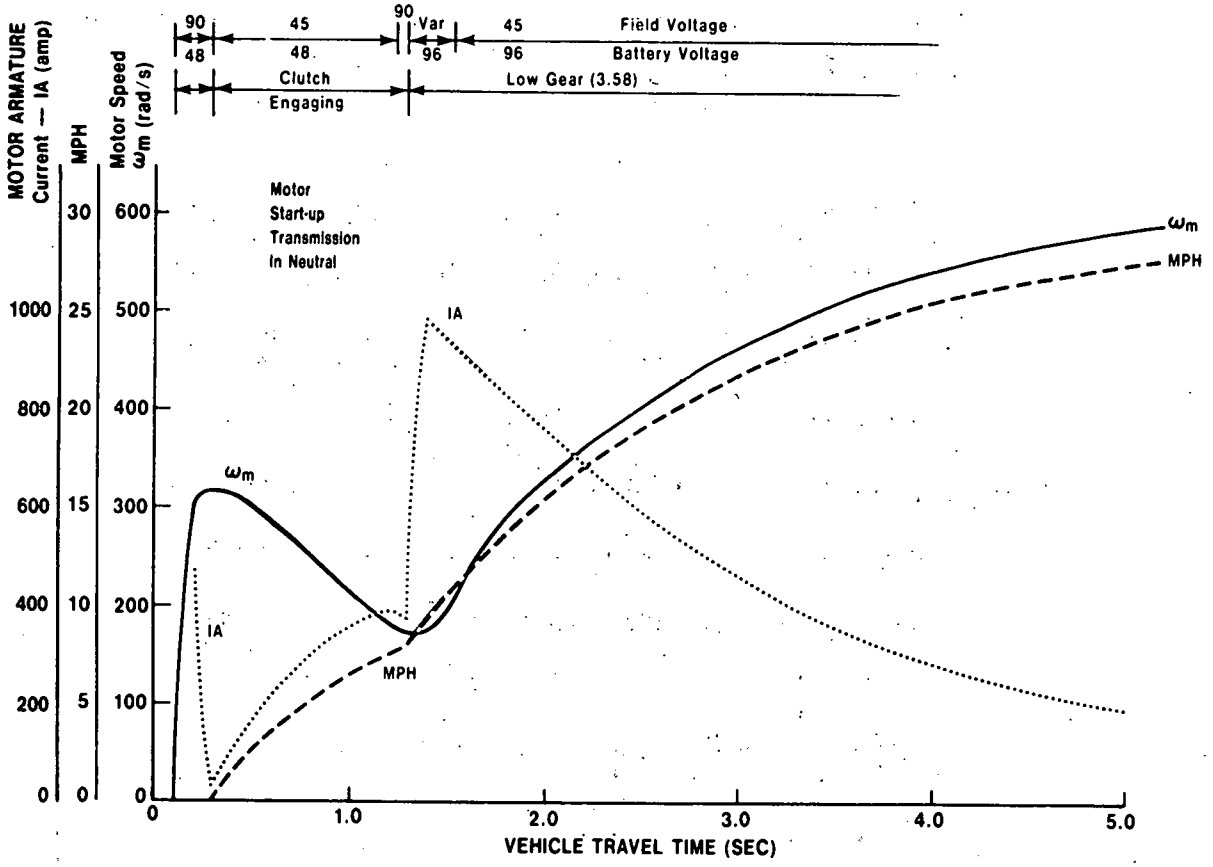

Figure V-16 Motor Speed & Armature Current vs. Vehicle Travel Time (Sec.)

The armature resistance chosen for this application is a GE stainless stell grid resistor type IC9141, which a resistance of 0.12 ohms at 25°C.

6. Panic Switch Assumptions

The manually operated contactors shown in Figure V-5 are supplied by means of a switch known as a "panic switch", since it can serve as the last means of protection during any type of fault in the drivetrain when other means of protection have failed to operate properly. It is used in a great many electric vehicles of all types in operation today. The proposed component is an Anderson Quick Disconnect (QD) and controller fault sensor, type TM. The Quick Disconnect opens the power wires between the battery and the drivetrain. Opening can result from signals from the controller fault sensor due to several types of faults in the motor or control system; from a contact on the car hood that is actuated every time the hood is raised; or from a "panic button" on the dash board. The contacts will be opened whenever the ignition is turned off. Opening of the quick disconnect for any reason requires manual resetting of the disconnect before the vehicle can be operated again. This will be performed, in the prototype vehicle, by means of a foot operated lever underneath the dashboard.

7. Component Weight And Size Summaries

The major drivetrain components have been summarized above. The estimated weights and sizes of the various components are given in Tables V-9 and V-10 respectively. The packaging of these components in the Fiesta is covered in the discussions to follow.

TABLE V-9 COMPARISON OF CONTROLLER WEIGHTS

COMPONENT	FIELD/CONTACTOR 32V	FIELD/CONTACTOR 48V	SERIES (1000-A)
1. ARMATURE CABLE			
SIZE	#2	#2	#2
LENGTH (FT)	30	30	40
WT. (LBS)	6.5	6.5	8.7
2. FIELD CABLE (LBS)	1.0(#6)	1.0(#6)	—
3. CONTACTORS			
NO. RQ'D.	7	4	4
WT. (LBS)	21	12	(INCLUDED IN ITEM #5)
4. ARMATURE RESISTOR (LBS)	15	10	—
5. POWER ELECTRONICS PACKAGE (LBS)	5	5	50
6. LOGIC PACKAGE (LBS)	10	10	10
TOTAL WT (LBS)	58.5	44.5	68.7

F. PRELIMINARY DESIGN AND ANALYSIS OF THE SERIES MOTOR SYSTEM

1. Need For An Alternate Drivetrain Design

During the course of this study, a number of questions were raised concerning the technical performance of the proposed field/contactor control system. At the time of the writing of this report, most of these questions appear to have been clarified satisfactorily.

a. The restrictions on the range of allowable speed and torque operating conditions, described in Figure V-14, and which are due to reduced torque limits on the motor inherent in field/contactor control, can be alleviated either by increasing the N/V ratio (RPM/MPH) in the mechanical power train as shown in Figure V-15, or by use of the 32/64/96-v battery connection scheme described in Section V-B above.

TABLE V-10 — ELECTRICAL COMPONENTS FOR NaS FIESTA EV

	Component	Dimensions	Location
1.	Contactors (4)	4.2" x 2" x 2.9"	1 under hood 3 on battery
2.	Contactors (3)	5.3" x 3" x 3.9"	on battery
3.	Resistor	18" x 6" x 11"	under hood
4.	Field control box **	4.5" x 6.5" x 11"	under hood
5.	Blower (for motor) *		under hood
	Blower:	8" dia. x 4.5" (300 CFM @ 1.8" H_2O)	
	Motor extension:	3.9" dia. x 6	
6.	Fuse, 1200A	1-1/2" dia. x 1-1/4" x 2" busbar	under hood
7.	Fuse, 100A	1" dia. x 1-1/4" x 1" busbar	under hood
8.	Shunt, 1000A	4" x 2" x 1"	under hood
9.	Shunt, 100A	2" x 2" x 1"	under hood
10.	Manual switch (Anderson QD)	4" x 3" x 2"	fire wall
11.	Air filter	8" dia. x 1"	under hood
12.	Logic package	8" x 4" x 4"	passenger area (rt. side of dash board)

* Mounted on Cortina motor.

** Ram-air cooled.

b. The use of an external armature circuit resistance for very short time intervals during battery switching reduces vehicle jerkiness.

c. The driving of the VW Electric Rabbit by members of the Ford Research Staff preparing this study was practical verification that good vehicle driveability can be achieved with this type of control.

Therefore, the need for some preliminary design for an alternate controller is not as pressing as during earlier stages of this study. However, some of the basic concepts of the alternate system, a series motor with an "off-the-shelf" control package, were developed and will be included here for completeness.

2. Series Motor Speed-Torque Characteristic Requirements

The same Cortina motor used for the analysis of the field/contactor system above was used in the series motor analysis since both types of field windings are available for this specific motor. The shunt field used in the field/contactor analysis has 130 turns/pole; the series field has 3 turns/pole.

Since the series motor is to be controlled by a full-range power semiconductor chopper, there is no need for battery switching. The following characteristics are based upon a 96-v battery system. These characteristics have been calculated by means of a BASIC computer analysis method. The motor internal parameters, except for the change in the field winding noted above, are identical to those used in the field/contactor analysis, including the magnetic characteristic shown in Figure V-7. The allowable speed-torque operating regions are shown in Figure V-17. This should be com-

pared with Figure V-13 for field/contactor control. The efficiency map of the series motor is given in Figure V-18.

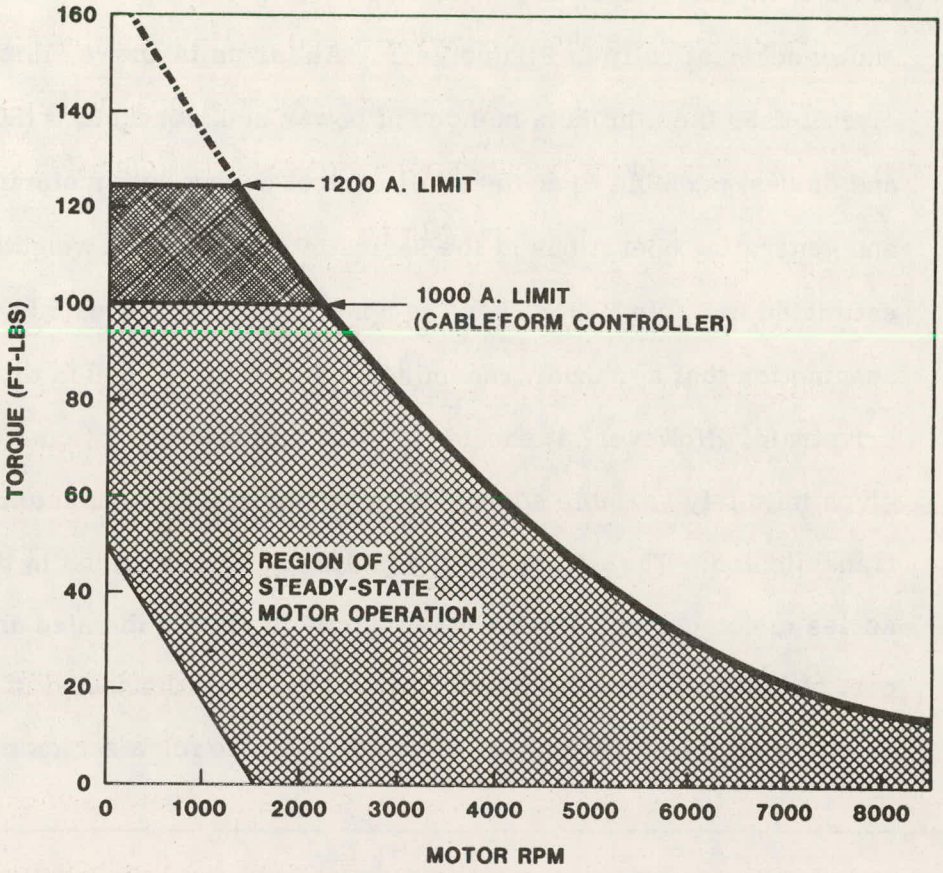

Figure V-17 Chopper — Series Motor Control Cortina Motor Torque vs. Speed

RPM →

T ↓

RPM

TORQUE (FT-LBS)	500	1000	1500	2000	3000	4000	5000	6000	7000	8000
10			.80	.83	.85	.86	.86	.85	.84	.83
20		.76	.81	.84	.87	.88	.88	.88	.88	
30		.75	.80	.84	.87	.88	.89	.89		
40		.73	.79	.83	.86	.88	.89			
50		.71	.77	.82	.86	.88				
60	.54	.69	.75	.81	.85					
70	.52	.67	.73	.79	.84					
80	.49	.65	.72	.78						
90	.47	.63	.70	.77						
100	.45	.62	.69							
110										

Figure V-18 Series Motor Efficiency (Motor Only)

3. Series Motor Controller Selection

The controller chosen for the series motor system is a commercially available system manufactured by Cableform Ltd. It is shown schematically in Figure V-19. As far as is known, this circuit uses the minimum number of power semiconductors (SCR's and diodes) possible to achieve full control during both motoring and generating operations of the series motor. System weights are estimated in Table V-9. These weights have been estimated with the assumption that a manual transmission will also be used in this drivetrain. However, it should be noted that this type of control gives infinitely variable speed characteristics just as an automatic transmission. The purpose of the multigear transmission in the series motor control system is primarily to reduce the size and cost of the motor and the controller, as has been discussed in Sub-Section B and Table V-3. A drive scenario for a series motor

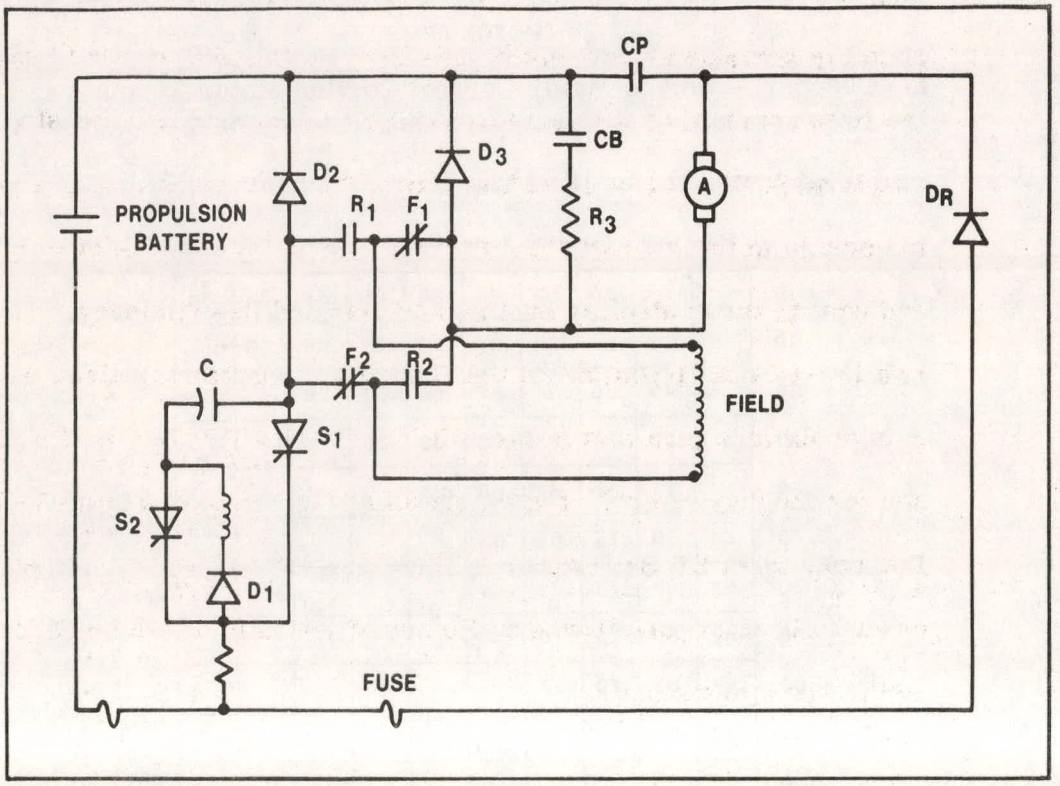

Figure V-19 Cableform — Series Motor Controller Wiring Schematic

system with a fixed ratio mechanical transmission has been prepared and is given as Table V-11. This system is further discussed as "System a" in Sub-Section B-1, and weight and cost estimates are given in Table V-3.

The control function of a series motor is the voltage applied across the armature and series field by the chopper controller. This control characteristic for the Cortina motor is shown as Figure V-20. It is seen that there is a "low-speed problem" with this type of control, also, but it is due to the nature of the controller power components rather than to motor torque instability as in the case of field/contactor control. From Figure V-20 it is seen that low torque operation at low speeds requires a very low applied armature voltage, V_{arm}. At the time of the Cortina EV conversion at Ford (1967), no power semiconductor components were available to control voltages in this range from a 100-v source (only power SCR's were available then). This required an inductance to be added in series with the motor armature and field in order to raise the time constant of the armature circuit to accomodate the slow response SCR's available at that time. The inductance, which had to operate in the high-current armature circuit, added both weight and cost to the controller system and reduced its efficiency. There is a low-torque limitation on the Cableform controller, also, although it is much less than that in the original Cortina EV; this is the reason for the "no-control" region shown at the origin of Figure V-17. For near term EV development, this "no-control" region can be essentially eliminated through the use of recently developed SCR's and power transistors.

TABLE V-11 — VEHICLE OPERATION WITH SERIES MOTOR CONTROL AND FIXED RATIO TRANSMISSION

A. Power Circuitry shown in Figure V-19.

B. Start-up

1. Turn on ignition key
   a. forward or reverse contactors (F or R) are closed and chopper (S_1, S_2, and D_1) is initialized
   b. there is zero power loss in this state of operation

C. Driving

1. A single accel pedal controls the driving by means of the rate at which S_1 is turned on and off; this controls average current through both armature and field.
2. With proper design, there should be infinitely variable control over the entire speed-torque range for which the drivetrain was designed.

D. Coasting

1. Coasting is accomplished by shutting off S_1 and there is zero power loss in the power circuitry under this condition.
2. Coasting down to zero speed is possible.

E. Regenerative Braking

1. To change from a driving or coasting mode to regenerative braking mode requires a series of switching events:
   a. the field must be connected in the reverse manner to the armature; this is done by using the other set of main contactors (either F or R)
   b. CP contactor must be opened
   c. the residual magnetism in the magnetic circuit of the motor must be reversed; this is done by momentarily closing contactor CB; in the standard Cableform con-

trollers, this contactor stays closed for about 3 seconds. The time delays required for this process may be objectionable for on-road vehicles; the opposite switching sequence (except for reversing the magnetism) must be made when going from braking to driving operation.

2. During regeneration, the current in the armature and field must be built up by means of S_1 with the motor shorted on itself through D_2. The energy stored in the armature and field inductance is then dumped into the battery through D_R, and the process is repeated. There must be residual magnetism (in the proper direction) to get the process started each time.

3. Braking (electrical) is possible down to zero speed, since, at low speeds, the system degenerates into a "plugging" mode of operation (see below).

F. Plugging

1. Plugging is an operation used for rapid stopping of crane and hoist motors, and can be built into the Cableform system.

   a. plugging is caused by reversing the field with respect to the armature while the motor is being driven from the battery; it causes a huge torque to be developed in the direction opposite to the direction of motion.

G. Dynamic Braking

1. This is also possible in the Cableform system; in dynamic braking, the kinetic energy due to vehicle motion is converted to electrical energy and dumped into a resistance (in this case, the armature resistance) rather than returned to the battery.

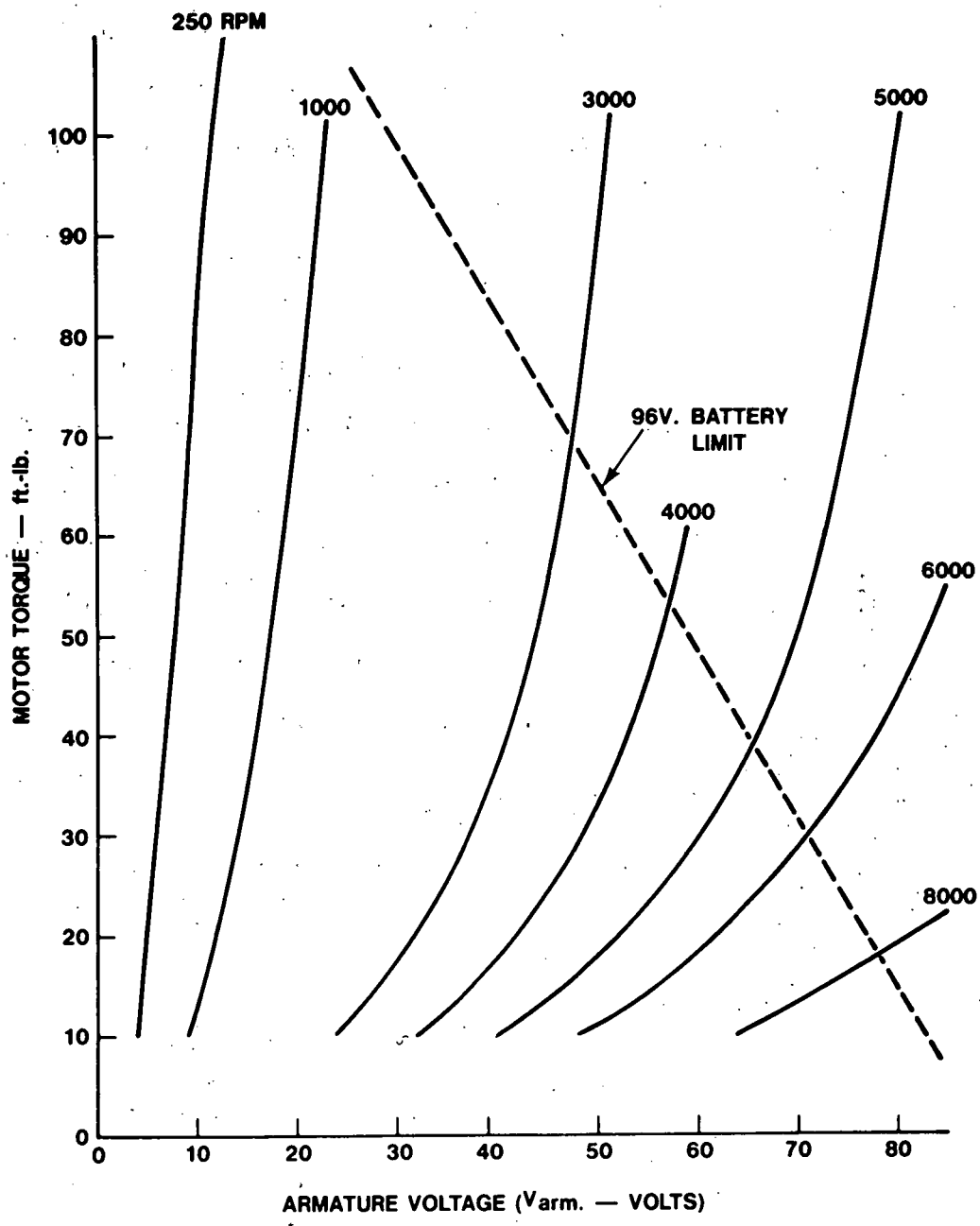

Figure V-20 Series Motor Torque vs. Armature Voltage for NaS Fiesta Ev

G. VEHICLE AUXILIARIES AND AUXILIARY POWER SOURCE

At first glance, the auxiliary power supply for a vehicle of any type would appear to be a straightforward application of techniques long used in the automotive industry. However, auxiliary power supplies and distribution systems are receiving careful scrutiny today in hopes of finding more energy efficient methods of supplying and using auxiliary power even in conventional vehicles and, as a result, many present practices and systems

may be altered in the near future. Secondly, the electric vehicle, as a power-short vehicle (in contrast to conventional vehicles), presents some unique problems to the development of energy-efficient and low-cost auxiliary power supplies.

1. EV Auxiliary Power Loads

The first question that arises in considering auxiliary power systems in an EV is, "Why have an auxiliary power system in a vehicle already loaded with batteries and a high-power distribution system?" At the present state of EV development, there is no firm evidence that an auxiliary power system is absolutely necessary, although, as far as is known, no EV has been built without such a system. The principal advantages of the use of an auxiliary power system are:

a. The main battery undergoes large swings of terminal voltage during driving, which would necessitate costly regulating systems for the supply of vehicle auxiliaries.

b. Low-cost electrical components, such as headlamps, are generally not available for the high voltages of the main EV battery.

c. Many control functions for the main drivetrain are better supplied from a separate source, electrically isolated from the main battery.

d. If an EV is to be developed by converting a conventional ICE vehicle, the use of the conventional auxiliary power system will reduce the cost and complexity of the conversion.

Auxiliary power on an EV includes many of the loads on a conventional vehicle plus some control loads unique to an EV. A recent Ford

estimate of auxiliary loads for a compact car listed the following loads which would also be required on an EV:

Load	Current (Amp:)	Power (Watts) (at a nominal 12v)
Side, tail & inst. lamps	4.10	49.0
Instruments	0.30	4.0
Head lamps	6.40	77.0
Wiper Motors	2.20	26.0
Heated backlamp	11.40	137.0
Backlight wiper	0.92	11.0
Radio	0.58	7.0
Driving lamps	2.40	29.0
Fog lamps	3.50	42.0
License lamps	0.50	6.0
Domo lamps	1.00	12.0
Turn signals	0.60	7.2
Horn	1.00	12.0
Heater blower	1.50	18.0
		437.2

The above listing does not include any loading for vehicle heating. In the proposed NaS Fiesta, an auxiliary hydro-carbon-fueled heater has been assumed. Loads related to the main drivetrain control system are:

Load	Current (A)	Power (w)
Contactor solenoids (assuming 4 energized concurrently @ 1.5A each)	6.0	72.0
Supply for vehicle logic	5.0	60.0
Panic Switch	1.0	12.0
Instrumentation	2.0	24.0
		168.0 w

This gives a theoretical maximum auxiliary load of approximately 600 watts. In a conventional ICE compact car, a 40-A alternator is used as a battery charger for a load of similar magnitude. Therefore, a 500-w auxiliary power source is considered adequate for the NaS Fiesta.

2. Power Supply for Auxiliary Load

The basic power supply for auxiliary loads will be a conventional lead acid SLI battery as in conventional vehicles. There are several options

for charging the auxiliary battery in an EV, however, which are not available in conventional vehicles:

a. External power supply: Since the main batteries require periodic charging, the auxiliary battery could be charged at the same time from the power distribution system using a simple, low-cost charger of the type used for conventional SLI batteries. A conventional SLI battery would be inadequate for this application, since such batteries are designed for high power, shallow discharge, floating charge service. Therefore, a lead-acid or a nickel-zinc traction battery would be required. Assuming an <u>average</u> auxiliary load current of 30 A, the following table indicates the length of service on one charge that could be expected from several brands of traction and industrial lead acid batteries:

Battery	Weight (lbs.)	Voltage (ave)	Wh/lb. @ 30A	Service Time (hr.)
Ford (Autolite) Industrial	60	11.5	12.45	2.1
ESB — EV106 Traction	65	6.0	14.40 (@ 60A)	2.6
Globe-Union GC2[26] (projected)	61	11.5	17.00	3.0

The service time for the main NaS battery in the electric Fiesta is designed (on city driving) for 100 miles/19.71 MPH ~ 5 hrs.; for constant-speed driving, the service time would be much longer. Thus, it is seen that none of the above batteries offers a service time comparable to that of the main battery. Also, the weight penalty of using a high-energy traction type battery is considerable.

b. Alternator: Since the electric Fiesta is a conversion, it is not unreasonable to assume that the Fiesta auxiliary power system could be adapted for use in the converted electric vehicle, with the alternator driven from the main drive motor. This is probably the lowest cost system available and would save weight over the use of a traction battery alone. The weight of the Fiesta alternator and regulator is 11 lbs.; an SLI battery assembly for a compact car is approximately 33 lbs. The disadvantages of this system are: low alternator efficiency, and the inability to charge or maintain good battery voltage at vehicle standstill, since there is no equivalent to engine idle in an EV.

c. Ford Disc Motor: The first disadvantage listed above could be appreciably reduced by the use of a higher quality alternator than that used on present small-sized conventional cars. A prime candidate for this application is the Ford Disc Motor, developed several years mainly as a traction motor for EV application. (20) As a generator, it has the advantage over conventional alternators of being able to generate down to almost zero speed, since its power output is determined by the pulse frequency of a reasonant circuit rather than by its rotational speed. Also, as an axial air-gap machine, it has very low windage losses. It can serve as an accurate motor shaft speed sensor with no modification, and it could be directly coupled to or built as an integral part of the drive motor. Its efficiency is good over a very wide range of speed and torque. It is still in the development stage, although several prototype motors have been built and tested. Its overall cost, including control, is estimated to be comparable to the present alternator/diode system.

d. DC/DC Converter: An obvious candidate for the auxiliary power supply is a DC/DC converter charging the SLI battery from the main battery. This could be of roughly the same weight as the alternator — SLI battery system. It could offer greater efficiency, less audible noise, and zero maintenance. A converter has a potentially low initial cost, comparable to the present automotive alternator system of equivalent size. A disadvantage of this system is the complication resulting from the switching of the main battery in the electric Fiesta. There are several options available for dealing with this problem:

(1) Design the input stages of the converter to operate off of either 32 or 96 volts. This would add considerable weight to the converter, especially its transformer.

(2) Operate a 32-volt converter off of one 32-volt section of the main battery. This will unbalance the state-of-charge among the three sections of the main battery, causing many problems in the charging and discharging of that battery. It is possible that the converter input could be altered among the three sections of the main battery, but it would still be difficult to insure charge balance among the sections.

(3) Operate the converter off of the entire main battery in either its 32-v or 96-v configuration. The latter is to be preferred since most driving is done at the higher voltage and the converter weight would be less when designed for 96 volts. A relatively simple control scheme could be developed to facilitate charging at vehicle standstill at either voltage.

3. Preliminary Converter Design

Although it is felt that the above options should all receive further consideration, a 96/12-v converter has been chosen for the auxiliary power supply in the Electric Fiesta. As far as is known, no commercial converter of this type is available. However, many acceptable circuits suitable for automotive application have been developed for various aerospace applications. A biased transformer converter is shown in Figure V-21 [27]. A second circuit requiring fewer semiconductors but larger capacitors is shown in Figure V-22 [28]. Both of these circuits provide electrical isolation, have demonstrated high efficiency, and are relatively light weight. A request for the cost of developing a prototype of the circuit of Figure V-22 has been sent to the California Institute of Technology.

A preliminary estimate of the size and weight of a 96/12-volt, 500-watt converter based upon Figure V-21 has been made. The principal components of this system are two 5-A, 200-v transistors,

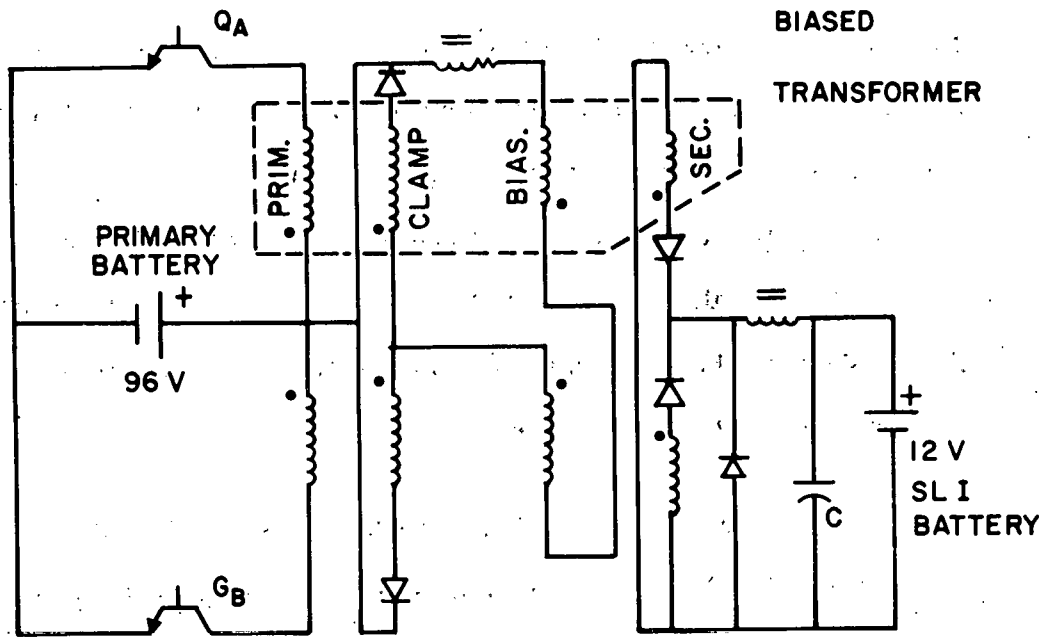

Figure V-21 Schematic or a Biased Transformer Converter For Charging SLI Battery

two 250-w transformers, five diodes rated 25A, 50 v, two choke coils, one capacitor, and heat sinks. Preliminary design of the reset transformers indicates a weight of 1.5 lbs. each; total converter package weight is estimated to be 10.5 lbs. Package size is 10-in. x 5-in. x 4-in.

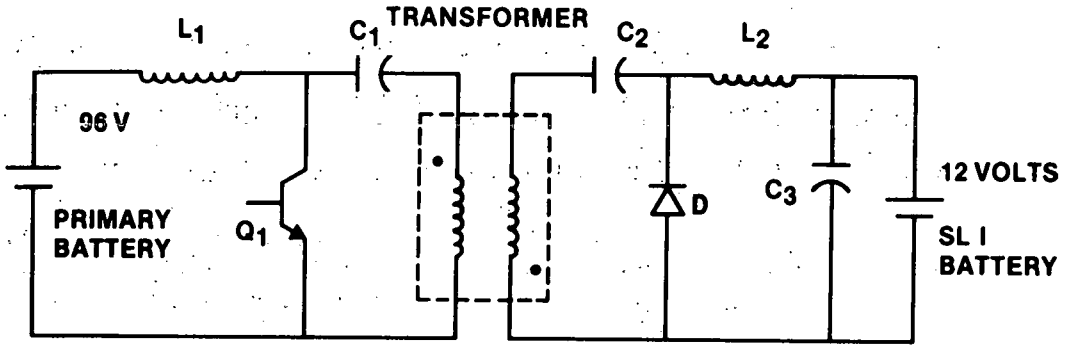

Figure V-22 Alternate Schematic or a Converter for Charging SLI Battery

H. PROTOTYPE DRIVETRAIN PACKAGE

The field/contactor type controller components, discussed previously in Sub-section E, have been "packaged" for installation in a Ford Fiesta EV 2-passenger car. The weights and volumes of the electrical components of the drivetrain have been summarized in Tables V-9 and V-10 and discussed in previous Sub-section G. Based upon size and volume estimates of selected drivetrain components, all of which are existing or "state-of-art" components, a wiring layout has been made and is shown schematically as Figure V-23. Most of the components shown in Figure V-23 can be found in their vehicle location in Figures IV-7 and IV-8 in Section IV of this final report.

Most of the concepts shown in Figure V-23 have already been discussed. The motor is to be connected directly to the Fiesta transaxle transmission, in a manner similar to the connection between the engine and transmission in the conventional Fiesta. Motor and battery cooling requirements of

the field controller can be met using vehicle ram air. The shunts shown in Figure V-23 are for current sensing required by the logic system or for instrumentation. The box designated "computer" in Figure V-23 has been termed, "logic box" in some Sections of this report, and represents the control logic to control and protect the motor, field controller, contactors, cooling systems, and batteries so that the drive scenarios stated in Tables V-5 and V-2 can be realized. By the time EV's are in any sort of commercial production, this control logic will certainly be living up to the name given it in Figure V-23. For details of cable layouts, components mounting structures, etc., refer to the vehicle layout drawings, Figures IV-7 and IV-8.

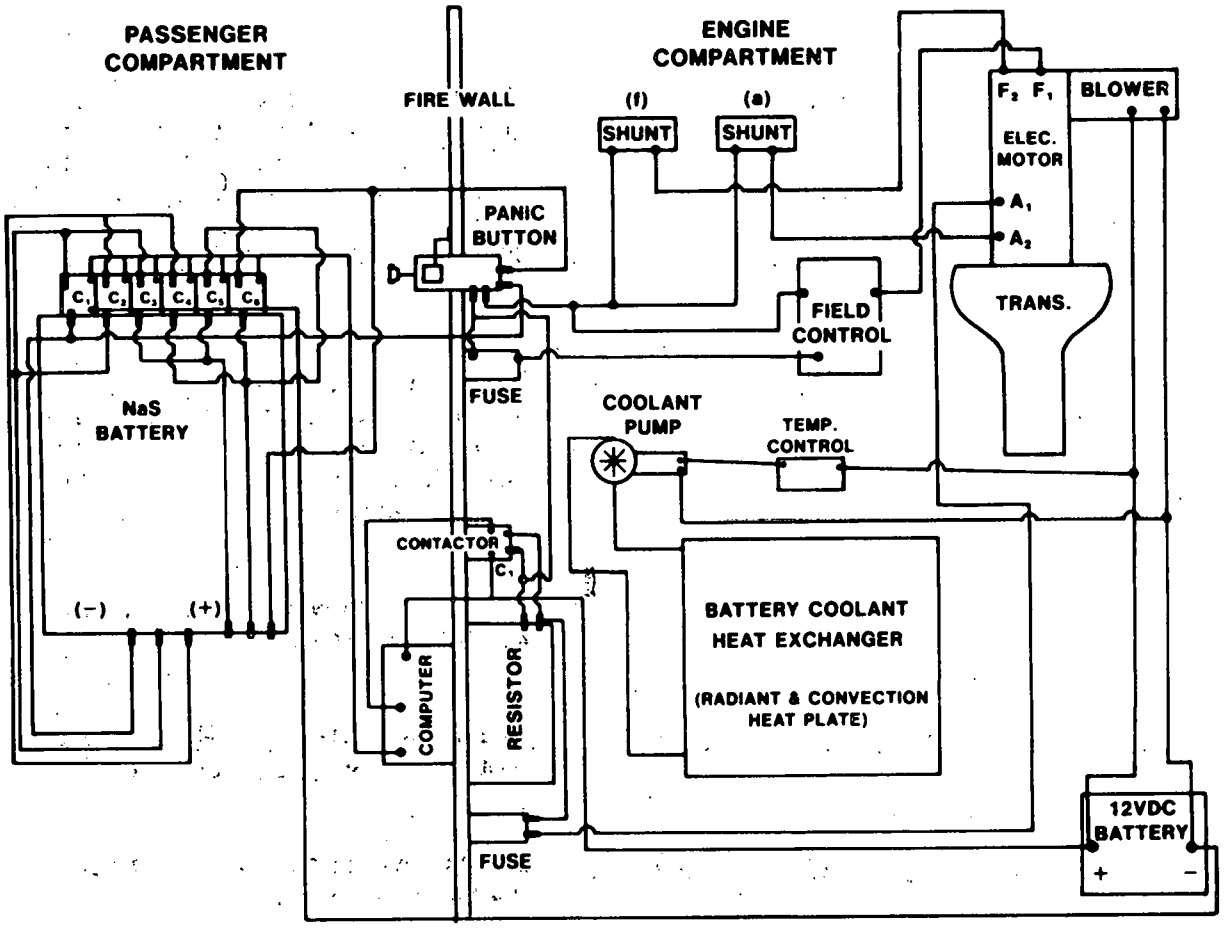

Figure V-23 Sodium-Sulfur Battery Vehicle Wiring Schematic

I. MOTOR AND CONTROLLER SPECIFICATIONS

As noted in previous sections of this report, the motor suggested for the prototype drivetrain was chosen because much test data was available for it, because it is an existing motor (not just a design), and because it had excellent characteristics for the Fiesta EV application. It is not necessarily an optimized motor for this vehicle weight class. In fact, as has been seen, it is somewhat oversized for the NaS Fiesta EV driving needs. Therefore, a motor specification, based upon the Fiesta EV requirements has been prepared.

This motor specification is based upon the speed torque characteristic shown in Figures V-1 and V-6. The following technology is used in the specification:

1. Max Torque: The maximum torque developed at the motor shaft which can be sustained without exceeding the motor thermal characteristic for one minute at motor speeds equal to and below the motor break speed (including zero speed)

2. Break Speed: The maximum speed at which max torque can be developed; it is the speed at which the torque characteristic ceases to be a horizontal line in Figures V-1 and V-6.

3. Max Power: The power based upon max torque and break speed.

4. Continuous Power: The power developed at the shaft that can be supplied continuously.

5. Max Operating Speed: The maximum speed at which maximum power can be supplied.

6. Max Safe Operating Speed: The speed above which the motor is unsafe even in an unloaded condition.

7. Energy Efficiency: The ratio of output shaft mechanical energy to input electrical energy (including field energy) during a variable-speed, variable torque cycle of operation to be specified by the purchaser. An appropriate voltage schedule for the machine windings must also be specified by the purchaser. For generator operation, energy efficiency is the reciprocal of this ratio.

It is assumed that other specifications used below are known to the reader. The present specification is based primarily upon the use of the motor with field/contactor control. However, the specification is general enough so that it can be applied to many other types of motors, including brushless motors.

1. Motor Specification:

- Armature Voltage: 120 v nominal
- Max Power: 60 H.P.
- Max Torque: 100 ft-lb
- Break Speed: 3150 RPM
- Max Operating Speed: 9000 RPM
- Max Safe Operating Speed: 12000 RPM
- Continuous Power: 24 H.P.
- Energy Efficiency (based on CVS cycle): 75%
- Max Ambient Temperature: 120°F
- Insulation Class: F or better
- Total Weight: 120 pounds maximum (100 lbs design goal)
- Vibration: According to Ford vehicles specifications

2. Field Chopper Specification:

- Continuous Output Current: 30A
- Input Voltage: 70 — 120 v

- Energy Efficiency: 90%
- Max Ambient Temperature: 120°F
- Vibration: According to Ford Specs for under-hood operation
- Noise: According to Ford specs

In Appendix A to follow, the performance and economy (P & E) studies which were conducted to give program guidance to the Electrical Systems Work Task, will be described.

J. REFERENCES:

1. Nelson, R. H., et al., "Electric Vehicle Simulation Program," Paper #782207, Fifth International Electric Vehicle Symposium, Philadelphia, Pennsylvania; October 1978

2. Rowland, E. A., "Evaluation of Battery Performance for an Electric Vehicle with Regenerative Braking;" ibid

3. Unnewehr, L. E., et al., "Energy Saving Potential of Engine-Electric Vehicular Drives;" Proceedings of the Eleventh Inter-society Energy Conversion Engineering Conference, SAE Paper #769063, September 1976

4. Unnewehr, L. E., Minck, R. W., and Owens, C., "Application of the Ford Sodium-Sulfur Battery in Electric Vehicles;" SAE Paper #770382, February 1977

5. "State-of-the-Art Assessment of Electric and Hybrid Vehicles," DOE Report HCP/M1011-01, January 1978

6. "Preliminary Power Train Design for a State-of-the-Art Electric Vehicle," Vol. 2: DOE Report DOE/NASA/0592-78/1; September 1978

7. Stockton, T. R., "Traction Transmission;" presentation at ERDA Contractors Co-ordinating Meeting, May 4-6, 1976; Ann Arbor, Michigan

8. Beachley, N. and Fran, A., "Continuously Variable Transmission Study," DOT Report #DOT-TST-75-2, Vol. I; December 1974

9. Foote, L. R., et al., "Electric Vehicle Systems Study, "Ford Scientific Research Staff Report #SR-73-132, October 1973

10. Foote, L. R., and Hough, J. F., "An Experimental Battery Powered Ford Cortina Estate Car," SAE Paper #700024, January 1970

11. Bader, C. and Stephen, W., "Comparison of Electric Drives for Road Vehicles," IEEE Transactions of Vehicular Technology, May, 1977; Vol. VT-26, #2

12. Thompson, F. T., "Advanced Electronic Control System for Electric Vehicles," IEEE Transactions of Vehicular Technology, Vol. VT-27, #3; August 1978

13. Zeisler, F., "Characteristics of Homopolar Motors and Generators," Ford Scientific Research Staff Report #SL 9-16, September 1962

14. Nagy, J. F., "Analysis of a Homopolar Transmission for a Fairlane-Size Vehicle," Ford Engineering and Research Staff Report AR65-23, July 1965

15. US Patent #4,124,086, "Electric Vehicle Drive Train Having Unipolar Motor," Adam Janotick, November 1978

16. Slabiak, W. and Collins, G. C., "Brushless Synchronous Propulsion Motor," SAE Paper #680455, June 1968

17. Turner, D., "The Double Ended Claw Motor," A Novel Form of Self-Synchronous Motor for Traction Purposes," Paper #782105 Fifth International Electric Vehicle Symposium, Philadelphia, Pennsylvania, October 1978

18. Richter, E., "Power Density Considerations for Permanent Magnet Machines," Electric Machines and Electromechanics, Vol. 3, No. 3., April-June 1979

19. Campbell, P., "The Permanent Magnet Disc Armature Motor — An Evaluation of Its Advantages Compared with Conventional Electric Vehicle Drives," Paper #782102, Fifth International Electric Vehicle Symposium, Philadelphia, Pennsylvania, October 1978

20. Unnewehr, L. E., and Koch, W., "An Axial Air-Gap Reluctance Motor for Variable Speed Applications," IEEE Transactions on Power Apparatus and Systems, Vol. PAS-93, No. 1, January 1974

21. Agarwal, P. D., "The GM High Performance Induction Motor Drive System," IEEE Winter Power Meeting, Paper #68 TP 107 PWR, January 1978

22. Rosenberg, S.A., Dewan, S.B., and Slemon, G.R., "Inverter-Fed Induction Motor Drive Using Power Factor Control," Paper #810, Conference Record, 1976 Annual Meeting of the IEEE Industry Applications Society, October 1976.

23. Middlebrook, R.D., "The Countertran; A New Controller for Traction Motors," Paper #312, ibid

24. "Characterization Study of an Electric Motor-Transmission System for Electric Vehicles," MTI Report 78TR2, September 1977; prepared for US-DOE

25. Miersch, R. and Stephan, W., "Design of a Sub-Compact Electric Passenger Car," Paper #782204, Fifth International Electric Vehicle Symposium, Philadelphia, Pennsylvania, October 1978

26. Weinlein, C.E., "Design Aspects of a Unique Lead-Acid EV Battery," Paper #783105, Fifth International EV Symposium, October 1978

27. Lillienstein, M. and Miller, R. S., "Biased Transformer DC-DC Power Converter," Record of the Power Electronics Specialist Conference, June 1976

28. Middlebrook, R. D. and Cuk, S., "Isolation and Multiple Output Extensions of a New Optimum Topology Switching DC-DC Converter," Record of the Power Electronics Specialist Conference, June 1978

APPENDIX A — SUPPORTING SYSTEM STUDIES

In this Appendix, three sub-tasks will be described which were supporting activities to the major work tasks presented in detail in Sections II through V.

I. PERFORMANCE AND ECONOMY STUDIES

To initiate the performance and economy projection study activities, a production Fiesta, having a curb weight of 1764 lbs., was chosen as the "image" vehicle.

To be able to make performance and economy comparisons between an ICE vehicle and a two-passenger NaS battery powered Fiesta style vehicle, a "198X", two-passenger paper design version of the production Fiesta was developed. The performance of the "198X" Fiesta engine was obtained by reducing the 1.6 L displacement of the 1979 production version to the level of 1.1 L, with a corresponding reduction in the Fiesta engine horsepower from 66 BHP to approximately 50 BHP.

The range goal of the NaS battery powered Fiesta EV was established to be 100 miles on the CVS driving cycle at 80% level of battery discharge. 125 miles maximum range was set as a goal, assuming that the remaining 20% of battery capacity would be used at a low constant vehicle driving speed. Consequently, the fuel requirements for the 198X Fiesta was estimated to be approximately 3.5 gals. to give comparable maximum range. The reductions in vehicle weight due to reducing on-board fuel capacity and reducing passenger seating from four to two, established the curb weight of the 198X-ICE Fiesta to be approximately 1620 lbs. with the weight breakdown as shown below:

DETERMINATION OF 198X-ICE FIESTA CURB WEIGHT

. Baseline Vehicle Curb Weight	=	1764 lbs.
. Less 2-Rear Seats and Trim (Est.)	=	-26.2 lbs.
		1737.8 lbs.
. Less Allowances for Reducing Gas Tank Volume from 10 gals. to 3.5 gals.	=	-48.8 lbs.
		1689.0 lbs.
. Weight allowance in downsizing 1.6 L engine to a 1.1 L engine	=	-69.0 lbs.
. 198X-ICE Fiesta Curb Weight	=	1620 lbs.

The weight penalty goal for the NaS battery powered Fiesta EV was defined in Section II to be 500 lbs. over the curb weight of a 2-passenger ICE powered Fiesta. Therefore the allowable curb weight and test weight of the Fiesta EV can be found as follows:

DETERMINATION OF NaS FIESTA CURB AND TEST WEIGHT

. Curb Weight of 198X — ICE 2-Passenger Fiesta	=	1620 lbs.
. Allowable Weight Penalty for NaS EV Fiesta	=	500 lbs.
. 198X — NaS EV Curb Weight	=	2120 lbs.
. Add Payload Weight (2-Passengers)	=	350 lbs. *
. 198X — NaS Ev Test Weight	=	2470 lbs.

The weight available for the EV powertrain (batteries, motor-controls, etc.) is determined by: (1) removing from the production Fiesta all ICE related systems/components to arrive at a stripped vehicle (or "bare") weight; and (2) developing a "base vehicle weight" which is arrived at by modifying the "bare" vehicle weight to account for vehicle adjustments required to have an operable EV, without the weight of the EV powertrain included. The ICE related items removed from the Fiesta are tabulated below:

* Corporate standard for 2-passenger vehicles.

REMOVAL OF ICE RELATED SYSTEMS

Items Removed from the ICE Fiesta	System Weight (Lbs.)
Engine	302.0
Engine Mounts	20.3
Alternator and Regulator	11.0
Exhaust System	32.1
Fuel Tank and Fluids (Gasoline, Oil, Coolants, etc.)	50.8
Heater Hoses and Blower	10.0
Total Weight Removed:	426.2 Lbs.

The bare Fiesta weight is arrived at by subtracting the removed weight from the ICE Fiesta curb weight as follows:

. 198X — ICE Fiesta Curb Weight	= 1620.0 Lbs.
. Less ICE Related Component Weight	= 426.2 Lbs.
Bare ICE Fiesta Weight:	= 1193.8 Lbs.

The NaS EV Fiesta will require some weight adjustments to the stripped ICE Fiesta to account for modifications to the suspension, newly added gasoline fired heater, structure beef-up, etc. To date, the only reasonably firm weight perturbation is the addition of a Southwind gasoline fired heater assembly (or its equivalent), which is estimated to be 60 lbs. (unit plus fuel). Therefore the NaS EV base vehicle weight is found to be:

. Bare ICE Fiesta Weight	= 1193.8 Lbs.
. Add Gasoline Heater Weight	= 60.0 Lbs.

NaS EV Base Vehicle Weight: = 1253.8 Lbs.

or 1254.0 Lbs.

The weight allowance for NaS batteries, mounting support brackets, cables, electrical components such as motor/controller, filters, switches, etc., and for battery insulation is found as follows:

. NaS EV Fiesta Curb Weight	= 2120.0 Lbs.
. Less NaS EV Fiesta Base Vehicle Weight	= -1254.0 Lbs.
Weight Allowance for EV Powertrain (and Related Components)	= 866.0 Lbs.

For P&E calculations the weight equation illustrated in Figure A-1 was used as a reference point:

For computer projections of Fiesta performance and economy, vehicle tests weights are required inputs. The curb weight and tests weights of the three reference Fiesta's are as follows:

	1979 Fiesta	198X ICE Fiesta	NaS EV Fiesta
. Curb Weight (Lbs.)	1764	1620	2120
. Payload (Lbs.)	350	350	350
Test Weight (Lbs.)	2064	1970	2470

The above values were used in a series of parametric performance and economy studies initiated early in the program. The computer program chosen for the NaS Fiesta EV P & E studies was developed by Ford Scientific Laboratory personnel over the past several years. This electric vehicle P & E computer program has been developed to be a flexible analytical tool which permits analyzing a variety of well defined production vehicles and a variety of batteries (e.g., lead-acid, nickel-cadmium,

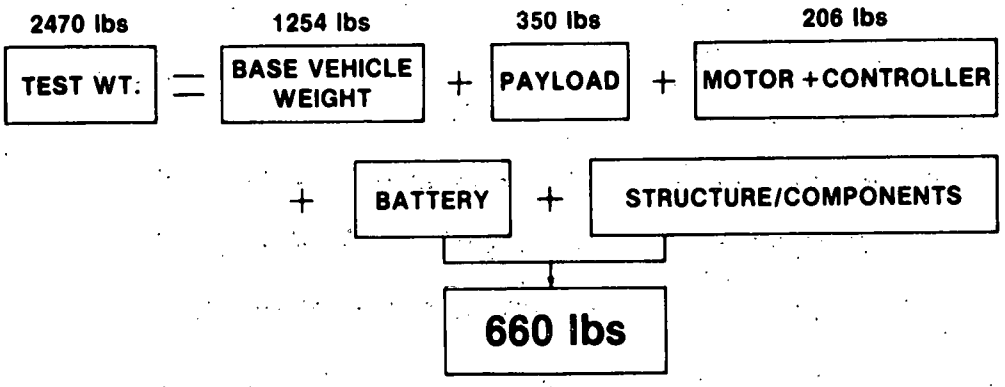

NaS ELECTRIC VEHICLE TEST WEIGHT

198X ICE FIESTA CURB WT. =	1620 lbs
ALLOWABLE WT. PENALTY =	500 lbs
CURB WEIGHT =	2120 lbs
PAYLOAD WT. =	350 lbs
TEST WEIGHT =	2470 lbs

Figure A-1 Reference Vehicle Weight Equation for P & E Analysis

nickel-zinc, and sodium-sulfur batteries), each coupled to a variety of traction motors and controllers. The program is also flexible enough to permit investigating hypothetical vehicles, providing that proper vehicle oriented input data are provided (e.g., drag coefficients, component efficiencies, N/V values, etc.).

The 198X-ICE Fiesta's performance and economy were computed using the Corporate proprietary P & E computer program while the NaS battery powered EV was computed using the Scientific Research Laboratory P & E Program developed for EV analysis, as described above.

1. Range and WOT Performance Studies

Parametric performance and economy studies were conducted to define the test weight spread of a NaS battery powered EV capable of 100 miles range when driven over the CVS cycle. The variations in test weight followed variations in assumed battery and battery support weight allowances, keeping all other terms in the weight equation of Figure A-1 constant. Table A-1 is a sample computer printout of a performance

and economy calculation for the so called reference Fiesta EV, which has been given the code name EV-4. Shown in the table are listings of vehicle test weight (2470 lbs.), battery weight of 635 lbs. (including allowance for battery insulation and container weight), motor/controller weight (206 lbs.), wide open throttle acceleration performance (e.g. 0-50 mph. in about 11.4 secs.), CVS driving cycle range (100 miles

TABLE A-1 SAMPLE COMPUTER PRINT OUT FOR A NaS POWERED ELECTRIC VEHICLE

VEH.WT	REGNPWR	BATT.WT	M-C WT	HP-CONT.	HP-MAX.	TE-MAX
2470.00	-39522.94	635.04	206.27	28.26	70.64	430.06

SMAX	MAXGRD	PWRDEN	KW(F=0)	KWH(C20)	T-MAX
176.06	79.71	58.82	37.35	30.62	106.00

OE OPEN THROTTLE RESULTS

IME (S)	MPH	FT	POWER
1.00	12.61	10.22	33.28
2.00	20.88	35.95	33.10
3.00	26.47	71.27	32.95
4.00	30.92	113.80	32.79
5.00	34.69	162.27	32.63
6.00	37.97	215.86	32.47
7.00	40.89	273.96	32.31
8.00	43.52	336.10	32.15
9.00	45.91	401.90	31.99
10.00	48.09	471.03	31.83
11.50	50.10	543.23	31.67
12.50	51.96	618.24	31.51
13.50	53.67	695.86	31.36
14.50	55.27	775.90	31.21
15.50	56.75	858.18	31.07
16.50	58.13	942.55	30.92
17.50	59.42	1028.88	30.78
18.50	60.62	1117.03	30.65
19.50	61.75	1206.88	30.52
20.50	62.80	1298.32	30.39
300.50	79.40		

TERY POWER LIMITED
PUT SGEAR1,SGEAR2,SGEAR3,SGEAR4 FOR DRIVE CYCLE

37. 44. 54. 54.

CVS CYCLE

MPH	RANGE-MI	BAT.KW	BAT.KWH	RL.KWH	SYS.EFF	M-C EFF	KWH/MI	F
20.00	148.67	3.28	25.61	12.19	0.476	0.496	0.196	0.802
40.00	122.67	7.69	25.70	16.70	0.571	0.709	0.238	0.804
50.00	64.00	19.44	25.71	14.55	0.498	0.702	0.457	0.805
5.00	6.83	15.88	25.74	10.09	0.345	0.465	4.284	0.806
19.70	100.49	34.51	25.56	17.47	0.601	0.673	0.289	0.800

AV.MPH	BKWAVE	IRMS	REGEN	CKWHM	CKWHG	CGEFF	CBMEFF
19.70	5.09	4747.09	-5.99	25.96	-4.035	0.674	1.015	99.879

based upon battery depth of discharge equal to 80%), battery power rating (37.35 kw @ zero depth of discharge), and battery energy rating (30.6 kw-hr. @ C/20 rate), etc. P & E calculations of this type were useful guides to both battery design and vehicle package studies.

Table A-2 summarizes these types of parametric calculations for an installed battery power density of 58.8 watts/lb. As can be seen, the reference vehicle, EV-4, does not quite meet the weight penalty goal of 500 lbs. over the ICE Fiesta counterpart, when the installed battery (clustered cells, electrical connections and battery container only) power density is only 58.8 watts/lb. That this is so can be seen in Table A-2 wherein only 25 lbs. are available for battery support structure and/or components (cables, switches, instrumentation, etc.). Increasing the NaS EV weight penalty to 600 lbs. will require an increase in the battery weight by 15 lbs. but will permit an increase in allowable structure weight of 85 lbs. for a total structure-plus-component weight of 110 lbs. This latter value should be adequate.

For EV-4 to be able to meet its weight goal, three system technology advances would need to occur in future follow-on programs. These technology advancements are:

a. Improvement in battery specific weight.
b. Reduction in motor/controller weight.
c. Reduction in base vehicle weight.

Items a. and b. above should be achievable through project follow-on design and development work. Item c., reduction in base Fiesta EV weight, will be difficult to achieve without resorting to modification and/or replacement of high weight components with light weight composite materials. In Figure A-2, the trade-off between "bare" battery

TABLE A-2 COMPARISON OF 198X-EV AND ICE "FIESTA" VEHICLES

COMPARISON OF 198X — E.V. AND ICE "FIESTA" VEHICLE

	1977 FIESTA	198X FIESTA	EV-1 KWH/MILE	EV-1 MPG	EV-2 KWH/MILE	EV-2 MPG	EV-3 KWH/MILE	EV-3 MPG	REF. EV-4 KWH/MILE	REF. EV-4 MPG	EV-5 KWH/MILE	EV-5 MPG
ECONOMY, MPG-CVS	34	38.7	.312	41.1	.305	42.0	.297	43.2	.289	44.4	.283	45.3
-HWY	46.8	51.2	.372	34.5	.369	34.7	.366	35.0	.360	35.6	.357	35.9
-M-H	38.8	43.9	.336	38.2	.331	38.8	.325	39.5	.317	40.4	.312	41.1
RANGE (MILE) - CVS	340	136.6	100.51		100.51		100.06		100.09		93.96	
- HWY	460	180.7	84.30		83.02		81.37		80.68		74.50	
- M-H	385	154	92.51		91.81		90.69		90.49		84.08	
ACCELERATION TIME (SEC.) 0-50 MPH	8.8	11.7	11.61		11.74		11.62		11.43		11.26	
WEIGHTS - CURB (LBS.)	1764	1620	2420		2320		2220		2120		2020	
- TEST (LBS.)	2064	1970	2770		2670		2570		2470		2370	
EV WEIGHT PENALTY (LBS)	-	-	800		700		600		500		400	
BATTERY — % TEST WEIGHT	-	-	24.75		25.09		25.33		25.71		24.52	
— KW (F=0)	-	-	40.33		39.41		38.29		37.35		34.18	
— KWH (C20)	-	-	33.06		32.25		31.35		30.62		28.05	
— POWER DENS. (W/LB.)	-	-	58.82		58.82		58.82		58.82		58.82	
— REQ'D BAT. KWH: CVS-	-	-	27.60		26.92		26.17		25.56		23.41	
HWY-	-	-	27.60		26.92		26.17		25.56		23.41	
— REQ'D BAT. KW: CVS-	-	-	38.46		37.14		35.82		34.51		33.21	
HWY-	-	-	34.22		33.22		32.25		31.27		30.52	
ENGINE — DISPLACEMENT	1.6	1.1	-		-		-		-		-	
— POWER	66HP	50 HP	-		-		-		-		-	
MOTOR — HP MAX (1 MIN RATING)			70.64		70.64		70.64		70.64		70.64	
— HP CONT.			28.26		28.26		28.26		28.26		28.26	
AVAIL. WEIGHT OF EV PROPULSION SYSTEM:*	-	-	1166		1066		966		866		786	
— BATTERY WT. (LBS.)	-	-	685		670		650		635		580	
— MOTOR-CONTROLLER WT. (LBS)	-	-	206		206		206		206		206	
— AVAIL. STRUCTURE/COMPONENT WEIGHT (LBS.)	-	-	+275		+190		+110		+25		0	

1. VEHICLE BASE WEIGHT = 1254 LB.
2. PAYLOAD = 350 LB.
3. ALL EV'S HAVE 4-SPD. MAN. TRANS. WITH 1ST THROUGH 4TH GEAR RATIOS OF 3.58, 2.06, 1.29, AND 1.00 AT N/V = 56.8
4. ONE (1) KWH = .078 GAL. OF GASOLINE
5. SHIFT SPEEDS: 1ST-2D: 37 MPH; 2D-3RD: 44 MPH; 3RD-4TH: 54 MPH
6. COMPUTATIONS BASED ON POWER PULSE = 20 KW
7. CASE EV-5 PENALIZED FOR BEING 20 LB. OVER TEST WEIGHT.

weight (viz. a battery assembly consisting of clustered modules only) and the allowable weight for battery electrical connections, insulation and container, battery support structure and power cables, and electrical switch gear, is shown for the reference vehicle, EV-4 whose test weight equals 2470 lbs. There are two cases illustrated in Figure A-2. The first case shows the weight increment allowable (150 lbs.) when the bare battery power density is equal to 73.5 watts/lb., and the second case shows the weight increment allowance (200 lbs.) when the "bare" battery power density equals 82.5 watts/lb. In the first case, the "bare" battery weight is approximately 510 lbs. and in the second case, the "bare" battery weight is reduced to approximately 460 lbs.

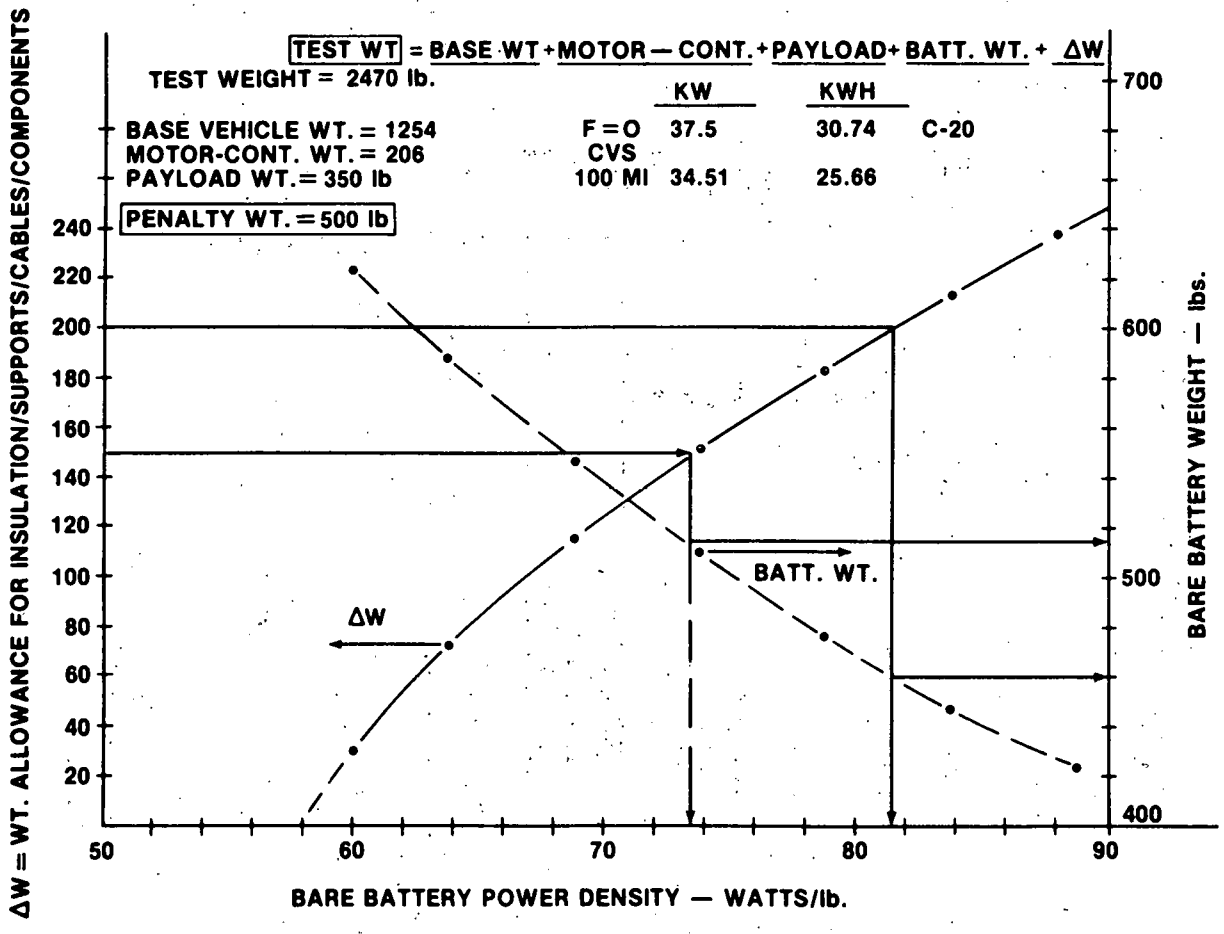

Figure A-2 Battery Power Density vs. Battery Structure Weight Allowance

If 50 lbs. can be reduced from the estimated weight for the Cortina motor/controller (presently assessed at 206 lbs.) then case 1 would be achievable with a "bare" battery specific power of 73.5 watts/lb. and an incremental weight allowance of 200 lbs., which is an adequate allowance for battery support hardware. It was these considerations which provided the incentive for performing the cell design optimization studies cited in Section III.

Other parametric studies were conducted from which parametric maps were created showing the effect on range for variations in vehicle test weight, battery power density (installed battery system including structural support), and battery energy density (installed battery

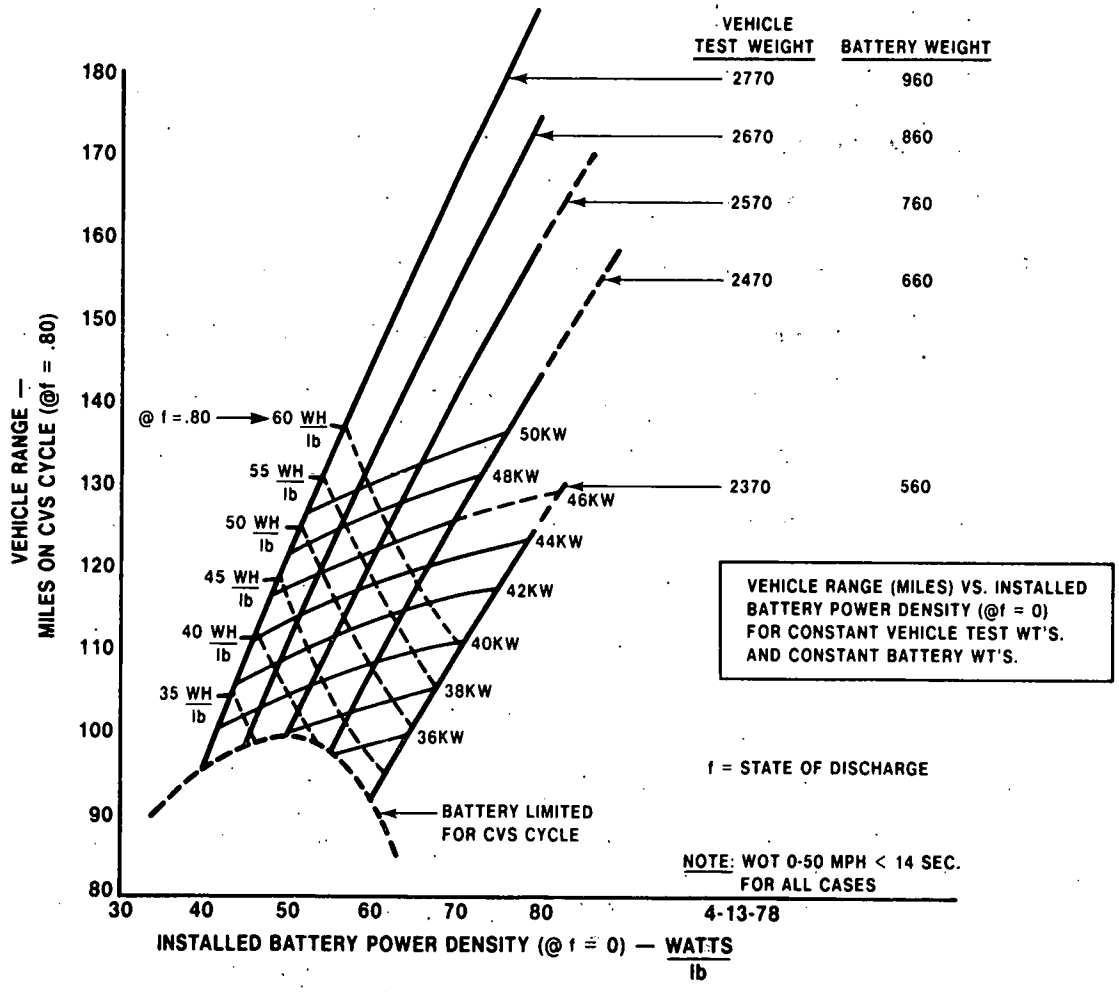

Figure A-3 Vehicle Range On CVS Cycle vs. Installed Battery Power Density

system based upon 80% depth of discharge). Figure A-3 is a parametric map of vehicle range (miles over CVS cycle at 80% depth of battery discharge) versus installed battery system power density (W/lb.) for variations in vehicle test weight (lbs.), variations in battery specific energy density (W-hr./lb.) and variations in battery power rating (Kw @ zero depth of discharge).

Figure A-4, is a parametric map of vehicle range versus installed battery specific energy (both vehicle range and energy density are based upon energy delivered by the battery to 80% depth of discharge), for variations in vehicle test weight (lbs.), variations in battery specific power (watt/lb.) and battery power rating (both specific power and power rating based upon zero depth of discharge).

Illustrated in both Figures A-3 and A-4, is the fact that there is a boundary limit on the ability of a given size battery (i.e. given weight, specific power, specific energy), to meet the power demands imposed by the CVS cycle. In both figures, this limit is identified by the broken line in the lower left hand corner of the parametric maps. This boundary limit occurs because of the fact that, for a given specific power value and on-board battery weight, the resulting power rating of the battery is too low to permit the vehicle to meet the CVS cycle acceleration demands (i.e. CVS peak power levels). While the vehicle can perhaps meet range goals at steady state speeds, it lacks enough battery power capacity to pass through a single CVS cycle, even once.

In addition to range and wide open throttle investigations, the P & E computer program was used to investigate other areas of system optimizations which would have an impact upon vehicle P & E projections. These supporting studies will be taken up next.

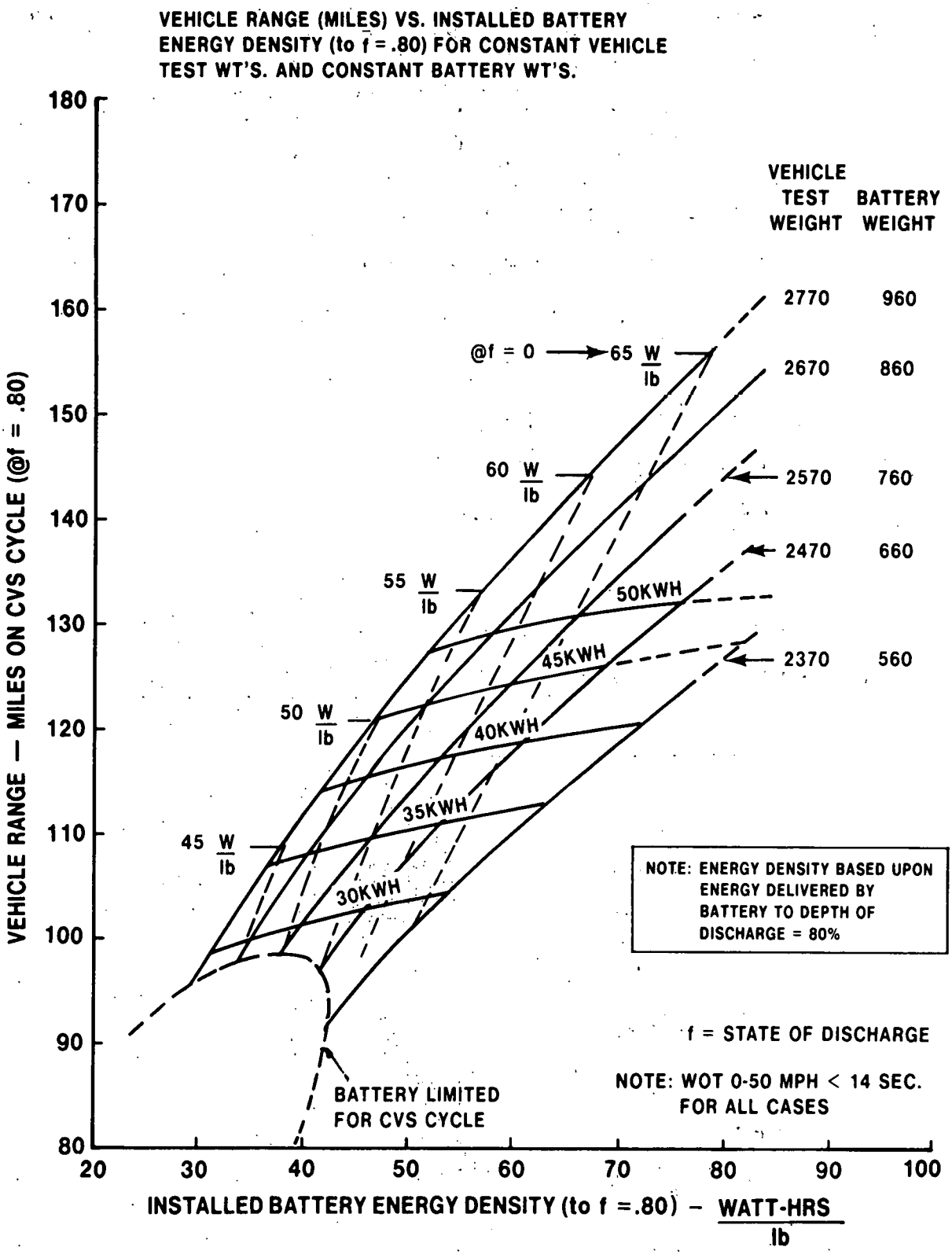

Figure A-4 Vehicle Range On CVS Cycle vs. Installed Battery Energy Density

2. Drive Methods and Shift Schedule Selections

The Scientific Research Laboratory P & E computer program was used to investigate the effect upon vehicle range and performance due to selecting a vehicle having a directly coupled motor-driveline system versus a vehicle having a traction motor coupled to a manual transmission for the EV powertrain. Concomitant with these driveline computer studies, an investigation was conducted regarding the effect on vehicle performance and economy by changing the shift schedule of a given manual transmission system. Each of these studies are separately discussed below:

a. Direct drive vs. manual shift: Table A-3 is a summary of P & E calculations in which a direct drive system is compared with a

TABLE A-3 POWERTRAIN TRADE-OFF STUDIES FOR VEHICLE TEST WEIGHT = 2470 LBS.

TRANSMISSION CHOICE	KWH/Mile 20 Mph	KWH/Mile 40 Mph	KWH/Mile 60 Mph	KWH/Mile CVS	RANGE CVS
I. DIRECT DRIVE					
A. Fixed Gear Ratio @ 4.50:1*	.187	.239	.385	.271	107.2*
B. Fixed Gear Ratio @ 3.58:1*	.194	.232	.385	.276	105.2*
C. Fixed Gear Ratio @ 2.70:1	.226	.229	.383	.294	98.9
II. MANUAL TRANSMISSION **					
A. Standard 4-Speed (3.58/2.06/1.29/1.00)	.194	.230	.433	.283	102.8
B. "Basic" 3-Speed (3.58/2.06/1.00)	.194	.230	.433	.287	101.4
C. Modified 4-Speed (4.50/2.50/1.75/1.00)	.187	.230	.433	.275	105.6
D. Modified 3-Speed (4.50/2.50/1.75)	.187	.230	.392	.273	106.5
E. Modified 3-Speed (4.50/2.50/1.00)	.187	.230	.433	.279	104.2

* Would require Cortina Motor Speeds in Excess of Max. Allowable Speed = 12,000 RPM

** All compared at Common Shift Schedules of: 37 mph (1-2nd Gear) 44 mph (2-3rd Gear) 54 mph (3-4th Gear)

manual transmission. Several fixed gear ratios were evaluated for the Direct Drive powertrain. As noted in Table A-3, for the N/V of the Fiesta equal to 56.8, fixed gear ratios greater than 2.70:1 cause the Cortina motor to exceed its maximum allowable speed of 12,000 rpm.

Five types of manual transmissions were investigated. Two transmissions are minor gear modifications to the standard production manual transmission which has gear ratios of 3.58 (list gear), 2.06 (2nd gear), 1.29 (3rd gear), 0.88 (4th gear). Manual transmission — "A" of Table A-3, is the same as the production transmission with the single exception that the fourth gear is a "lock-up" or direct drive gear, viz. 1:1 ratio. Manual transmission — "B" differs from "A" only the fact that the 1.29:1 gear of transmission — "A" is dropped to provide a 3-speed gear set with 1st and 2nd gear ratios for transmission — "B" the same as "A".

Transmission "C", "D" and "E" are variations of a manual transmission whose gear ratios are selected to be higher in any given shift range than its counterpart in a standard production transmission. The gear ratios for the last three manual transmissions were selected to keep the motor speed as high as possible in all gear ranges without however, exceeding the motor maximum speed rating.

From Table A-3 several useful conclusions can be established. The first conclusion to be drawn is that of the direct drive cases studied, only one, Case C, is feasible for the standard Fiesta driveline having an N/V of 56.8. Cases A and B, while meeting meeting the CVS range goal of 100 miles, require that Cortina

motor to exceed its safe operating speed at 60 mph, and beyond. The second conclusion to be made is that all of the manual transmissions studied meet the CVS range goal of 100 miles and that, while cases "C", "D" and "E" for the manual transmission study are measurably better than either of Case "A" and "B", they would significant changes to the production transmission. Since Case "A" requires minimum modification to a standard production manual transmission, and since it meets the 100 mile CVS driving range, it would be the preferred transmission for the first NaS Fiesta EV test bed/demonstrated vehicle. In later follow-on program phases, when all powertrain components have undergone thorough testing, new P & E optimization studies can be performed to select best manual transmission gear ratios.

b. Shift schedule selection studies: As a companion effort to the transmission study previously described, P & E calculations were conducted to investigate the effect of various shift schedules on vehicle range. Table A-4 lists two transmission, a four-speed and a three-speed, both are based on slight modifications to the Fiesta production transmission described earlier. For the 4-speed transmission, three cases of shift selection variation are illustrated in Table A-4. The first case, the EPA designated shift schedule, was selected as a reference point. As can be seen in the table, the EPA shift schedule of 15 mph (1st — 2nd), 25 mph (2nd — 3rd) and 40 mph (3rd — 4th) is a poor match with the efficiency map of the Cortina motor. Shift schedule "A", line A.2 of Table A-4, is still too low in its shift points, as can be seen by the low CVS range of 75 miles calculated for this case. By raising the shift points to 37 mph/44 mph/54 mph for Shift schedule — "B", line A.3 in Table A-4, other range goal of 100

miles over the CVS cycle can be met; hence, this schedule was selected for all P & E studies based on use of the 4-speed transmission.

For the three-speed transmission shift schedule study, Case "B" in Table A-4, six (6) variations were calculated. The EPA shift schedule for the 3-speed transmission has shift points at 15 mph and 25 mph. As can be seen in Table A-4, this schedule is no better matched to the Cortina drive motor efficiency map than was the case for the 4-speed transmission discussed above, as evidenced by the same low — 75 mile range over the CVS cycle.

Raising the shift speeds to 25 mph and 40 mph, i.e., a "modified EPA" shift schedule, improved considerably the range capability,

TABLE A-4 MANUAL TRANSMISSION SHIFT SCHEDULE STUDIES

VEHICLE TEST WEIGHT = 2470 lbs

MANUAL TRANSMISSION	KWH/Mile 20 Mph	KWH/Mile 40 Mph	KWH/Mile 60 Mph	KWH/Mile CVS	RANGE CVS
A. 4-Speed Manual (3.58/2.06/1.29/1.00)					
1. EPA Shift Schedule: 15 mph/25 mph/40 mph	.248	.257	.433	.319	75.3
2. Shift Schedule — "A" 18 mph/31 mph/50 mph	.248	.279	.433	.312	75.4
3. Shift Schedule — "B" 37 mph/44 mph/54 mph	.194	.230	.433	.283	102.8
B. 3-Speed Manual (3.58/2.06/1.29)					
1. EPA Shift Schedule 15 mph/25 mph	.246	.274	.402	.312	75.3
1.A EPA Shift Schedule (Modified) 25 mph/40 mph	.194	.279	.402	.295	97.7
2.0 Shift Schedule - "A" 18 mph/31 mph	.248	.279	.402	.308	75.4
2.A Modified Shift Schedule — "A" 31 mph/50 mph	.194	.230	.402	.280	103.7
3.0 Shift Schedule — "B" 37 mph/44 mph	.194	.230	.402	.280	103.6
3.A Modified Shift Schedule — "B" 44 mph/50 mph	.194	.232	.402	.279	104.3

although 100 miles was not quite attainable. This case illustrates once again the need to keep the Cortina motor speed in the middle-to-high speed range for best vehicle economy over the CVS cycle.

The results of shift schedule — "A", line B.2 of Table A-4, is identical to the disappointing result obtained for shift schedule – "A" for the 4-speed transmission, see line A.2. However, by raising the shift point speeds to 31 mph and 50 mph, the resulting improvement in range is dramatic, as can be seen in line B.2.a of Table A-4, where in the range goal of 100 miles has been easily met.

Both shift schedule — "B" and its modification for the 3-speed manual transmission, see lines B.3 and B.3.a. in the Table, meet the 100 mile range goal. It is interesting to note that both of these cases give CVS range results practically identical to study case B.2.a., which indicates that moving the first shift point to 30 mph-plus produces the most dramatic range improvement. Whether the second shift point is set at 44 mph or 50 mph has little overall effect on range results.

II. VEHICLE HANDLING AND SAFETY REVIEWS

In support of the battery packaging and vehicle packaging work tasks, design reviews were conducted for each conceptual layout design developed to ascertain whether major vehicle handling and/or safety issues existed. Company Vehicle Safety representatives were contacted for consultation on vehicle handling and safety considerations peculiar to both the specific battery configuration proposed for EV use and the method of installation and specific location of the battery inside of the vehicle.

As mentioned in Section IV of this report, battery thermal management considerations ruled against dividing up the battery into several small

packages for ease of vehicle storage. Consequently all battery conceptual designs were single packages, located in the rear of the vehicle, e.g. behind the front seats. Thermal management considerations as well as vehicle tear up considerations ruled against arranging the battery in either a long slim rectangular configuration or in a thin profiled "T-shaped" configuration, such as has been tried by other EV developers, using lead-acid batteries for propulsion purposes. Review of design reports and movie films taken by EV developers showing their vehicle mock-ups and test bed vehicles impacting a barrier under simulated 30 mph vehicle crash conditions, clearly demonstrated that vehicle installations having these long rectangular battery packages installed down the center of the vehicle would be unsuitable for the NaS battery package configurations. The reason that these vehicle centerline battery installations are unsuitable for the Fiesta NaS battery packaging, is that the NaS cells cannot take major deformations and certainly not crush in the same manner that the lead-acid of Ni-Zn cells can for the purpose of energy absorption. Nearly all Lead Acid of Ni-Zn centerline vehicle installations depend upon an appreciable amount of crush of the battery cases, plates, and separators, plus electrolyte hydraulic pressure resistance to absorb impact energy developed during front end or rear end crashes. If the NaS cells were to receive comparable container crush and/or deformation, the resultant breakage of the alumina electrolyte would cause a significant release of thermal energy due to the highly exothermic reaction between the molten sodium and molten sulfur, which are suddenly allowed to co-mix.

The same reasoning rules heavily against a front end installation of the NaS battery in the Fiesta Vehicle, due to the fact that complete front end crush (up to the firewall) is relied-upon for full energy absorption. If a

NaS battery package were mounted "up-front" so to speak, then the front end structure would have to be made completely rigid to protect the battery package during impact, otherwise the resultant battery fire would, more than likely, pose a major hazard to the vehicle occupants and the vehicle surroundings. Building a rigid frame structure in the front end of the Fiesta to provide full battery protection during front end crashes would be a major vehicle rework and feasibility is none too certain.

Following several design review meetings with Company Vehicle Safety Engineers, it was concluded that the best in-vehicle installation of the NaS battery was in the rear of the vehicle, directly behind the front seats. In this position the battery container can be installed in a protective structural cage, which offers not only positive tie down protection in the event of front or rear end impacts, but some measure of protection to side impacts as well. The protective cage structure can be affixed to the existing front rails of the Fiesta to insure transfer of battery inertia loads to the front structure of the vehicle when the vehicle is subjected to 30 mph FMVSS crash tests. By following these design safety concepts, which are detailed in Figures IV-7 and IV-8 in Section IV, the battery will remain in a fixed position in the vehicle while the vehicle impact energy is absorbed by the crush of either the front end or rear end structure.

Placing the battery behind the front seats raised questions concerning the safe handling of the Fiesta EV due to the possible shift in weight distribution from front to rear, in comparison to a standard ICE powered Fiesta having a curb weight front wheel-to-rear wheel weight percentage distribution of 63% front and 37% rear. When the ICE production Fiesta is fully loaded, viz. 4-passengers plus 100 lbs. of cargo, the weight distribution shifts to about 50% front wheels and 50% rear wheels. An

early investigation into the situation was based upon assuming that the battery, support structure and selected electrical support components weighed approximately 800 lbs. The motor-controller system weight was estimated at 206 lbs. and was located in the vehicle front end with the motor mounted to the transaxle transmission and the controller components mounted to the firewall and the fender aprons. From weight balance calculations it was concluded that, for a fully loaded Fiesta EV, the weight distribution that, for a fully loaded Fiesta EV, the weight distribution would become about 47% front end and 53% rear end, as reported in Figure IV-6, Section IV. When the battery cell optimization studies were completed and the liquid cooled battery configuration illustrated in Figure III-8, Section III, was selected for vehicle packaging, the weight distribution was re-estimated to be about 50% front and 50% rear as a result of the reduction in battery weight (800 lbs. down to 665 lbs.) and a reduction in battery width from 28 inches to about 20 inches, with a resultant forward shift in the battery center-of-gravity. The fact that the Fiesta EV, when fully loaded, has an estimated weight distribution nearly identical to the ICE powered production Fiesta is a basis for believing that the handling characteristics of the two Fiestas will be very similar. This belief will have to be tested in any future follow-on work, since, for now, it is an open issue along with other vehicle handling open issues, such as:

1. Adequacy of the brakes to meet FMVSS because of increased vehicle loads.

2. Adequacy of the production suspension system to handle the Fiesta EV weight increase, e.g. 2170 lbs. curb weight for the Fiesta EV versus 1764 lbs. curb weight for the production ICE Fiesta.

III. THERMAL MANAGEMENT STUDIES

The short duration and the somewhat limited work scope of the NaS EV feasibility study program limited supporting studies, such as heat transfer studies, to a minimum level. Consequently, the main lines of thermal management investigations were confined to brief preliminary analyses aimed at establishing the feasibility of such thermal design concepts as:

1. Use of super insulation techniques to restrict the heat loss from a battery container enclosing high temperature NaS cell clusters and cell modules.

2. Use of novel cooling and heating techniques to maintain the battery temperature within the desired operating range of 300-350^{o}C.

3. Use of new materials and designs for lead throughs (power leads, instrumentation leads, coolant lines, etc.) which must penetrate the battery thermal insulation-container structure.

Brief summaries of each of the above study areas will be presented.

Battery Container Thermal Loss Control

The high operating temperature (300 — 350^{o}C) level of the NaS battery necessary for its efficient operation requires methods which can maintain this temperature level over reasonably long periods of time without requiring large amounts of input thermal energy. Because of the size of the battery required to meet the NaS Fiesta EV performance goals defined in Section II, the large temperature difference between the battery bulk temperature of approximately 620^{o}F (avg.) and an environmental temperature range of -40 to 110^{o}F requires high performance battery insulation. The only

high performance insulation concept of merit for this high temperature application is the so called "super insulation" designs based upon the combined use of a vacuum jacket around the hot battery mass (to reduce to nearly zero the convection and conduction heat losses), and a multi-reflective foil jacket inside the walls of the vacuum jacket (to greatly reduce the thermal radiation heat exchange between the walls of the vacuum jacket). After a brief survey of vendors having experience in "super insulation" applications, the vacuum thermal insulation, called MULTI-FOIL, produced by the THERMO ELECTRON CORP. was selected for preliminary design purposes. The foil design selected for this study consists of a zirconium-oxide coated, thin (.001 inch or less) aluminum sheet which is then stacked in multiple layers to form the thermal insulation blanket. The ZrO_2 particles, which are sparsely sprayed on the surfaces (10% or less area coverage) of the aluminum foils, serve the function of foil separaters to reduce the chance of thermal contact between foil sheets. Vendor supplied test data indicates that at 350^{o} C (660^{o}F) the use of approximately 40 layers of Al ZrO_2 MULTI-FOIL insulation would limit the heat losses to approximately .0025 watts/cm^2 (7.93 BTU/hr/ft^2). Under ideal conditions, the battery package illustrated in Figures III-8 and III-9, Section III, (approximately 39" x 20" x 20") would lose a maximum of 63.3 watts (216 Btu/hr) through all four sides for the liquid cooled battery design. This thermal loss value may turn out to be somewhat conservative because of the added insulating effect of the glass microspheres which are used inside the inner container as void filler material surrounding the cell sub-modules. These glass microspheres were selected for the following design/performance reasons:

1. An evacuated inner container was chosen in order to insure that sodium and/or sulfur fires could not occur in the event that one or more cells failed during battery life. With vacuum inside the inner container, convection and conduction processes are virtually nil. Consequently, heat transfer to and from cell sub-modules would have to be by radiation heat transfer. By arranging the cooling plates and heating strips in a parallel-transverse arrangement similar to the arrangement shown in Figure III-10, Section III, high radiation view factors could be obtained. However, the close spacing required between the cell sub-modules and the heat sink plates to achieve minimum battery volume, created a high risk for electrical shorts due to plate and/or sub-module shift during high vibration or g-loads. By placing glass microspheres in the void space between the cell sub-modules and the heat sink plates, both components are electrically insulated from one another, both components are held in position during vibrating loads due to the packing and force damping capabilities of the glass microspheres, and both components can exchange heat via conduction through the packed microspheres. The glass microspheres have a packed density of approximately 9-12 lbs/cu. ft. using sodium boro-silicate glass and, therefore, offer a light weight means for immobilizing the cell sub-modules and the heat sink-heater components inside the inner container.

2. The thermal conductivity of the packed microsphere is low (.70 — .80 (Btu)·(In)/(hr) (1 sq. ft.) (^{o}F)) and therefore the packed spacing between the cell modules and the heat sink-heater plates must be made small to insure adequate heat

conduction for cell-to-plate temperature differences of 300-350°-F. (1/16-3/16" is adequate). However, around the sides and ends of the assembled battery, the spacing between the assembled and interconnected modules and the walls of the inner container is on the order of 3/4 to 1.0 inches, see Figure III-10, Section III. When this perimeter spacing is filled with packed microspheres (100-300 microns in diameter), an added thermal blanket is provided to supplement the MULTI-FOIL vacuum insulation.

3. The filling of all voids within the inner container-structure with low cost, light weight microspheres prior to final sealing of the inner container assembly, permits the inner container walls to be constructed of thin wall aluminum and/or stainless steel for minimum weight. By packing the inner container with microspheres, the thin inner container walls are restricted from collapsing when the inner container is totally evacuated (to approximately 10^{-3} - 10^{-5} torr.) of gases and/or air molecules. The final sealed and evacuated inner container can be handled as a "solid assembly" for final build up of the battery assembly, including MULTI-FOIL wrapping and installation of the outer container, power leads, instrumentation leads, coolant lines, etc.

For design reference purposes, the glass microspheres produced by Emerson & Cumins, Inc., were selected and all engineering data used was based upon the brochure information supplied by this vendor.

The heating and cooling of the battery is accomplished by the use of heat sink plates cooled by a high temperature, low-vapor pressure, non-toxic, pumped (on demand only) heat transfer fluid.

Heating of the battery is accomplished by the use of foil-type heaters which are available commercially for service at temperatures up to 1000 deg.-F. The heat sink plates are formed into heat exchangers by designing onto the plate surface, profiles of the headers and parallel flow-paths which are then fabricated into physical shapes within the bonded seams of the heat sink plates by the so called "Roll-Bond" (T.M.) process. This fabrication process is a low cost commercial fabrication technique used extensively to fabricate heat exchange/heat sink plates for applications in the home appliance and chemical process industries.

For the battery assembly previously shown in Figures III-8 through III-11, in Section III, eighteen (18) heat sink plates are installed transversely in the inner container in the spacing formed between the series connected (electrically speaking) cell sub-modules. The heat sink plates are contoured to closely follow the undulating profile formed by the cell clusters defining a battery sub-module, see Figure III-10, Section III. By proper contouring the heat sink plate, a constant spacing between the surfaces of the clustered cells and the heat sink plate, can be maintained. For the planview shown in Figure III-10, Section III, a 3/16 inch gap filled with glass microspheres, was established between the clustered cells and the heat sink plate for the final battery package design.

Provision for heating of the inner battery assembly to achieve either initial battery warmup or to maintain a temperature regime for efficient battery operation, was accomplished by using strip-type foil heater sheets bonded to part of the surfaces of the "Roll-Bond" fabricated heat sink plates. These strategically located foil strip heaters conduct heat through the approximately 3/16 inch microsphere filled gap separating the heat sink-heater plates and the cell sub-modules. For reference purposes, in the battery design activity, the technical design information supplied by Safeway Products Inc., (makers

of THIN-HEET foil shaped appliance heaters), was used in establishing geometrical designs of the foil heaters. Foil heaters capable of 1000 deg.-F service are commercially available from several vendors.

The cooling fluid selected for the removal of excess heat generated by either high battery load demand caused by vehicle driving conditions, such as long hill climbing, long WOT operation or driving into high head winds, was a commercial heat transfer fluid produced by Monsanto, called Therminol-66. It's two outstanding features are (a) stable operation up to 650 deg.-F, and (b) low vapor pressure at 650 deg.-F (650 mm of Hg.). The fact that its viscosity is low in the operating range of 300°F - 600°F (.5 - 1.5 centistokes) is decided plus, since its pumping power will be low. Table A-5 is a list of

TABLE A-5 - TYPICAL PROPERTIES OF BATTERY COOLANT

(Ref: MONSANTO BULLETIN NO. IC/FF-35)

Composition	Modified terphenyl
Appearance	Clear, pale yellow liquid
Specific Gravity 25/15.5°C	1.004
Kinematic Viscosity @ 100°F	30 cSt
Moisture Content	100 ppm
Pour Point	-18°F (-27.8°C)
Flash Point COC	352°F (178°C)
Fire Point COC	380°F (194°C)
AIT (ASTM D-2155)	705°F (374°C)
Coefficient of Thermal Expansion	0.00039°F-' (0.00070°C-')
Boiling Range	
10%	643°F (339°C)
90%	668°F (353°C)
Heat of Vaporization (Calculated)	105 BTU/LB. (83 cal/g.)

typical properties, as supplied by Monsanto. Since the Flash Point is given as 352°F, the heat transfer fluid would be kept 12°F below this value, viz. at 340°F. The design of the coolant circuit is such that the coolant is pumped through the battery assembly only upon demand. The demand would be established by thermocouple pick-ups showing a need for cooling in the event that either local hot spots are detected or the bulk mean temperature of the battery begins to rise above a pre-determined level (e.g. to 700°F). The flow rate is adjusted for a maximum outlet temperature of 340°F. The discharged coolant is transferred to a coolant plate, also formed into a heat exchanger surface by the "Roll-Bond" technique, wherein the heated plate radiates its heat to the roadway. It has been estimated that as much as 1.75 kw of internal heat energy could be generated by the battery during hill driving or by extended driving into strong headwinds. This amount of energy could be dissipated to the roadway, if it were at an ambient of 110°F, by a radiation surface sized to be about 4 feet long by 3.32 feet wide, if the plate had an emissivity of .91 and a mean surface temperature of 330°F. If the bottom of the coolant plate has extended surfaces (short enough and spaced far enough apart so as to not reduce the plate view factor much below 1.00) for heat transfer by conduction during vehicle travel, then the size of the coolant radiative plate can be made appreciably smaller.

A fluid reservoir and sump pump is built into the bottom coolant radiation plate assembly. Heat transfer fluid would not be allowed to reside inside of the battery but, instead, would be pumped through the battery only upon demand. As soon as the temperature of the battery reached an acceptable equilibrium value, the pump system would automatically switch to a by-pass mode and the battery coolant fluid would be drained into the low-point sump in the coolant radiation plate located beneath the vehicle. This procedure, controlled by the on-board computer, would insure that the coolant should not see high wall temperatures for extended periods of time.

In addition to preliminary investigations of thermal management concepts for controlling the heat loss from the battery package via either the container walls or by forced convection heat removal, or both, design studies were conducted to evaluate the means for minimizing heat leaks via the battery container penetrations caused by the battery power leads, instrumentation leads, coolant lines, etc. In the course of various configuration design exercises, it became apparent that all of the battery package configurations under study had two common requirements:

1. The outer battery container should be constructed from a light weight, easily formable material which, in an emergency, could function well at temperatures in the range of 600-800°F.
2. The lead throughs (power, instrumentation, etc.) should be buried in some type of easily formable material which has excellent electrical and thermal insulation qualities. This material should permit the design the fabrication of hermetically sealed feed through assemblies to insure vacuum leak tightness at the points where penetrations of the double walled container occur.

For the outer container material consideration was given to both metals and non-metals. It was finally decided that from weight, electrical insulation, thermal insulation, and low cost fabrication points of view, moldable plastics would be preferable, if any could be found with high strength properties at elevated temperatures (300 - 600°F). After a materials search, moldable polyimide compounds capable of continuous use at high temperatures (400 - 600°F continuous use, and intermittent use at 800°F) was selected. One polyimide formulation prepared by the TRIBOL Division of Flurocarbon, called "Tribolon" PI-600, appeared attractive since it had the highest con-

tinuous temperature rating 600°F, and is reported to be able to be used intermittently at 800°F. It is reported by the supplier to have the following key application properties:

Tensile strength (psi)	12,000
Flexural strength (psi)	
@ 70°F	19,000
@ 600°F	6,399
Flexural modulus (psi)	650,000

The injection molding capability permits forming the outer container walls into strong rigid shapes such as the series of connected truncated cones illustrated in Figures III-8 thru III-11 in Section III. This particular geometry has been previously used in light weight structures for high loading applications such as load-floors and wall panels in commercial aircraft. Injection molding of polyimide materials also permits the direct forming or "O ring" seal channels for use in vacuum sealing the battery container, see Figures III-11 and III-12 in Section III for typical details.

The next material investigation focused on the use of high temperature materials which could be used in the temperature range of 500-1000°F, be machined and easily fabricated into complex shapes. Ceramoplastics were finally selected since they offered the following advantages, for use as not only structural materials but as finished assemblies, as well:

1. Excellent dimensional stability
2. Operating temperature range (-273°F - 1800°F)
3. Impervious to moisture
4. Resists thermal cycling
5. Does not out gas
6. Thermal expansion can approximate metal inserts
7. Can be plated with metals

8. Can be formed by plastic manufacturing techniques in large complex shapes
9. Can be machined like metal (e.g. drilled, tapped, milled and lathe turned).
10. Low thermal conductivity

The ceramoplastic selected as a design reference material was a glass-bonded-mica compound formulated by the Mykroy Ceramics Corporation, and labeled MyKroy — 761. Key properties of this ceramoplastic are cited below:

- Specific gravity 3.60
- Density 13
  Thermal Conductivity
  (10^{-4} cal/sec/cm^2/^{o}C/Cm) 13.0
  BTU-in/Hr. Ft^2 ^{o}F 3.77
- Coeff. of thermal expansion
  (10^{-6} x in/in/^{o}F) 6.0
  (10^{-6} x in/in/^{o}C) 10.8
- Specific heat
  (Cal/gm/^{o}C) 0.24
- Max. continuous operating Temp. (^{o}C) 750.0
- Tensile strength (psi) 7000
- Compressive strength (psi) 29,000
- Dielectric strength (V/m) 350
- Vol. Resistivity (ohm-cm @ 70^{o}F) . . . . . 10^{14}

The areas in which Mykroy has been applied in the design of the Fiesta battery assembly are listed below (refer to Figure III-10, III-11 and III-12, Section III):

a. Molded base plate for holding cell sub-modules into correct position and spacing. The base support plate

has power conductors molded directly into the ceramo-plastic base plate (Figure III-11 and III-12).

b. Cell spacers at the top of the clustered cells in each sub-module. These spacers "lock-in" the top sub-module bus bars with the cell cluster top retainer band (Figure III-11).

c. The wavy-formed heat sink plates are locked into position during battery assembly by Mykroy inserts sitting on top of the battery base plate (Figure III-11).

d. A Mykroy top retaining plate has been provided to insure that cell submodule remain stationary during vehicle rough road travel. This molded retaining plate is spring loaded, as shown in Figure III-11.

e. The power leads (both main battery leads and electrical heater leads) leaving the battery container are pre-fabricated in molded Mykroy to reduce chances of electrical shorts between leads which could occur if conventional insulation were used due to thermal breakdown of the insulation when subjected to high temperature service (400-650^{o}F). The low thermal conductivity of Mykroy (.29-.31 BTU-Ft/hr-sq. ft-^{o}F) makes it an excellent choice for reducing thermal convection and conduction losses from the power leads. As shown in Figures III-11 and III-12, Section III, the power and coolant lines leaving the battery container are encapsulated in their own tubular shaped housings which are evacuated to reduce radial thermal losses by conduction and convection from these lines. The longitudinal losses are

controlled by the length of line insulation; generally 1-1/2 to 2 feet is adequate.

The use of polyimide materials, glass microspheres, and glass bonded mica parts played major roles in the overall design of the battery system to minimize the unwanted thermal losses from the battery, while at the same time satisfying other structural, and/or electrical design requirements.

The preliminary NaS battery design effort needs considerably more thermal analyses to be performed prior to producing any hard line drawings of the battery assembly and vehicle packaging. In any follow-on NaS battery research, development and application activities, both thermal loss studies and thermal stress studies should be defined as Major Work Tasks.

APPENDIX B

PROFESSIONAL STAFF

A. Topouzian — Program Manager

L. Bell — Research Engineer

W. Chase — Research Engineer

R. Freedman — Research Engineer

R. Layne — Designer, Technical Services Inc. Agency

B. Macauley — Staff Engineer

R. Minck — Principal Staff Engineer

P. Nicholls — Staff Engineer

M. Pulick — Principal Staff Engineer

L. Unnewehr — Principal Staff Engineer

N. Waugh — Research Engineer

APPENDIX C

LIST OF MONTHLY REPORTS

Ford/DOE — Sodium Sulfur Battery Electric Vehicle and Demonstration Phase I

Progress Report No. 27	October 1-31, 1977
Progress Report No. 29	December 1-31, 1977
Progress Report No. 31	January 1-31, 1978
Progress Report No. 38	March 1-31, 1978
Progress Report No. 39	April 1-31, 1978
Progress Report No. 43	June 1-31, 1978
Progress Report No. 45	July 1-31, 1978
Progress Report No. 46	August 1-31, 1978
Progress Report No. 47	September 1-30, 1978

LIST OF QUARTERLY REPORTS

Ford/DOE — Sodium Sulfur Battery Electric Vehicle and Demonstration Phase I

Quarterly Progress Report No. 33

September 1 - November 30, 1977

Quarterly Progress Report No. 37

December 1 - February 28, 1977

Quarterly Progress Report No. 42

March 1 - May 31, 1977

APPENDIX D

LIST OF PUBLIC PRESENTATIONS

1. Electric and Hybrid Vehicle Program Contractors Meeting

   Germantown, Maryland June 26-28, 1978

   . Presenter: M. A. Pulick, Ford, Principal Staff Engineer

2. Sodium-Sulfur Battery Review

   Newport Beach, California November 1, 1978

   . Presenter: M. A. Pulick, Ford, Principal Staff Engineer

☆U.S. GOVERNMENT PRINTING OFFICE: 1980-640-258 2117